

Measurement of the production cross section for a Higgs boson in association with a vector boson in the $H \rightarrow WW \rightarrow \ell\nu\ell\nu$ channel in pp collisions at $\sqrt{s}=13$ TeV with the ATLAS detector

ATLAS Collaboration; Newman, Paul

DOI:

[10.1016/j.physletb.2019.134949](https://doi.org/10.1016/j.physletb.2019.134949)

License:

Creative Commons: Attribution (CC BY)

Document Version

Publisher's PDF, also known as Version of record

Citation for published version (Harvard):

ATLAS Collaboration & Newman, P 2019, 'Measurement of the production cross section for a Higgs boson in association with a vector boson in the $H \rightarrow WW \rightarrow \ell\nu\ell\nu$ channel in pp collisions at $\sqrt{s}=13$ TeV with the ATLAS detector', *Physics Letters B*, vol. 798, 134949. <https://doi.org/10.1016/j.physletb.2019.134949>

[Link to publication on Research at Birmingham portal](#)

Publisher Rights Statement:

ATLAS Collaboration & Newman, P (2019), 'Measurement of the production cross section for a Higgs boson in association with a vector boson in the HWW channel in pp collisions at $\sqrt{s}=13$ TeV with the ATLAS detector', *Physics Letters B*, vol. 798, 134949. ©2019 The Author(s). <https://doi.org/10.1016/j.physletb.2019.134949>

General rights

Unless a licence is specified above, all rights (including copyright and moral rights) in this document are retained by the authors and/or the copyright holders. The express permission of the copyright holder must be obtained for any use of this material other than for purposes permitted by law.

- Users may freely distribute the URL that is used to identify this publication.
- Users may download and/or print one copy of the publication from the University of Birmingham research portal for the purpose of private study or non-commercial research.
- User may use extracts from the document in line with the concept of 'fair dealing' under the Copyright, Designs and Patents Act 1988 (?)
- Users may not further distribute the material nor use it for the purposes of commercial gain.

Where a licence is displayed above, please note the terms and conditions of the licence govern your use of this document.

When citing, please reference the published version.

Take down policy

While the University of Birmingham exercises care and attention in making items available there are rare occasions when an item has been uploaded in error or has been deemed to be commercially or otherwise sensitive.

If you believe that this is the case for this document, please contact UBIRA@lists.bham.ac.uk providing details and we will remove access to the work immediately and investigate.



Measurement of the production cross section for a Higgs boson in association with a vector boson in the $H \rightarrow WW^* \rightarrow \ell\nu\ell\nu$ channel in pp collisions at $\sqrt{s} = 13$ TeV with the ATLAS detector

ATLAS Collaboration^{*}

ARTICLE INFO

Article history:

Received 26 March 2019

Received in revised form 28 August 2019

Accepted 16 September 2019

Available online 23 September 2019

Editor: M. Doser

ABSTRACT

A measurement of the Higgs boson production cross sections via associated WH and ZH production using $H \rightarrow WW^* \rightarrow \ell\nu\ell\nu$ decays, where ℓ stands for either an electron or a muon, is presented. Results for combined WH and ZH production are also presented. The analysis uses events produced in proton–proton collisions collected with the ATLAS detector at the Large Hadron Collider in 2015 and 2016. The data correspond to an integrated luminosity of 36.1 fb^{-1} recorded at a centre-of-mass energy of 13 TeV. The products of the $H \rightarrow WW^*$ branching fraction times the WH and ZH cross sections are measured to be $0.67^{+0.31}_{-0.27}(\text{stat.})^{+0.18}_{-0.14}(\text{syst.}) \text{ pb}$ and $0.54^{+0.31}_{-0.24}(\text{stat.})^{+0.15}_{-0.07}(\text{syst.}) \text{ pb}$ respectively, in agreement with the Standard Model predictions.

© 2019 The Author(s). Published by Elsevier B.V. This is an open access article under the CC BY license (<http://creativecommons.org/licenses/by/4.0/>). Funded by SCOAP³.

1. Introduction

Higgs boson production in association with a W or Z boson, which is respectively denoted by WH and ZH , and collectively referred to as VH associated production in the following, provides direct access to the Higgs boson couplings to weak bosons. In particular, in the WH mode with subsequent $H \rightarrow WW^*$ decay, the Higgs boson couples only to W bosons, at both the production and decay vertices.

This paper presents a measurement of the corresponding production cross sections through the decay $H \rightarrow WW^* \rightarrow \ell\nu\ell\nu$, using proton–proton collisions at a centre-of-mass energy of $\sqrt{s} = 13$ TeV. The data correspond to an integrated luminosity of 36.1 fb^{-1} and were recorded by the ATLAS detector at the Large Hadron Collider (LHC). Previous measurements at $\sqrt{s} = 8$ TeV were performed by the ATLAS [1] and CMS [2] Collaborations and recently at $\sqrt{s} = 13$ TeV with 35.9 fb^{-1} of data by the CMS Collaboration [3]. Recent results at $\sqrt{s} = 13$ TeV on VH production in other decay modes can be found in Refs. [4–9].

The analysis is performed using events with three (3ℓ) or four (4ℓ) charged leptons (electrons or muons) in the final state, targeting the WH and ZH channels respectively. Leptonic decays of τ leptons, from $H \rightarrow WW^* \rightarrow \tau\nu\tau\nu$ or $H \rightarrow WW^* \rightarrow \tau\nu\ell\nu$ or from the associated vector bosons, are considered as signal, while no specific selection is performed for events with hadronically decaying τ leptons in the final state. Events from VH production with

$H \rightarrow \tau\tau$ are considered as background. The leading-order Feynman diagrams for the WH and ZH production processes are depicted in Fig. 1.

In the WH channel, multivariate discriminants are used to maximise the sensitivity to the Higgs boson signal, while in the ZH channel the analysis is performed through selection requirements. The distribution of these WH discriminants, together with event counts in background control regions and the signal regions in the ZH channel, are combined in a binned maximum-likelihood fit to extract the signal yield and the background normalisations. The maximum-likelihood fit provides results for the WH and the ZH channels separately and for their combination VH , assuming the Standard Model (SM) prediction for the relative cross sections of the two production processes.

2. ATLAS detector

The ATLAS experiment [10–12] is a multi-purpose particle detector with a forward–backward symmetric cylindrical geometry and a near 4π coverage in solid angle.¹ It consists of an in-

¹ ATLAS uses a right-handed coordinate system with its origin at the nominal interaction point (IP) in the centre of the detector and the z -axis along the beam pipe. The x -axis points from the IP to the centre of the LHC ring, and the y -axis points upwards. Cylindrical coordinates (r, ϕ) are used in the transverse plane, ϕ being the azimuthal angle around the z -axis. The pseudorapidity is defined in terms of the polar angle θ as $\eta = -\ln \tan(\theta/2)$. Angular distance is measured in units of $\Delta R \equiv \sqrt{(\Delta\eta)^2 + (\Delta\phi)^2}$. Transverse momentum and energy are defined as $p_T = p \sin \theta$ and $E_T = E \sin \theta$ respectively.

^{*} E-mail address: atlas.publications@cern.ch.

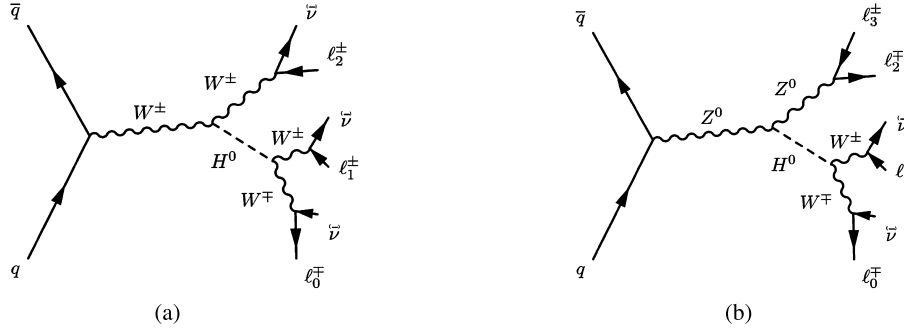


Fig. 1. Tree-level Feynman diagrams for the $VH(H \rightarrow WW^*)$ topologies considered in this paper: (a) 3ℓ channel and (b) 4ℓ channel.

Table 1

Monte Carlo generators used to model the signal and background processes. Alternative generators, underlying event and parton-showering models, used to estimate systematic uncertainties, are shown in parentheses. In the last column the prediction order for the total cross section is shown. “PYTHIA6” refers to version 6.428, “PYTHIA8” refers to versions 8.210 or 8.186.

Process	Generator (alternative)	UEPS model (alternative)	Prediction order for total cross section
$q\bar{q} \rightarrow WH$	PowHEG-Box v2 MiNLO	PYTHIA8 (HERWIG 7)	NNLO QCD + NLO EW [16–18]
$q\bar{q} \rightarrow ZH$	PowHEG-Box v2 MiNLO	PYTHIA8 (HERWIG 7)	NNLO QCD + NLO EW [16–18]
$gg \rightarrow ZH$	PowHEG-Box v2	PYTHIA8 (HERWIG 7)	NLO + NLL [19]
$ggF\ H$	PowHEG-Box v2 NNLOPS	PYTHIA8	NNNLO QCD + NLO EW [20]
$VBF\ H$	PowHEG-Box v2	PYTHIA8	NNLO QCD + NLO EW [21]
$t\bar{t}$	PowHEG-Box v2	PYTHIA8 (HERWIG 7)	NNLO+NNLL [22]
Wt	(SHERPA 2.2.1) PowHEG-Box v1	(SHERPA 2.2.1) PYTHIA6	NLO [23]
$t\bar{t}W/Z$	MG5_AMC@LO	PYTHIA8	NLO [24,25]
tZ	MG5_AMC@LO	PYTHIA6	LO [26]
$q\bar{q}/qg \rightarrow \ell\nu\ell\ell$	SHERPA 2.2.2 (PowHEG-Box v2)	SHERPA 2.2.2 (HERWIG++)	NLO [27]
$q\bar{q}/qg \rightarrow \ell\ell\ell\ell$	SHERPA 2.1/2.2.2 (PowHEG-Box v2)	SHERPA 2.1/2.2.2 (HERWIG++)	NLO [27]
$gg \rightarrow \ell\ell\ell\ell$	SHERPA 2.1.1	SHERPA 2.1.1	NLO [28]
VVV	SHERPA 2.2.2 (MG5_AMC@NLO)	SHERPA 2.2.2 (PYTHIA8)	NLO [29]

ner tracking detector (ID) surrounded by a thin superconducting solenoid providing a 2 T axial magnetic field, electromagnetic (EM) and hadronic calorimeters, and a muon spectrometer (MS). The inner tracking detector covers the pseudorapidity range $|\eta| < 2.5$. It consists of silicon pixel, silicon micro-strip, and transition-radiation tracking detectors. Lead/liquid-argon (LAr) sampling calorimeters provide electromagnetic energy measurements with high granularity. A hadronic (steel/scintillator-tile) calorimeter covers the central pseudorapidity range ($|\eta| < 1.7$). The endcap and forward regions are instrumented with LAr calorimeters for both EM and hadronic energy measurements up to $|\eta| = 4.9$. The muon spectrometer surrounds the calorimeters and is based on three large air-core toroidal superconducting magnet systems that provide a field integral between 2.0 and 6.0 Tm across most of the detector. The muon spectrometer includes a system of precision tracking chambers covering the region $|\eta| < 2.7$ and fast detectors for triggering within the range $|\eta| < 2.4$. A two-level trigger system is used to select events [13].

3. Signal and background Monte Carlo simulation

Monte Carlo (MC) event generators are used to model signal and background processes. All signal samples were generated with a Higgs boson mass of 125 GeV [14,15]. For most processes, sep-

arate programs were used to generate the hard scattering process and to model the underlying event and the parton showering (UEPS). A description of the MC samples is given in Table 1. They are normalised to cross-section predictions calculated with the QCD and electroweak (EW) orders specified in the last column of Table 1.

The $q\bar{q} \rightarrow WH$ and $q\bar{q} \rightarrow ZH$ processes were generated with PowHEG-Box v2 [30] MiNLO interfaced to PYTHIA8 [31], with the AZNLO set of tuned parameters (tune) [32] for underlying event, showering and hadronisation. The $gg \rightarrow ZH$ process was simulated with PowHEG-Box v2 + PYTHIA8 with the AZNLO tune for underlying event, showering and hadronisation. For the VH samples, the PDF4LHC15 parton distribution function (PDF) set [33] was used for the hard scattering process in PowHEG-Box v2 and the CTEQ6L1 PDF set [34] was used for the parton showering in PYTHIA8. HERWIG 7 [35], with the MMHT2014lo68cl PDF set [36], was used as an alternative parton-showering model for VH . The uncertainty due to the PDF choice is smaller than the uncertainty obtained by using HERWIG as an alternative parton shower model (Section 7).

The gluon-gluon fusion (ggF) events were generated with PowHEG-Box v2 NNLOPS [37] interfaced to PYTHIA8 with the AZNLO tune. The vector-boson fusion (VBF) events were generated with PowHEG-Box v2, interfaced to PYTHIA8. For the ggF and

VBF samples, the PDF4LHC15 PDF set was used for the hard scattering process in PowHEG-Box v2 and the CTEQ6L1 PDF set was used for the parton showering in PyTHIA8. The contribution from the $t\bar{t}H$ and tH production modes is negligible.

The top-quark pair production ($t\bar{t}$) was simulated with PowHEG-Box v2 [38] using the NNPDF 3.0 NNLO PDF set [39] and interfaced to PyTHIA8 using the NNPDF 2.3 PDF set [40] for parton showering, with the A14 tune [41]. For $t\bar{t}$ production, SHERPA [42] 2.2.1, with the NNPDF 3.0 PDF set, was used as an alternative generator while HERWIG 7, with the MMHT2014lo68cl PDF set, was used as an alternative UEPS model. The single-top-quark production Wt was generated with PowHEG-Box v1 [23] interfaced to PyTHIA6 [43] for parton showering with the PERUGIA2012 tune [44]. EvtGEN 1.2.0 [45] was used for the simulation of b -quark and c -quark decays. The $t\bar{t}W/Z$ and tZ processes were generated at leading order (LO) with MG5_AMC@LO [25] version 2.2.2 ($t\bar{t}W/Z$) and 2.2.1 (tZ) interfaced to PyTHIA8 ($t\bar{t}W/Z$) and PyTHIA6 (tZ), using the NNPDF2.3 LO PDF set.

The $q\bar{q}/gg \rightarrow VV^*$ samples with final states $\ell\nu\ell\ell$ and $\ell\ell\ell\ell$ [46] were generated with SHERPA 2.2.2, with the exception of the ZZ^* sample in the WH analysis for which SHERPA 2.1 was used; the CT10 PDF set [47] and the NNPDF 3.0 PDF set were used for versions 2.1 and 2.2.2, respectively. PowHEG-Box v2 [48] was used as an alternative generator for VV^* , with HERWIG++, using the CTEQ6L1 PDF set, for parton showering. Among the loop-induced gg -initiated diboson processes, the only relevant process in this analysis is $gg \rightarrow ZZ^*$, for which a K -factor of 1.55 was used [28]. This process was simulated with SHERPA 2.1.1, using the CT10 PDF set.

The triboson VVV samples were generated with SHERPA 2.2.2 and the NNPDF 3.0 PDF set. MG5_AMC@NLO was used as an alternative generator for VVV , with PyTHIA8, using the NNPDF2.3 LO PDF set. The same PDF sets were used for the hard scattering and the parton showering in all the SHERPA samples described above.

All simulated samples include the effect of pile-up from multiple interactions in the same and neighbouring bunch crossings. This was achieved by overlaying minimum-bias events, simulated using PyTHIA8 with the A2 tune [49] and MSTW2008LO PDF set [50]. All samples were processed through the GEANT 4 [51] ATLAS detector simulation [52].

4. Event reconstruction

Candidate signal events are selected using triggers that require a single isolated lepton with minimum transverse momentum (p_T) thresholds between 24 GeV and 26 GeV for electrons and between 20 GeV and 26 GeV for muons, depending on the data-taking period. At least one of the leptons reconstructed offline is required to have triggered the event and to have a p_T higher than the nominal trigger threshold by at least 1 GeV. The single-lepton trigger efficiencies on the plateau are approximately 70% for single muons with $|\eta| < 1.05$, 90% for single muons in the range $1.05 < |\eta| < 2.40$ and greater than 90% for single electrons in the range $|\eta| < 2.47$. The trigger efficiency for the signal events, estimated after the preselection, is 94% for WH and 98.5% for ZH .

Selected events are required to have at least one primary vertex reconstructed from at least two associated tracks, each with transverse momentum $p_T > 400$ MeV, as described in Ref. [53]. If an event has more than one reconstructed primary vertex, the vertex with the largest track $\sum p_T^2$ is selected for the analysis.

Electrons are reconstructed from clusters of energy deposits in the EM calorimeter matched to ID tracks, and are identified using criteria based on the calorimeter shower shape, the quality of the match between the track and the cluster and the amount of transition radiation emitted in the ID, as described in Ref. [54]. Electrons

are required to satisfy $|\eta| < 2.47$, excluding $1.37 < |\eta| < 1.52$, which corresponds to the transition region between the barrel and the endcap EM calorimeters. The efficiency for electron identification ranges from 88% to 94%, depending on electron p_T and η . Muons are reconstructed by combining ID and MS tracks with consistent trajectories and curvatures. An overall fit of hits from the ID track, energy loss in the calorimeter and the hits of the track in the muon system is used to form muon candidates, as described in Ref. [55]. The efficiency for muon identification is close to 95% over the full instrumented η range. To suppress particles misidentified as leptons, several identification requirements as well as impact parameter, calorimeter and track isolation criteria [54,55] are applied.

Jets are reconstructed using the anti- k_t algorithm with radius parameter $R = 0.4$ [56,57]. The four-momenta of jets are corrected for the effects of calorimeter non-compensation, energy loss in non-instrumented regions, and contributions from pile-up [58]. Jets are required to have $|\eta| < 4.5$, with $p_T > 25$ GeV for the region $|\eta| < 2.5$ and $p_T > 30$ GeV for the region $2.5 < |\eta| < 4.5$. A multivariate selection [59] is used to suppress jets with $p_T < 60$ GeV and $|\eta| < 2.4$ originated from pile-up. Furthermore, to suppress pile-up jets in the forward region, jet shapes and topological jet correlations in pile-up interactions are exploited [60]. Jets with $p_T > 20$ GeV and $|\eta| < 2.5$ containing b -hadrons (b -jets) are identified using a multivariate technique [61] with an efficiency of 85%, estimated from simulated $t\bar{t}$ events. The multivariate technique gives rejection factors against jets originating from a light quark or gluon and jets containing c -hadrons of 33 and 3, respectively.

The missing transverse momentum \vec{p}_T^{miss} with magnitude E_T^{miss} in each event is calculated from the negative vectorial sum of the transverse momenta of electrons, muons, and jets. It uses both track-based and calorimeter-based measurements [62].

5. Event selection

In the WH channel, exactly three isolated leptons with $p_T > 15$ GeV are required with a total charge of ± 1 . The lepton with unique charge is labelled ℓ_0 , the lepton closest to ℓ_0 in angular distance ΔR is labelled ℓ_1 , and the remaining lepton is labelled ℓ_2 . In signal events leptons ℓ_0 and ℓ_1 are most likely to originate from the $H \rightarrow WW^*$ decay, with probabilities of 99% and 85% respectively.

The most prominent background processes to the WH channel are $WZ/W\gamma^*$ production and top-quark processes with either three prompt leptons, e.g. $t\bar{t}V$, or two prompt leptons and one non-prompt lepton from a b -hadron decay, e.g. $t\bar{t}$. Other important background processes are ZZ^* (including $Z\gamma^*$), $Z\gamma$ and Z -jets production; they may satisfy the signal selection requirements if a lepton is undetected, in the case of ZZ^* , or if they contain a misidentified or non-prompt lepton, in the case of $Z\gamma$ and Z -jets production. Processes with three prompt leptons in the final state such as tribosons, in particular WWW , also contribute to the background. Contributions from background processes that include more than one misidentified lepton, such as W -jets production and inclusive $b\bar{b}$ pair production, are negligible. The background from top-quark production is suppressed by vetoing events if they contain any b -tagged jet.

The analysis of the WH channel separates events with at least one same-flavour opposite-sign charge (SFOS) lepton pair from events with zero SFOS lepton pairs, which have different signal-to-background ratios. Due to the presence of $Z \rightarrow \ell\ell$ decays as a dominant background, the former is hereafter referred to as the Z -dominated category, while the latter is referred to as the Z -depleted category. In the Z -dominated category, the major background processes are those involving Z bosons. Events are ve-

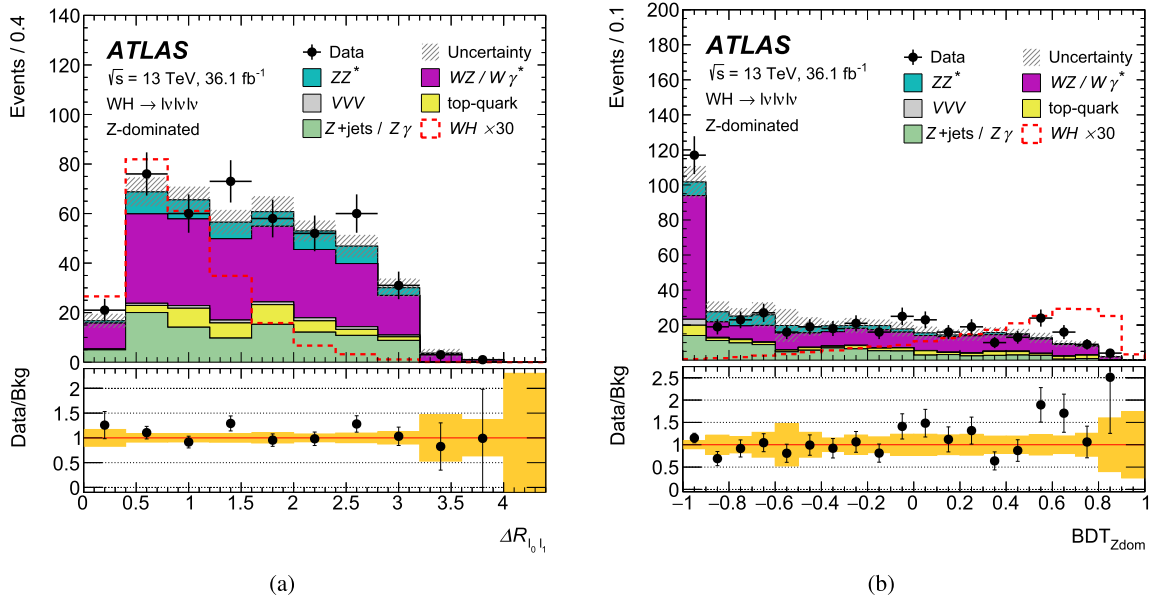


Fig. 2. Distribution of (a) angular separation $\Delta R_{\ell_0\ell_1}$ and (b) $\text{BDT}_{Z\text{dom}}$ distribution in the Z-dominated category. The dashed line shows the WH signal scaled by a factor of 30. The hatched band in the upper panel and the shaded band in the lower panel show the total statistical and experimental systematic uncertainty in background predictions. The $WZ/W\gamma^*$ and top-quark background processes are normalised with the normalisation factors from the control region analysis (Table 4). The Z +jets and $Z\gamma$ background processes are estimated with the data-driven technique described in Section 6.

toed if they contain more than one jet. This requirement further suppresses top-quark events with an additional non-prompt lepton from b -hadron decays. In order to select final states with neutrinos, E_T^{miss} is required to be above 30 GeV. The invariant masses $m_{\ell\ell}$ of all SFOS pairs are required to satisfy a Z-veto selection: $|m_{\ell\ell} - m_Z| > 25$ GeV. The last two requirements suppress $WZ/W\gamma^*$ and ZZ^* events, and improve the Z +jets rejection. In order to suppress background events from heavy-flavour quarkonia, the smallest invariant mass of SFOS pairs is required to be greater than 12 GeV. The signal efficiency of this selection with respect to the preselection is 34.6%. A discriminant based on a boosted decision tree (BDT) [63,64] is used to achieve a further separation between signal and background processes. The main purpose of the multivariate classifier, named $\text{BDT}_{Z\text{dom}}$, is to distinguish between signal and the dominant $WZ/W\gamma^*$ and ZZ^* background processes, and hence it is trained against these two background processes. The $\text{BDT}_{Z\text{dom}}$ uses seven input variables. They are the magnitude of the vectorial sum of lepton transverse momenta ($|\Sigma p_{T\ell}|$), the invariant masses of the first lepton pair ($m_{\ell_0\ell_1}$) and of the three leptons ($m_{\ell\ell\ell}$), the angular distance $\Delta R_{\ell_0\ell_1}$, E_T^{miss} and the pseudorapidity separation between the leptons with the same charge ($\Delta\eta_{\ell_1\ell_2}$). Moreover the BDT uses the transverse mass

$$m_T^W = \sqrt{2 p_T^{\ell_W} \cdot E_T^{\text{miss}} \cdot (1 - \cos \Delta\phi(\ell_W, \vec{p}_T^{\text{miss}}))},$$

built from the \vec{p}_T^{miss} and the lepton ℓ_W which is the lepton not belonging to the SFOS lepton pair with invariant mass closer to the Z boson mass, and could be either ℓ_1 or ℓ_2 . Fig. 2 shows the distribution of $\Delta R_{\ell_0\ell_1}$, which is the most powerful variable in the $\text{BDT}_{Z\text{dom}}$ training, and the $\text{BDT}_{Z\text{dom}}$ distribution in the Z-dominated category, before applying any selection requirement on the $\text{BDT}_{Z\text{dom}}$ score.

The Z-dominated signal region (SR), defined as the events with high-ranking $\text{BDT}_{Z\text{dom}}$ score ($\text{BDT}_{Z\text{dom}} > 0.3$), is divided into three bins with increasing sensitivity: $0.3 \leq \text{BDT}_{Z\text{dom}} < 0.5$, $0.5 \leq \text{BDT}_{Z\text{dom}} < 0.7$ and $0.7 \leq \text{BDT}_{Z\text{dom}} < 1.0$. This binning is the result of an optimisation to find the minimal number of BDT bins that gives the highest sensitivity. The expected signal-to-background ra-

tio in these bins is about 0.05, 0.09 and 0.19, respectively. The full Z-dominated event selection is summarised in Table 2.

In the Z-depleted category, the two major background processes are $WZ/W\gamma^*$ with $Z/\gamma^* \rightarrow \tau\tau$ and $t\bar{t}$, where $WZ/W\gamma^*$ has the same signature of the signal, namely three prompt leptons, while $t\bar{t}$ contains a misidentified or non-prompt lepton from a jet. Two separate BDTs, named BDT_{WZ} and $\text{BDT}_{t\bar{t}}$, are trained to allow an optimal background rejection. The BDT_{WZ} uses 11 input variables, of which three common to the $\text{BDT}_{Z\text{dom}}$ are $m_{\ell_0\ell_1}$, E_T^{miss} and $\Delta\eta_{\ell_1\ell_2}$; the other variables are the transverse momenta of the three leptons ($p_T^{\ell_0}$, $p_T^{\ell_1}$, $p_T^{\ell_2}$), the transverse mass ($m_T^{\ell_0\ell_1}$) built from ℓ_0 , ℓ_1 and \vec{p}_T^{miss} , the invariant mass of the electrons with same-sign charge (m_{ee}), the transverse impact parameter significances of the lepton with lowest p_T ($|d_{0,\text{sig,min}}|$), the transverse impact parameter significances of the lepton with second-lowest p_T and opposite charge with respect to the lepton with lowest p_T ($|d_{0,\text{sig,mid}}|$) and the compatibility of the event with the WZ hypothesis F_α .²

A definition of the most likely lepton from heavy-flavour decays (ℓ_{HFL}) is crucial for an optimal performance of the $\text{BDT}_{t\bar{t}}$. For this purpose, a BDT_{HFL} is trained purely on data using track and calorimeter isolation as well as impact-parameter variables as input. The lepton with the minimal BDT_{HFL} output is selected as ℓ_{HFL} . The $\text{BDT}_{t\bar{t}}$ uses nine input variables, of which two common to the $\text{BDT}_{Z\text{dom}}$ and BDT_{WZ} are $m_{\ell_0\ell_1}$ and $\Delta\eta_{\ell_1\ell_2}$, one common to the $\text{BDT}_{Z\text{dom}}$ is $\Delta R_{\ell_0\ell_1}$, and the other input variables are the number of jets (N_{jet}), the transverse momentum of the leading jet (p_T^{lead}), the invariant mass of the leptons with same-sign charge ($m_{\ell_1\ell_2}$), and three ℓ_{HFL} -related variables: its BDT_{HFL} output, its transverse momentum, $p_T^{\ell_{\text{HFL}}}$, and the invariant mass built from it together

² Given the reconstructed charged-lepton momenta and the \vec{p}_T^{miss} , the event kinematics can be calculated under the WZ with $Z \rightarrow \tau\tau$ hypothesis and using the collinear approximation for the τ decays with one remaining unknown, e.g. the ratio of one τ energy to the energy of the lepton from this τ decay. This unknown is varied and the number of physical kinematic solutions is taken as a measure of the compatibility with the WZ hypothesis.

Table 2

Event selection criteria used to define the signal regions in the WH and ZH analyses. The symbols are defined in the text.

Category	WH		ZH	
	3 isolated leptons ($p_T > 15$ GeV) total lepton charge ± 1		4 isolated leptons ($p_T > 10$ GeV) total lepton charge 0	
	Z-dominated	Z-depleted	2-SFOS	1-SFOS
Number of SFOS	2 or 1	0	2	1
Number of jets	≤ 1	—	≤ 1	≤ 2
Number of b -jets	0	0	0	0
E_T^{miss} [GeV]	> 30	—	> 45	—
p_T^{le} [GeV]	—	—	> 45	—
$m_{\ell\ell}$ [GeV]	> 12 (min. SFOS)	—	> 10	> 10
$ m_{\ell\ell} - m_Z $ [GeV]	> 25 (SFOS)	—	< 10 ($m_{\ell_2\ell_3}$)	< 10 ($m_{\ell_2\ell_3}$)
$m_{\ell_0\ell_1}$ [GeV]	—	—	< 55	< 60
$\Delta\phi_{\ell_0\ell_1}^{\text{boost}}$	—	—	< 2.3	< 1.9
$m_{\tau\tau}$ [GeV]	—	—	—	< 50
$\Delta\phi_{\ell_0\ell_1, \vec{p}_T^{\text{miss}}}$ [rad]	—	—	—	> 0.4
$m_{4\ell}$ [GeV]	—	—	> 140	—
BDT	$\text{BDT}_{\text{Zdom}} > 0.3$	$\text{BDT}_{\ell\bar{\ell}} > 0.2 \& \text{BDT}_{WZ} > 0.15$	—	—

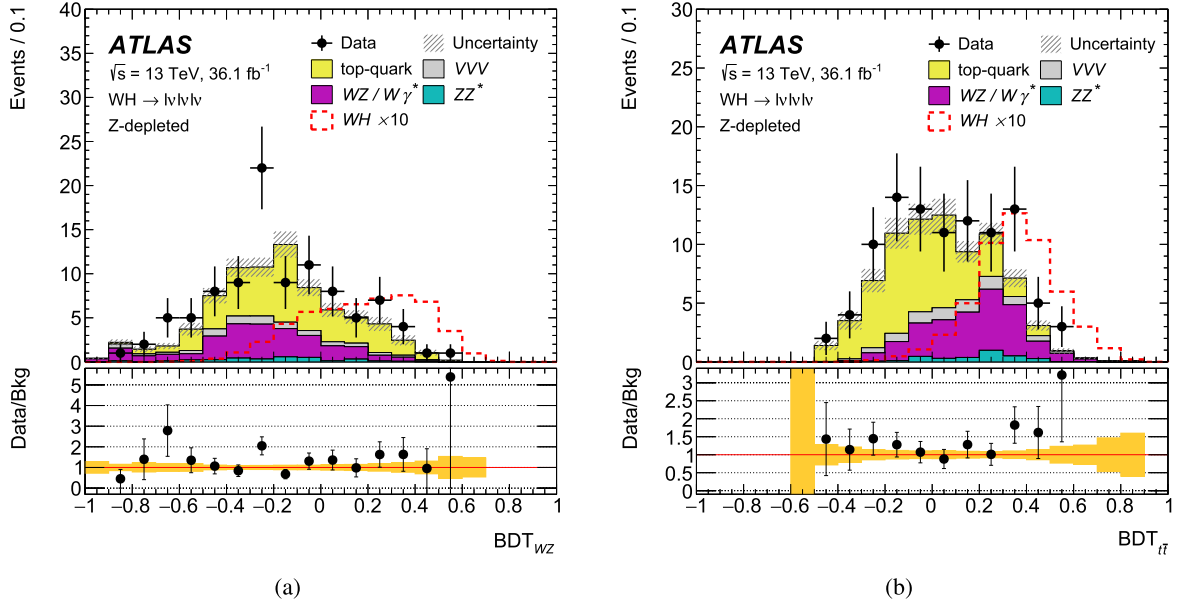


Fig. 3. Distribution of (a) BDT_{WZ} and (b) $\text{BDT}_{\ell\bar{\ell}}$ in the Z-depleted category. The dashed line shows the WH signal scaled by a factor of 10. The hatched band in the upper panel and the shaded band in the lower panel show the total statistical and experimental systematic uncertainty in background predictions. The $WZ/W\gamma^*$ and top-quark background processes are normalised with the normalisation factors from the control region analysis (Table 4).

Table 3

Summary of the Z-depleted fit regions.

Bin 1	Bin 2	Bin 3	Bin 4	Bin 5	Bin 6
$0.2 \leq \text{BDT}_{\ell\bar{\ell}} < 0.3$		$0.3 \leq \text{BDT}_{\ell\bar{\ell}} < 0.45$		$0.45 \leq \text{BDT}_{\ell\bar{\ell}}$	
$0.15 \leq \text{BDT}_{WZ} < 0.35$	$0.35 \leq \text{BDT}_{WZ}$	$0.15 \leq \text{BDT}_{WZ} < 0.35$	$0.35 \leq \text{BDT}_{WZ}$	$0.15 \leq \text{BDT}_{WZ} < 0.35$	$0.35 \leq \text{BDT}_{WZ}$

with the closest opposite-charge lepton ($m_{\ell_{\text{HFL}}\ell_{\text{cloc}}}$). Fig. 3 shows the outputs of BDT_{WZ} and $\text{BDT}_{\ell\bar{\ell}}$ in the Z-depleted category, before applying any selection requirements on the BDT scores.

The choice of input variables for the different BDTs was the result of an optimisation study where several thousand different BDTs using different set of input variables have been compared and the best performing BDTs have been selected for the final analysis.

The full Z-depleted event selection is summarised in Table 2. The events with high-ranking BDT scores ($\text{BDT}_{\ell\bar{\ell}} > 0.2$ and $\text{BDT}_{WZ} > 0.15$) are used to define the Z-depleted SR. In this region, the BDT scores are used as discriminant variables in the statistical analysis, with three bins in $\text{BDT}_{\ell\bar{\ell}}$, each being subdivided into

two bins in BDT_{WZ} as shown in Table 3. The expected signal-to-background ratio in these bins ranges from about 0.07 in the first bin up to about 3.6 in the last bin. The signal efficiency with respect to the preselection, before any cut on the BDT scores, is 23.5%.

The ZH channel requires events to contain four isolated leptons with $p_T > 10$ GeV and total electric charge of zero. Events that contain a SFOS lepton pair with $m_{\ell\ell} < 10$ GeV are rejected to suppress the contamination from heavy-flavour quarkonia. Following this preselection, events are classified according to the number of SFOS lepton pairs: 1-SFOS and 2-SFOS. Events with no SFOS lepton pairs are not considered.

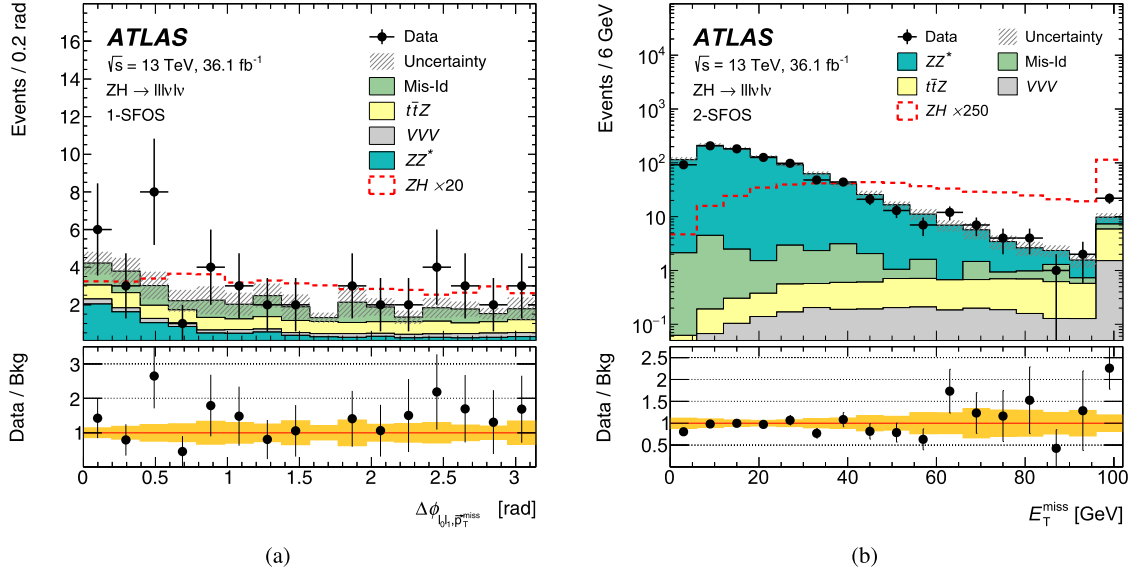


Fig. 4. Distributions of (a) the azimuthal separation between the Higgs-candidate lepton pair and the missing transverse momentum $\Delta\phi_{\ell_0\ell_1, \vec{p}_T^{\text{miss}}}$ in 1-SFOS events and (b) the missing transverse momentum E_T^{miss} in 2-SFOS events, after preselection. For the latter the last bin contains overflow events. The dashed line shows the ZH signal scaled by a factor 20 (left) and by a factor 250 (right). The hatched band in the upper panel and the shaded band in the lower panel show the total statistical and experimental systematic uncertainty in background predictions. The ZZ^* background process is normalised in the 2-SFOS case with the normalisation factor from the control region analysis (Table 4). The Mis-Id background is estimated with the data-driven technique described in Section 6.

The reconstruction of the ZH process proceeds through the identification of the leptons from the Z boson, called ℓ_2 and ℓ_3 , as the SFOS lepton pair with invariant mass closest to the Z boson mass, m_Z . Then, the remaining two leptons, labelled ℓ_0 and ℓ_1 , are candidates for originating from the Higgs boson decay. The background in the ZH channel is almost exclusively due to ZZ^* production. This constitutes $\sim 92\%$ of the total background after the preselection is applied. Processes with four prompt leptons in the final state such as triboson production, in particular ZWW , which has the same signature as the signal, and $t\bar{t}Z$ also contribute to the background. Other background processes such as $WZ/W\gamma^*$, Z +jets and tV may contribute when at least one jet, hadron or a converted photon is misidentified as a lepton.

In order to suppress the $t\bar{t}Z$ process, events containing b -tagged jets are rejected and at most one and two jets are allowed in 2-SFOS and 1-SFOS classes, respectively. To reduce the ZZ^* background process in events with two SFOS lepton pairs, a threshold of 45 GeV is applied to the E_T^{miss} and to the vector sum of the lepton transverse momenta, $p_T^{4\ell}$. The invariant mass of ℓ_2 and ℓ_3 , $m_{\ell_2\ell_3}$, is required to satisfy $|m_{\ell_2\ell_3} - m_Z| < 10$ GeV, and the invariant mass of ℓ_0 and ℓ_1 , $m_{\ell_0\ell_1}$, is required to be between 10 GeV and 60 GeV (55 GeV) in 1-SFOS (2-SFOS) events. The variable $\Delta\phi_{\ell_0\ell_1}^{\text{boost}}$ denotes the difference in azimuthal angle between the leptons from the Higgs boson candidate in the frame where the Higgs boson p_T is zero. The Higgs boson transverse momentum is approximated with $\vec{p}_T^H \approx -\vec{p}_T^Z$, or $\vec{p}_T^H \approx -\vec{p}_T^Z - \sum \vec{p}_T^{\text{jet}}$ if at least one jet is present in the event. Events are required to satisfy $\Delta\phi_{\ell_0\ell_1}^{\text{boost}} < 1.9$ (2.3) rad in the 1-SFOS (2-SFOS) class. In 1-SFOS events the ZZ^* process contributes through the $Z \rightarrow \tau\tau$ decay, therefore the reconstructed mass of the τ pair, $m_{\tau\tau}$ is required to be below 50 GeV; $m_{\tau\tau}$ is computed using the collinear approximation method [65]. In addition, the azimuthal separation between the Higgs-candidate lepton pair and the \vec{p}_T^{miss} , $\Delta\phi_{\ell_0\ell_1, \vec{p}_T^{\text{miss}}}$, is required to be above 0.4 rad. The final selection of these variables is optimised in order to maximise the signal significance. Fig. 4(a) illustrates the discriminating power of the $\Delta\phi_{\ell_0\ell_1, \vec{p}_T^{\text{miss}}}$ variable for 1-SFOS events after the preselection. This variable reduces the ZZ^*

contribution which becomes the dominant background source after the b -tagged jet veto and $m_{\ell_0\ell_1}$ selection are applied. Fig. 4(b) shows the E_T^{miss} distribution for 2-SFOS events after the preselection. In order to be orthogonal to the $H \rightarrow ZZ^*$ analysis of Ref. [66], 2-SFOS events are required to have an invariant mass of the four-lepton system, $m_{4\ell}$, above 140 GeV. The full event selection for ZH is summarised in Table 2.

The total efficiency times acceptance of this selection for the process WH with subsequent $H \rightarrow WW^*$ decay is about 0.073% while for ZH it is about 0.026%. These numbers are given with respect to all W and Z decays.

6. Background estimation

The main background contamination originates from processes with the same final state as the signal, namely diboson production ($WZ/W\gamma^*$, ZZ^*), top-quark processes with three or four prompt leptons such as $t\bar{t}V$, and triboson production. Other relevant background contributions arise from processes, such as $t\bar{t}$ or Z +jets, where the reconstructed leptons either originate from non-prompt decays of heavy-flavour hadrons or from jets misidentified as leptons.

Two dedicated regions, hereafter named control regions (CRs), are used to estimate the normalisation factors (NFs) of the main prompt background processes by fitting the expected yields from simulation to data: $WZ/W\gamma^*$ for the WH channel and ZZ^* for the ZH channel in the 2-SFOS SR. In the 1-SFOS SR, ZZ^* is estimated purely from simulation.

The CRs are made orthogonal to the corresponding SRs by inverting various selection criteria with respect to the SR definitions. The WZ CR is defined by reversing the Z -veto in the Z -dominated WH signal region. To improve the purity of the WZ CR, the minimum E_T^{miss} is increased from 30 GeV to 50 GeV. The ZZ CR is defined by inverting the $m_{\ell_0\ell_1}$ requirement defined in the ZH 2-SFOS SR. In order to increase the number of events, the E_T^{miss} , $\Delta\phi_{\ell_0\ell_1}^{\text{boost}}$, $p_T^{4\ell}$, and $m_{4\ell}$ requirements are removed. Table 4 summarises the event selection for the WZ and ZZ CRs and the NFs for the background processes, obtained from the fit described in

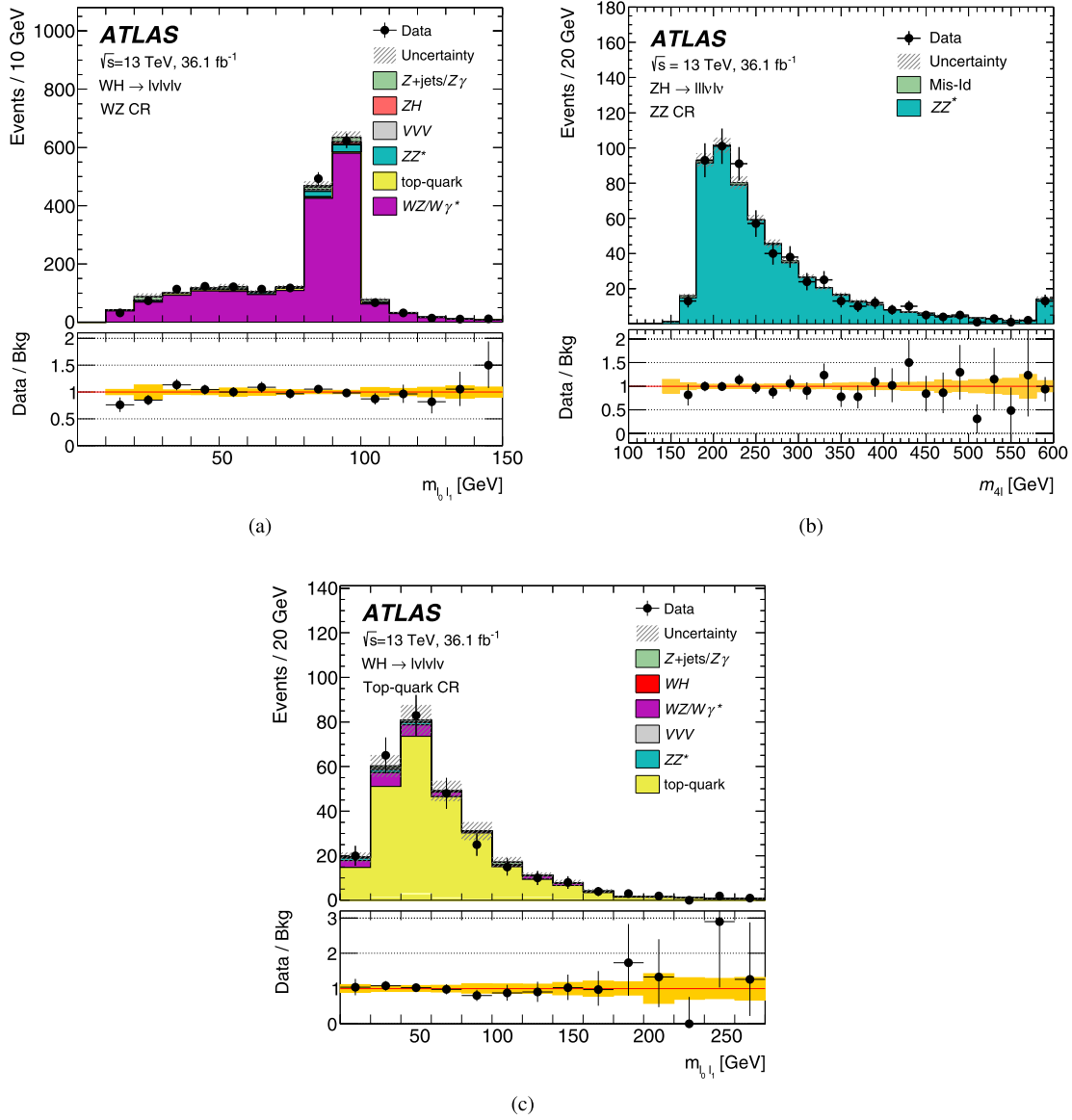


Fig. 5. Post-fit distributions of the dilepton invariant mass $m_{\ell_0 \ell_1}$ in the WZ CR (a) and of the four-lepton invariant mass $m_{4\ell}$ in the ZZ CR (b). For the latter the last bin contains overflow events. Post-fit distributions of the dilepton invariant mass $m_{\ell_0 \ell_1}$ is shown also in the top-quark CR (c). The hatched band in the upper panel and the shaded band in the lower panel show the total statistical and experimental systematic uncertainty in background predictions. The Mis-Id background is estimated with the data-driven technique described in Section 6.

Table 4

Definition of control regions in the WH and ZH analyses. Selections indicated in boldface font are designed to ensure the control region (CR) is orthogonal to the relevant SR. In the last line normalisation factors which scale the corresponding yields in the signal region are shown with their uncertainties, including both the statistic and the systematic uncertainties.

Channel (Category)	WH (Z-dominated and Z-depleted)		ZH (2-SFOS)
CR	WZ	Top-quark	ZZ
Number of leptons	3	3	4
Total lepton charge	± 1	± 1	0
Number of SFOS	2 or 1	≤ 2	2
Number of jets	≤ 1	≥ 1	≤ 1
Number of b-jets	0	≥ 1	0
E_T^{miss} [GeV]	> 50	> 50 (2 or 1 SFOS)	—
$ m_{\ell\ell} - m_Z $ [GeV]	$< \mathbf{25}$	> 25 (2 or 1 SFOS)	< 10 ($m_{\ell_2 \ell_3}$)
$m_{\ell_0 \ell_1}$ [GeV]	—	—	$> \mathbf{55}$
$m_{\ell\ell}$ (min. SFOS) [GeV]	> 12	> 12 (2 or 1 SFOS)	—
Normalisation factors	0.99 ± 0.05	0.97 ± 0.08	1.13 ± 0.06

Section 8. The NFs are hereby completely dominated by the CR statistics and their values do not change when only the control regions are used in the fit. Figs. 5(a) and 5(b) show the distributions of $m_{\ell_0 \ell_1}$ in the WZ CR and the invariant mass of the four leptons in the ZZ CR, as obtained from the final fit in the statistical analysis (post-fit) described in Section 8.

The background contributions with misidentified leptons are estimated using different techniques. The top-quark background in the WH channels is normalised using a CR (top-quark CR) defined by requiring at least one b -tagged jet. To improve the purity of the top-quark CR, the minimum E_T^{miss} is increased from 30 GeV to 50 GeV if at least one SFOS pair is present in the event. Processes with one misidentified lepton ($t\bar{t}$ and Wt) constitute 94% of the top-quark CR, the remaining events contain three prompt leptons from $t\bar{t}W$ decays. The full selection requirements applied to define the top-quark CR and the measured NF are also summarised in Table 4. Fig. 5(c) shows the $m_{\ell_0 \ell_1}$ distribution in the top-quark CR as obtained from the final fit.

Table 5

Post-fit predictions and data yields in the four SRs. The uncertainties include those from the sample statistics, and the theoretical and experimental systematic uncertainties. The sum of the single contributions may differ from the total value due to rounding. Moreover, the total uncertainty differs from the sum in quadrature of the single-process uncertainties due to the correlations. “Other Higgs” contains Higgs production mechanisms and decay processes different from VH and $H \rightarrow WW^*$ respectively, except for the $H \rightarrow ZZ^*$ contribution which is included in the “ ZZ^* ” row. The corresponding pre-fit predictions for the background processes differ only by the normalization factors listed in Table 4.

Process	WH		ZH	
	Z-dominated	Z-depleted	1-SFOS	2-SFOS
WH	11 ± 6	5.8 ± 2.8	—	—
ZH	1.1 ± 0.6	0.61 ± 0.34	3.3 ± 1.7	1.8 ± 0.9
$WZ/W\gamma^*$	40.1 ± 2.8	1.7 ± 0.5	—	—
ZZ^*	2.4 ± 1.1	0.27 ± 0.09	0.14 ± 0.14	1.2 ± 0.3
VVV	1.5 ± 0.1	0.71 ± 0.11	0.32 ± 0.05	0.20 ± 0.03
$tV/t\bar{t}V$	0.14 ± 0.03	0.13 ± 0.03	0.04 ± 0.02	0.03 ± 0.01
Other top-quark	8.4 ± 2.6	1.9 ± 0.8	—	—
Other Higgs	0.31 ± 0.03	0.06 ± 0.01	< 0.01	0.04 ± 0.01
Misid. leptons	9.7 ± 3.4	< 0.1	0.19 ± 0.08	0.36 ± 0.12
Total background	62 ± 5	4.7 ± 1.0	0.65 ± 0.17	1.8 ± 0.3
Observed	76	10	5	2

A data-driven technique is used to estimate the Z +jets and $Z\gamma$ contribution in both the WH and ZH channels and the contributions from $WZ/W\gamma^*$ and top-quark processes in the ZH channel. These contributions typically have one misidentified lepton (Z +jets and $Z\gamma$ in the WH channel, and $WZ/W\gamma^*$ and $tZ/t\bar{t}W$ in the ZH channel) or two misidentified leptons (Z +jets and $tW/t\bar{t}$ in the ZH channel). A control sample where one or two of the lepton candidates fail to meet the nominal identification or isolation criteria but satisfy looser identification criteria, referred to as anti-identified leptons, is used. The contribution from misidentified leptons in the SR is then obtained by scaling the number of events in the control sample by extrapolation factors measured in a data sample enriched in Z +jets events. The latter is obtained by selecting events with two prompt leptons from a Z boson decay and a loosely identified lepton considered to be the misidentified lepton candidate. The extrapolation factors are defined as the ratio of the number of misidentified lepton candidates that pass the nominal identification criteria to the number that pass the anti-identification criteria. In both the control sample and the data samples enriched in Z +jets events, the contribution from background events not estimated with this method is subtracted using MC expectations. Details of this method can be found in Ref. [67]. The uncertainty in the data-driven background processes described in this section includes the statistical uncertainty in the Z +jets enriched sample, the uncertainty from Z +jets MC modelling, and the theory uncertainty from the subtraction of other processes. For the ZH channel, which can have events with two prompt leptons and two misidentified leptons, the uncertainty in the extrapolation from the control sample to the SRs is also included.

7. Systematic uncertainties

The systematic uncertainties can be categorised into those arising from experimental sources and those from theoretical sources. The dominant experimental uncertainties come from the misidentification of leptons (see Section 6), the mismodelling of the impact-parameter significance, the b -tagging efficiency [61] and the jet energy scale and resolution [58]. Other sources of uncertainty are due to the modelling of pile-up, the calibration of the missing transverse momentum measurement [62], and the luminosity measurement. The uncertainty in the combined 2015+2016 integrated luminosity is 2.1%. It is derived from the calibration of

the luminosity scale using x-y beam-separation scans, following a methodology similar to that detailed in Ref. [68], and using the LUCID-2 detector for the baseline luminosity measurements [69].

The impact of the uncertainties on lepton energy (momentum) scale and resolution, and identification and isolation criteria [54, 55, 70] is negligible. The experimental uncertainties are varied in a correlated way across all background processes and all signal- and control-region bins, so that uncertainties in the extrapolation from control to signal regions are correctly propagated. The luminosity uncertainty is only applied to background processes that are normalised to theoretical predictions, and to the Higgs boson signal. The theoretical uncertainties are evaluated by comparing nominal and alternative event generators and UEPS models as described in Section 3 and by varying PDF sets and the QCD renormalisation and factorisation scales. The uncertainty due to the PDF choice for the signal process is 1% while the uncertainty obtained by using HERWIG as an alternative parton shower model is 3–10%, depending on the signal region. All uncertainties are propagated through the full analysis chain and treated as being bin-dependent and region-dependent, i.e. potentially modifying not only the normalisation but also the shape of the BDT output distributions. Whenever the influence on the shape is found to be negligible, as in the case of the PDF and scale variations, only the normalisation uncertainties are used. A list of the systematic uncertainty sources and their impact on the cross-section measurement are shown later in Section 8.

8. Results

A binned likelihood function is constructed as a product of Poisson probability terms over the eleven bins of the different SRs defined in Section 5. The function has two independent scaling parameters: the signal strength parameter μ , defined as the ratio of the measured signal yield to that predicted by the SM, for each of the WH and the ZH processes. Additionally, one Poisson probability term is added for each CR to determine simultaneously the normalisation of the corresponding background processes. Systematic uncertainties enter as nuisance parameters in the likelihood function and their correlations are taken into account. The final results are obtained using the profile likelihood method [71]. The resulting post-fit prediction and data yields in the four SRs are shown in Table 5.

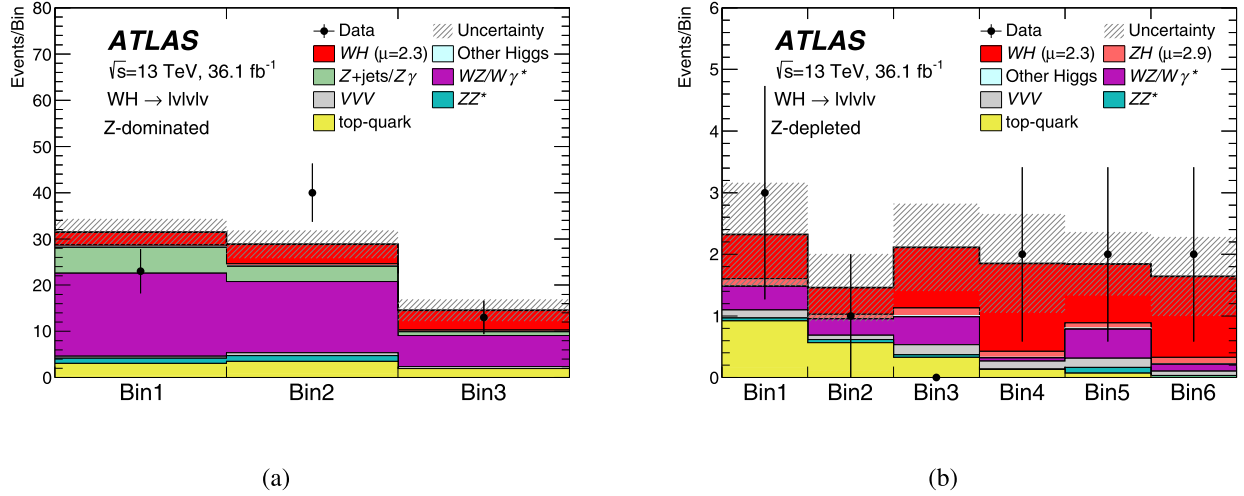


Fig. 6. Post-fit BDT-score distributions (a) in the WH Z-dominated SR and (b) for the two-dimensional grid in $BDT_{t\bar{t}}$ and BDT_{WZ} in the WH Z-depleted SR. The shaded band includes statistical and systematic uncertainties on both signal and background as estimated by the fit.

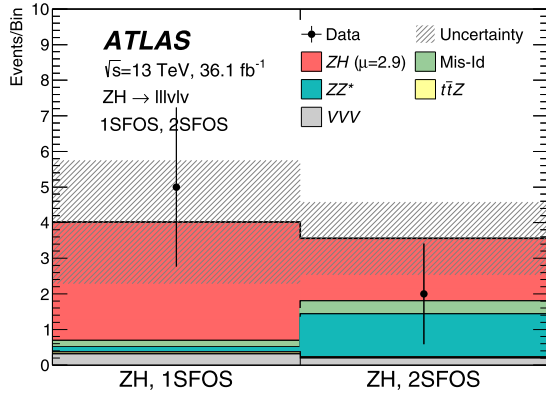


Fig. 7. Post-fit event yields in the ZH 1-SFOS and 2-SFOS SRs. The shaded band includes statistical and systematic uncertainties on both signal and background as estimated by the fit.

Fig. 6 shows the post-fit distribution of BDT scores in the WH Z-dominated and Z-depleted SRs. The post-fit event yields in the ZH 1-SFOS and 2-SFOS SRs are shown in Fig. 7.

The measured signal strengths for the WH and ZH production modes in the $H \rightarrow WW^*$ decay channel are simultaneously determined to be

$$\mu_{WH} = 2.3^{+1.1}_{-0.9}(\text{stat.})^{+0.49}_{-0.36}(\text{exp syst.})^{+0.41}_{-0.33}(\text{theo syst.}) = 2.3^{+1.2}_{-1.0},$$

$$\mu_{ZH} = 2.9^{+1.7}_{-1.3}(\text{stat.})^{+0.54}_{-0.28}(\text{exp syst.})^{+0.66}_{-0.27}(\text{theo syst.}) = 2.9^{+1.9}_{-1.3},$$

compared to the expected results of $\mu_{WH} = 1.0^{+0.86}_{-0.69}(\text{stat.})^{+0.40}_{-0.30}(\text{exp syst.})^{+0.32}_{-0.26}(\text{theo syst.}) = 1.0^{+1.0}_{-0.8}$ and $\mu_{ZH} = 1.0^{+1.3}_{-0.9}(\text{stat.})^{+0.41}_{-0.20}(\text{exp syst.})^{+0.32}_{-0.16}(\text{theo syst.}) = 1.0^{+1.4}_{-0.9}$. The observed (expected) significances of WH and ZH production modes are 2.6 (1.3) standard deviations and 2.8 (1.2) standard deviations above the SM background, including other Higgs-boson processes, respectively. When determining the significance for WH production, the ZH signal-strength parameter is left floating in the fit, and vice versa. The combination of the WH and ZH channels leads to an observed (expected) significance for the combined VH production mode of 4.1 (1.9) standard deviations above the SM background, including other Higgs-boson processes. The p -value with respect to the value predicted by the SM corresponds to about two stan-

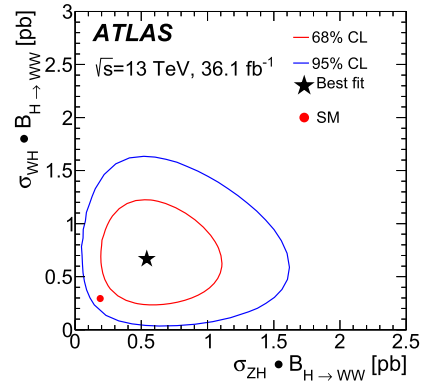


Fig. 8. Two-dimensional likelihood contours of $\sigma_{WH} \cdot \mathcal{B}_{H \rightarrow WW^*}$ vs. $\sigma_{ZH} \cdot \mathcal{B}_{H \rightarrow WW^*}$ for 68% and 95% confidence level (CL) compared with the prediction from the Standard Model.

dard deviations. The validity of the asymptotic approximation used in deriving these results was tested using pseudo-experiments. The combined signal strength for VH is measured to be

$$\mu_{VH} = 2.5^{+0.8}_{-0.7}(\text{stat.})^{+0.30}_{-0.23}(\text{exp syst.})^{+0.37}_{-0.26}(\text{theo syst.}) = 2.5^{+0.9}_{-0.8}$$

with an expected signal strength of $\mu_{VH} = 1.0^{+0.66}_{-0.54}(\text{stat.})^{+0.26}_{-0.17}(\text{exp syst.})^{+0.22}_{-0.17}(\text{theo syst.}) = 1.0^{+0.7}_{-0.6}$.

The cross-section times branching-fraction values, $\sigma_{WH} \cdot \mathcal{B}_{H \rightarrow WW^*}$ and $\sigma_{ZH} \cdot \mathcal{B}_{H \rightarrow WW^*}$, are simultaneously determined to be:

$$\sigma_{WH} \cdot \mathcal{B}_{H \rightarrow WW^*} = 0.67^{+0.31}_{-0.27}(\text{stat.})^{+0.14}_{-0.11}(\text{exp syst.})^{+0.11}_{-0.09}(\text{theo syst.}) \text{ pb},$$

$$\sigma_{ZH} \cdot \mathcal{B}_{H \rightarrow WW^*} = 0.54^{+0.31}_{-0.24}(\text{stat.})^{+0.10}_{-0.05}(\text{exp syst.})^{+0.11}_{-0.05}(\text{theo syst.}) \text{ pb}.$$

The main contributions to the uncertainties in $\sigma_{WH} \cdot \mathcal{B}_{H \rightarrow WW^*}$ and $\sigma_{ZH} \cdot \mathcal{B}_{H \rightarrow WW^*}$ are summarised in Table 6. The predicted cross-section times branching-fraction values are 0.293 ± 0.007 pb and 0.189 ± 0.007 pb for WH and ZH [72], respectively. The 68% and 95% confidence level two-dimensional contours of $\sigma_{WH} \cdot \mathcal{B}_{H \rightarrow WW^*}$ and $\sigma_{ZH} \cdot \mathcal{B}_{H \rightarrow WW^*}$ are shown in Fig. 8. The corresponding one-dimensional results, where the other parameter is left

Table 6

Breakdown of the main contributions to the total uncertainty in $\sigma_{WH} \cdot \mathcal{B}_{H \rightarrow WW^*}$ (left) and $\sigma_{ZH} \cdot \mathcal{B}_{H \rightarrow WW^*}$ (right). The individual sources of systematic uncertainties are grouped together. The sum in quadrature of the individual components differs from the total uncertainty due to correlations between the components. Systematic uncertainties that affect the shape of the fitted distribution are indicated by an asterisk.

Source	$\Delta\sigma_{WH} \cdot \mathcal{B}_{H \rightarrow WW^*}$ [%]	Source	$\Delta\sigma_{ZH} \cdot \mathcal{B}_{H \rightarrow WW^*}$ [%]
Data statistics in SR	43	Data statistics in SR	50
Data statistics in CR	6	Data statistics in CR	< 1
Theoretical uncertainties	16	Theoretical uncertainties	15
$WZ/W\gamma^{(*)}$	12	ZH signal	14
Top-quark(*)	8	Top-quark	1
WH signal(*)	4	$WZ/W\gamma^{(*)}$	< 1
ZZ^*	2	ZZ^*	< 1
Experimental uncertainties	12	Experimental uncertainties	7
Impact parameter mismodelling	8	Misidentified leptons	3
Misidentified leptons	8	b -tagging	1
b -tagging	1		
MC statistics	9	MC statistics	11
Luminosity	3	Luminosity	2
TOTAL	49	TOTAL	54

floating in the fit, are consistent with the SM predictions within 1.3σ for WH and 1.5σ for ZH .

9. Conclusion

Measurements of the inclusive production of a Higgs boson in association with a W or Z boson are presented. Results of the WH and ZH production cross section times branching fraction for $H \rightarrow WW^*$ are obtained selecting the leptonic decays $W \rightarrow \ell\nu$ and $Z \rightarrow \ell\ell$, with $\ell = e, \mu$, in $\sqrt{s} = 13$ TeV proton–proton collisions recorded with the ATLAS detector at the LHC in a data sample corresponding to an integrated luminosity of 36.1 fb^{-1} . The products of the $H \rightarrow WW^*$ branching fraction times the WH and ZH cross sections are measured to be $0.67^{+0.31}_{-0.27}(\text{stat.})^{+0.18}_{-0.14}(\text{syst.}) \text{ pb}$ and $0.54^{+0.31}_{-0.24}(\text{stat.})^{+0.15}_{-0.07}(\text{syst.}) \text{ pb}$, respectively, compatible with the Standard Model predictions of $0.293 \pm 0.007 \text{ pb}$ for WH and $0.189 \pm 0.007 \text{ pb}$ for ZH within up to 1.5σ . The WH channel with $H \rightarrow WW^*$ is purely sensitive to the HW coupling and this measurement is to date the most precise measurement of this channel.

Acknowledgements

We thank CERN for the very successful operation of the LHC, as well as the support staff from our institutions without whom ATLAS could not be operated efficiently.

We acknowledge the support of ANPCyT, Argentina; YerPhI, Armenia; ARC, Australia; BMWFW and FWF, Austria; ANAS, Azerbaijan; SSTC, Belarus; CNPq and FAPESP, Brazil; NSERC, NRC and CFI, Canada; CERN; CONICYT, Chile; CAS, MOST and NSFC, China; COLCIENCIAS, Colombia; MSMT CR, MPO CR and VSC CR, Czech Republic; DNRF and DNSRC, Denmark; IN2P3-CNRS, CEA-DRF/IRFU, France; SRNSFG, Georgia; BMBF, HGF, and MPG, Germany; GSRT, Greece; RGC, Hong Kong SAR, China; ISF and Benoziyo Center, Israel; INFN, Italy; MEXT and JSPS, Japan; CNRS, Morocco; NWO, Netherlands; RCN, Norway; MNiSW and NCN, Poland; FCT, Portugal; MNE/IFA, Romania; MES of Russia and NRC KI, Russian Federation; JINR; MESTD, Serbia; MSSR, Slovakia; ARRS and MIZŠ, Slovenia; DST/NRF, South Africa; MINECO, Spain; SRC and Wallenberg Foundation, Sweden; SERI, SNSF and Cantons of Bern and Geneva, Switzerland; MOST, Taiwan; TAEK, Turkey; STFC, United Kingdom; DOE and NSF, United States of America. In addition, individual groups and members have received support from BCKDF, Canarie, CRC and Compute Canada, Canada; COST, ERC, ERDF, Horizon 2020, and Marie Skłodowska-Curie Actions, European Union;

Investissements d’Avenir Labex and Idex, ANR, France; DFG and AvH Foundation, Germany; Herakleitos, Thales and Aristeia programmes co-financed by EU-ESF and the Greek NSRF, Greece; BSF-NSF and GIF, Israel; CERCA Programme Generalitat de Catalunya, Spain; The Royal Society and Leverhulme Trust, United Kingdom.

The crucial computing support from all WLCG partners is acknowledged gratefully, in particular from CERN, the ATLAS Tier-1 facilities at TRIUMF (Canada), NDGF (Denmark, Norway, Sweden), CC-IN2P3 (France), KIT/GridKA (Germany), INFN-CNAF (Italy), NL-T1 (Netherlands), PIC (Spain), ASGC (Taiwan), RAL (UK) and BNL (USA), the Tier-2 facilities worldwide and large non-WLCG resource providers. Major contributors of computing resources are listed in Ref. [73].

References

- [1] ATLAS Collaboration, Study of $(W/Z)H$ production and Higgs boson couplings using $H \rightarrow WW^*$ decays with the ATLAS detector, J. High Energy Phys. 08 (2015) 137, arXiv:1506.06641 [hep-ex].
- [2] CMS Collaboration, Measurement of Higgs boson production and properties in the WW decay channel with leptonic final states, J. High Energy Phys. 01 (2014) 096, arXiv:1312.1129 [hep-ex].
- [3] CMS Collaboration, Measurements of properties of the Higgs boson decaying to a W boson pair in pp collisions at $\sqrt{s} = 13$ TeV, Phys. Lett. B 791 (2019) 96, arXiv:1806.05246 [hep-ex].
- [4] ATLAS Collaboration, Measurements of Higgs boson properties in the diphoton decay channel with 36 fb^{-1} of pp collision data at $\sqrt{s} = 13$ TeV with the ATLAS detector, Phys. Rev. D 98 (2018) 052005, arXiv:1802.04146 [hep-ex].
- [5] ATLAS Collaboration, Measurement of the Higgs boson coupling properties in the $H \rightarrow ZZ^* \rightarrow 4\ell$ decay channel at $\sqrt{s} = 13$ TeV with the ATLAS detector, J. High Energy Phys. 03 (2018) 095, arXiv:1712.02304 [hep-ex].
- [6] ATLAS Collaboration, Observation of $H \rightarrow b\bar{b}$ decays and VH production with the ATLAS detector, Phys. Lett. B 786 (2018) 59, arXiv:1808.08238 [hep-ex].
- [7] ATLAS Collaboration, Search for the decay of the Higgs boson to charm quarks with the ATLAS experiment, Phys. Rev. Lett. 120 (2018) 211802, arXiv:1802.04329 [hep-ex].
- [8] CMS Collaboration, Observation of Higgs boson decay to bottom quarks, Phys. Rev. Lett. 121 (2018) 121801, arXiv:1808.08242 [hep-ex].
- [9] CMS Collaboration, Search for the associated production of the Higgs boson and a vector boson in proton–proton collisions at $\sqrt{s} = 13$ TeV via Higgs boson decays to τ leptons, J. High Energy Phys. (2018), arXiv:1809.03590 [hep-ex].
- [10] ATLAS Collaboration, The ATLAS experiment at the CERN large hadron collider, J. Instrum. 3 (2008) S08003.
- [11] ATLAS Collaboration, ATLAS Insertable B-Layer Technical Design Report, ATLAS-TDR-19, 2010, <https://cds.cern.ch/record/1291633>; ATLAS insertable B-layer technical design report addendum, ATLAS-TDR-19-ADD-1, <https://cds.cern.ch/record/1451888>, 2012.
- [12] B. Abbott, et al., Production and integration of the ATLAS insertable B-layer, J. Instrum. 13 (2018) T05008, arXiv:1803.00844 [physics.ins-det].

- [13] ATLAS Collaboration, Performance of the ATLAS trigger system in 2015, *Eur. Phys. J. C* 77 (2017) 317, arXiv:1611.09661 [hep-ex].
- [14] ATLAS, CMS Collaborations, Combined measurement of the Higgs boson mass in pp collisions at $\sqrt{s} = 7$ and 8 TeV with the ATLAS and CMS experiments, *Phys. Rev. Lett.* 114 (2015) 191803, arXiv:1503.07589 [hep-ex].
- [15] ATLAS Collaboration, Measurement of the Higgs boson mass in the $H \rightarrow ZZ^* \rightarrow 4\ell$ and $H \rightarrow \gamma\gamma$ channels with $\sqrt{s} = 13$ TeV pp collisions using the ATLAS detector, *Phys. Lett. B* 784 (2018) 345, arXiv:1806.00242 [hep-ex].
- [16] T. Han, S. Willenbrock, QCD correction to the $pp \rightarrow WH$ and ZH total cross sections, *Phys. Lett. B* 273 (1991) 167.
- [17] O. Brein, A. Djouadi, R. Harlander, NNLO QCD corrections to the Higgs-strahlung processes at hadron colliders, *Phys. Lett. B* 579 (2004) 149, arXiv:hep-ph/0307206.
- [18] M.L. Ciccolini, S. Dittmaier, M. Krämer, Electroweak radiative corrections to associated WH and ZH production at hadron colliders, *Phys. Rev. D* 68 (2003) 073003, arXiv:hep-ph/0306234.
- [19] L. Altenkamp, S. Dittmaier, R.V. Harlander, H. Rzehak, T.J.E. Zirke, Gluon-induced Higgs-strahlung at next-to-leading order QCD, *J. High Energy Phys.* 02 (2013) 078, arXiv:1211.5015 [hep-ph].
- [20] C. Anastasiou, et al., High precision determination of the gluon fusion Higgs boson cross-section at the LHC, *J. High Energy Phys.* 05 (2016) 058, arXiv:1602.00695 [hep-ph].
- [21] M. Ciccolini, A. Denner, S. Dittmaier, Strong and electroweak corrections to the production of a Higgs boson + 2 jets via weak interactions at the large hadron collider, *Phys. Rev. Lett.* 99 (2007) 161803, arXiv:0707.0381 [hep-ph].
- [22] M. Czakon, P. Fiedler, A. Mitov, Total top-quark pair-production cross section at hadron colliders through $O(\alpha_s^4)$, *Phys. Rev. Lett.* 110 (2013) 252004, arXiv:1303.6254 [hep-ph].
- [23] E. Re, Single-top Wt -channel production matched with parton showers using the POWHEG method, *Eur. Phys. J. C* 71 (2011) 1547, arXiv:1009.2450 [hep-ph].
- [24] S. Frixione, V. Hirschi, D. Pagani, H.-S. Shao, M. Zaro, Electroweak and QCD corrections to top-pair hadroproduction in association with heavy bosons, *J. High Energy Phys.* 06 (2015) 184, arXiv:1504.03446 [hep-ph].
- [25] J. Alwall, et al., The automated computation of tree-level and next-to-leading order differential cross sections, and their matching to parton shower simulations, *J. High Energy Phys.* 07 (2014) 079, arXiv:1405.0301 [hep-ph].
- [26] J. Campbell, R.K. Ellis, R. Röntsch, Single top production in association with a Z boson at the LHC, *Phys. Rev. D* 87 (2013) 114006, arXiv:1302.3856 [hep-ph].
- [27] F. Cascioli, et al., Precise Higgs-background predictions: merging NLO QCD and squared quark-loop corrections to four-lepton + 0,1 jet production, *J. High Energy Phys.* 01 (2014) 046, arXiv:1309.0500 [hep-ph].
- [28] F. Caola, M. Dowling, K. Melnikov, R. Röntsch, L. Tancredi, QCD corrections to vector boson pair production in gluon fusion including interference effects with off-shell Higgs at the LHC, *J. High Energy Phys.* 07 (2016) 087, arXiv:1605.04610 [hep-ph].
- [29] T. Binoth, G. Ossola, C.G. Papadopoulos, R. Pittau, NLO QCD corrections to tri-boson production, *J. High Energy Phys.* 06 (2008) 082, arXiv:0804.0350 [hep-ph].
- [30] G. Luisoni, P. Nason, C. Oleari, F. Tramontano, $HW^\pm/HZ + 0$ and 1 jet at NLO with the POWHEG BOX interfaced to GoSam and their merging within MiNLO, *J. High Energy Phys.* 10 (2013) 083, arXiv:1306.2542 [hep-ph].
- [31] T. Sjöstrand, S. Mrenna, P.Z. Skands, A brief introduction to PYTHIA 8.1, *Comput. Phys. Commun.* 178 (2008) 852, arXiv:0710.3820 [hep-ph].
- [32] ATLAS Collaboration, Measurement of the Z/γ^* boson transverse momentum distribution in pp collisions at $\sqrt{s} = 7$ TeV with the ATLAS detector, *J. High Energy Phys.* 09 (2014) 145, arXiv:1406.3660 [hep-ex].
- [33] J. Butterworth, et al., PDF4LHC recommendations for LHC Run II, *J. Phys. G* 43 (2016) 023001, arXiv:1510.03865 [hep-ph].
- [34] J. Pumplin, et al., New generation of parton distributions with uncertainties from global QCD analysis, *J. High Energy Phys.* 07 (2002) 012, arXiv:hep-ph/0201195.
- [35] J. Bellm, et al., Herwig 7.0/Herwig++ 3.0 release note, *Eur. Phys. J. C* 76 (2016) 196, arXiv:1512.01178 [hep-ph].
- [36] L.A. Harland-Lang, A.D. Martin, P. Motylinski, R.S. Thorne, Parton distributions in the LHC era: MMHT 2014 PDFs, *Eur. Phys. J. C* 75 (2015) 204, arXiv:1412.3989 [hep-ph].
- [37] K. Hamilton, P. Nason, E. Re, G. Zanderighi, NNLOPS simulation of Higgs boson production, *J. High Energy Phys.* 10 (2013) 222, arXiv:1309.0017 [hep-ph].
- [38] S. Frixione, P. Nason, G. Ridolfi, A positive-weight next-to-leading-order Monte Carlo for heavy flavour hadroproduction, *J. High Energy Phys.* 09 (2007) 126, arXiv:0707.3088 [hep-ph].
- [39] R.D. Ball, et al., Parton distributions for the LHC Run II, *J. High Energy Phys.* 04 (2015) 040, arXiv:1410.8849 [hep-ph].
- [40] R.D. Ball, et al., Parton distributions with LHC data, *Nucl. Phys. B* 867 (2013) 244, arXiv:1207.1303 [hep-ph].
- [41] ATLAS Collaboration, ATLAS Pythia 8 tunes to 7 TeV data, ATL-PHYS-PUB-2014-021, <https://cds.cern.ch/record/1966419>, 2014.
- [42] T. Gleisberg, et al., Event generation with SHERPA 1.1, *J. High Energy Phys.* 02 (2009) 007, arXiv:0811.4622 [hep-ph].
- [43] T. Sjöstrand, S. Mrenna, P.Z. Skands, PYTHIA 6.4 physics and manual, *J. High Energy Phys.* 05 (2006) 026, arXiv:hep-ph/0603175.
- [44] P.Z. Skands, Tuning Monte Carlo generators: the Perugia tunes, *Phys. Rev. D* 82 (2010) 074018, arXiv:1005.3457 [hep-ph].
- [45] D.J. Lange, The EvtGen particle decay simulation package, *Nucl. Instrum. Methods A* 462 (2001) 152.
- [46] ATLAS Collaboration, Multi-boson simulation for 13 TeV ATLAS analyses, ATL-PHYS-PUB-2016-002, <https://cds.cern.ch/record/2119986>, 2016.
- [47] H.-L. Lai, et al., New parton distributions for collider physics, *Phys. Rev. D* 82 (2010) 074024, arXiv:1007.2241 [hep-ph].
- [48] P. Nason, G. Zanderighi, W^+W^- , WZ and ZZ production in the POWHEG-BOX-V2, *Eur. Phys. J. C* 74 (2014) 2702, arXiv:1311.1365 [hep-ph].
- [49] ATLAS Collaboration, Summary of ATLAS Pythia 8 tunes, ATL-PHYS-PUB-2012-003, <https://cds.cern.ch/record/1474107>, 2012.
- [50] A.D. Martin, W.J. Stirling, R.S. Thorne, G. Watt, Parton distributions for the LHC, *Eur. Phys. J. C* 63 (2009) 189, arXiv:0901.0002 [hep-ph].
- [51] S. Agostinelli, et al., GEANT4: a simulation toolkit, *Nucl. Instrum. Methods A* 506 (2003) 250.
- [52] ATLAS Collaboration, The ATLAS simulation infrastructure, *Eur. Phys. J. C* 70 (2010) 823, arXiv:1005.4568 [physics.ins-det].
- [53] ATLAS Collaboration, Reconstruction of primary vertices at the ATLAS experiment in Run 1 proton–proton collisions at the LHC, *Eur. Phys. J. C* 77 (2017) 332, arXiv:1611.10235 [physics.ins-det].
- [54] ATLAS Collaboration, Electron reconstruction and identification in the ATLAS experiment using the 2015 and 2016 LHC proton–proton collision data at $\sqrt{s} = 13$ TeV, *Eur. Phys. J. C* (2019), arXiv:1902.04655 [hep-ex].
- [55] ATLAS Collaboration, Muon reconstruction performance of the ATLAS detector in proton–proton collision data at $\sqrt{s} = 13$ TeV, *Eur. Phys. J. C* 76 (2016) 292, arXiv:1603.05598 [hep-ex].
- [56] M. Cacciari, G.P. Salam, G. Soyez, The anti- k_t jet clustering algorithm, *J. High Energy Phys.* 04 (2008) 063, arXiv:0802.1189 [hep-ph].
- [57] M. Cacciari, G.P. Salam, G. Soyez, FastJet user manual, *Eur. Phys. J. C* 72 (2012) 1896, arXiv:1111.6097 [hep-ph].
- [58] ATLAS Collaboration, Jet energy scale measurements and their systematic uncertainties in proton–proton collisions at $\sqrt{s} = 13$ TeV with the ATLAS detector, *Phys. Rev. D* 96 (2017) 072002, arXiv:1703.09665 [hep-ex].
- [59] ATLAS Collaboration, Performance of pile-up mitigation techniques for jets in pp collisions at $\sqrt{s} = 8$ TeV using the ATLAS detector, *Eur. Phys. J. C* 76 (2016) 581, arXiv:1510.03823 [hep-ex].
- [60] ATLAS Collaboration, Identification and rejection of pile-up jets at high pseudorapidity with the ATLAS detector, *Eur. Phys. J. C* 77 (2017) 580, arXiv:1705.02211 [hep-ex], Erratum: *Eur. Phys. J. C* 77 (2017) 712.
- [61] ATLAS Collaboration, Measurements of b -jet tagging efficiency with the ATLAS detector using $t\bar{t}$ events at $\sqrt{s} = 13$ TeV, *J. High Energy Phys.* 08 (2018) 089, arXiv:1805.01845 [hep-ex].
- [62] ATLAS Collaboration, Performance of missing transverse momentum reconstruction with the ATLAS detector using proton–proton collisions at $\sqrt{s} = 13$ TeV, *Eur. Phys. J. C* 78 (2018) 903, arXiv:1802.08168 [hep-ex].
- [63] A. Hoecker, et al., TMVA - toolkit for multivariate data analysis, arXiv:physics/0703039 [physics.data-an], 2008.
- [64] F. Pedregosa, et al., Scikit-learn: machine learning in Python, *J. Mach. Learn. Res.* 12 (2011) 2825, arXiv:1201.0490 [cs.LG].
- [65] T. Plehn, D.L. Rainwater, D. Zeppenfeld, Method for identifying $H \rightarrow \tau^+\tau^- \rightarrow e^\pm \mu^\mp p_T$ at the CERN LHC, *Phys. Rev. D* 61 (2000) 093005, arXiv:hep-ph/9911385.
- [66] ATLAS Collaboration, Measurement of inclusive and differential cross sections in the $H \rightarrow ZZ^* \rightarrow 4\ell$ decay channel in pp collisions at $\sqrt{s} = 13$ TeV with the ATLAS detector, *J. High Energy Phys.* 10 (2017) 132, arXiv:1708.02810 [hep-ex].
- [67] ATLAS Collaboration, Observation and measurement of Higgs boson decays to WW^* with the ATLAS detector, *Phys. Rev. D* 92 (2015) 012006, arXiv:1412.2641 [hep-ex].
- [68] ATLAS Collaboration, Luminosity determination in pp collisions at $\sqrt{s} = 8$ TeV using the ATLAS detector at the LHC, *Eur. Phys. J. C* 76 (2016) 653, arXiv:1608.03953 [hep-ex].
- [69] G. Avoni, et al., The new LUCID-2 detector for luminosity measurement and monitoring in ATLAS, *J. Instrum.* 13 (2018) P07017.
- [70] ATLAS Collaboration, Electron and photon energy calibration with the ATLAS detector using 2015–2016 LHC proton–proton collision data, *J. Instrum.* 14 (2019) P03017, arXiv:1812.03848 [hep-ex].
- [71] G. Cowan, K. Cranmer, E. Gross, O. Vitells, Asymptotic formulae for likelihood-based tests of new physics, *Eur. Phys. J. C* 71 (2011) 1554, arXiv:1007.1727 [physics.data-an], Erratum: *Eur. Phys. J. C* 73 (2013) 2501.
- [72] LHC Higgs Cross Section Working Group, Handbook of LHC Higgs cross sections: 4. Deciphering the nature of the Higgs sector, arXiv:1610.07922 [hep-ph], 2016.
- [73] ATLAS Collaboration, ATLAS computing acknowledgements, ATL-GEN-PUB-2016-002, <https://cds.cern.ch/record/2202407>.

The ATLAS Collaboration

G. Aad ¹⁰¹, B. Abbott ¹²⁸, D.C. Abbott ¹⁰², O. Abidinov ^{13,*}, A. Abed Abud ^{70a,70b}, K. Abeling ⁵³, D.K. Abhayasinghe ⁹³, S.H. Abidi ¹⁶⁷, O.S. AbouZeid ⁴⁰, N.L. Abraham ¹⁵⁶, H. Abramowicz ¹⁶¹, H. Abreu ¹⁶⁰, Y. Abulaiti ⁶, B.S. Acharya ^{66a,66b,n}, B. Achkar ⁵³, S. Adachi ¹⁶³, L. Adam ⁹⁹, C. Adam Bourdarios ¹³², L. Adamczyk ^{83a}, L. Adamek ¹⁶⁷, J. Adelman ¹²¹, M. Adersberger ¹¹⁴, A. Adiguzel ^{12c,ah}, S. Adorni ⁵⁴, T. Adye ¹⁴⁴, A.A. Affolder ¹⁴⁶, Y. Afik ¹⁶⁰, C. Agapopoulou ¹³², M.N. Agaras ³⁸, A. Aggarwal ¹¹⁹, C. Agheorghiesei ^{27c}, J.A. Aguilar-Saavedra ^{140f,140a,ag}, F. Ahmadov ⁷⁹, X. Ai ^{15a}, G. Aielli ^{73a,73b}, S. Akatsuka ⁸⁵, T.P.A. Åkesson ⁹⁶, E. Akilli ⁵⁴, A.V. Akimov ¹¹⁰, K. Al Khoury ¹³², G.L. Alberghi ^{23b,23a}, J. Albert ¹⁷⁶, M.J. Alconada Verzini ⁸⁸, S. Alderweireldt ¹¹⁹, M. Aleksa ³⁶, I.N. Aleksandrov ⁷⁹, C. Alexa ^{27b}, D. Alexandre ¹⁹, T. Alexopoulos ¹⁰, A. Alfonsi ¹²⁰, M. Alhroob ¹²⁸, B. Ali ¹⁴², G. Alimonti ^{68a}, J. Alison ³⁷, S.P. Alkire ¹⁴⁸, C. Allaire ¹³², B.M.M. Allbrooke ¹⁵⁶, B.W. Allen ¹³¹, P.P. Allport ²¹, A. Aloisio ^{69a,69b}, A. Alonso ⁴⁰, F. Alonso ⁸⁸, C. Alpigiani ¹⁴⁸, A.A. Alshehri ⁵⁷, M. Alvarez Estevez ⁹⁸, B. Alvarez Gonzalez ³⁶, D. Álvarez Piqueras ¹⁷⁴, M.G. Alviggi ^{69a,69b}, Y. Amaral Coutinho ^{80b}, A. Ambler ¹⁰³, L. Ambroz ¹³⁵, C. Amelung ²⁶, D. Amidei ¹⁰⁵, S.P. Amor Dos Santos ^{140a}, S. Amoroso ⁴⁶, C.S. Amrouche ⁵⁴, F. An ⁷⁸, C. Anastopoulos ¹⁴⁹, N. Andari ¹⁴⁵, T. Andeen ¹¹, C.F. Anders ^{61b}, J.K. Anders ²⁰, A. Andreazza ^{68a,68b}, V. Andrei ^{61a}, C.R. Anelli ¹⁷⁶, S. Angelidakis ³⁸, A. Angerami ³⁹, A.V. Anisenkov ^{122b,122a}, A. Annovi ^{71a}, C. Antel ^{61a}, M.T. Anthony ¹⁴⁹, M. Antonelli ⁵¹, D.J.A. Antrim ¹⁷¹, F. Anulli ^{72a}, M. Aoki ⁸¹, J.A. Aparisi Pozo ¹⁷⁴, L. Aperio Bella ³⁶, G. Arabidze ¹⁰⁶, J.P. Araque ^{140a}, V. Araujo Ferraz ^{80b}, R. Araujo Pereira ^{80b}, C. Arcangeletti ⁵¹, A.T.H. Arce ⁴⁹, F.A. Arduh ⁸⁸, J.-F. Arguin ¹⁰⁹, S. Argyropoulos ⁷⁷, J.-H. Arling ⁴⁶, A.J. Armbruster ³⁶, L.J. Armitage ⁹², A. Armstrong ¹⁷¹, O. Arnaez ¹⁶⁷, H. Arnold ¹²⁰, A. Artamonov ^{111,*}, G. Artoni ¹³⁵, S. Artz ⁹⁹, S. Asai ¹⁶³, N. Asbah ⁵⁹, E.M. Asimakopoulou ¹⁷², L. Asquith ¹⁵⁶, K. Assamagan ²⁹, R. Astalos ^{28a}, R.J. Atkin ^{33a}, M. Atkinson ¹⁷³, N.B. Atlay ¹⁵¹, H. Atmani ¹³², K. Augsten ¹⁴², G. Avolio ³⁶, R. Avramidou ^{60a}, M.K. Ayoub ^{15a}, A.M. Azoulay ^{168b}, G. Azuelos ^{109,aw}, M.J. Baca ²¹, H. Bachacou ¹⁴⁵, K. Bachas ^{67a,67b}, M. Backes ¹³⁵, F. Backman ^{45a,45b}, P. Bagnaia ^{72a,72b}, M. Bahmani ⁸⁴, H. Bahrasemani ¹⁵², A.J. Bailey ¹⁷⁴, V.R. Bailey ¹⁷³, J.T. Baines ¹⁴⁴, M. Bajic ⁴⁰, C. Bakalis ¹⁰, O.K. Baker ¹⁸³, P.J. Bakker ¹²⁰, D. Bakshi Gupta ⁸, S. Balaji ¹⁵⁷, E.M. Baldin ^{122b,122a}, P. Balek ¹⁸⁰, F. Balli ¹⁴⁵, W.K. Balunas ¹³⁵, J. Balz ⁹⁹, E. Banas ⁸⁴, A. Bandyopadhyay ²⁴, Sw. Banerjee ^{181,i}, A.A.E. Bannoura ¹⁸², L. Barak ¹⁶¹, W.M. Barbe ³⁸, E.L. Barberio ¹⁰⁴, D. Barberis ^{55b,55a}, M. Barbero ¹⁰¹, T. Barillari ¹¹⁵, M.-S. Barisits ³⁶, J. Barkeloo ¹³¹, T. Barklow ¹⁵³, R. Barnea ¹⁶⁰, S.L. Barnes ^{60c}, B.M. Barnett ¹⁴⁴, R.M. Barnett ¹⁸, Z. Barnovska-Blenessy ^{60a}, A. Baroncelli ^{60a}, G. Barone ²⁹, A.J. Barr ¹³⁵, L. Barranco Navarro ¹⁷⁴, F. Barreiro ⁹⁸, J. Barreiro Guimarães da Costa ^{15a}, S. Barsov ¹³⁸, R. Bartoldus ¹⁵³, G. Bartolini ¹⁰¹, A.E. Barton ⁸⁹, P. Bartos ^{28a}, A. Basalaev ⁴⁶, A. Bassalat ^{132,ap}, R.L. Bates ⁵⁷, S.J. Batista ¹⁶⁷, S. Batlamous ^{35e}, J.R. Batley ³², B. Batool ¹⁵¹, M. Battaglia ¹⁴⁶, M. Bause ^{72a,72b}, F. Bauer ¹⁴⁵, K.T. Bauer ¹⁷¹, H.S. Bawa ^{31,l}, J.B. Beacham ⁴⁹, T. Beau ¹³⁶, P.H. Beauchemin ¹⁷⁰, F. Becherer ⁵², P. Bechtel ²⁴, H.C. Beck ⁵³, H.P. Beck ^{20,q}, K. Becker ⁵², M. Becker ⁹⁹, C. Becot ⁴⁶, A. Beddall ^{12d}, A.J. Beddall ^{12a}, V.A. Bednyakov ⁷⁹, M. Bedognetti ¹²⁰, C.P. Bee ¹⁵⁵, T.A. Beermann ⁷⁶, M. Begalli ^{80b}, M. Begel ²⁹, A. Behera ¹⁵⁵, J.K. Behr ⁴⁶, F. Beisiegel ²⁴, A.S. Bell ⁹⁴, G. Bella ¹⁶¹, L. Bellagamba ^{23b}, A. Bellerive ³⁴, P. Bellos ⁹, K. Beloborodov ^{122b,122a}, K. Belotskiy ¹¹², N.L. Belyaev ¹¹², D. Benchekroun ^{35a}, N. Benekos ¹⁰, Y. Benhammou ¹⁶¹, D.P. Benjamin ⁶, M. Benoit ⁵⁴, J.R. Bensinger ²⁶, S. Bentvelsen ¹²⁰, L. Beresford ¹³⁵, M. Beretta ⁵¹, D. Berge ⁴⁶, E. Bergeas Kuutmann ¹⁷², N. Berger ⁵, B. Bergmann ¹⁴², L.J. Bergsten ²⁶, J. Beringer ¹⁸, S. Berlendis ⁷, N.R. Bernard ¹⁰², G. Bernardi ¹³⁶, C. Bernius ¹⁵³, F.U. Bernlochner ²⁴, T. Berry ⁹³, P. Berta ⁹⁹, C. Bertella ^{15a}, I.A. Bertram ⁸⁹, G.J. Besjes ⁴⁰, O. Bessidskaia Bylund ¹⁸², N. Besson ¹⁴⁵, A. Bethani ¹⁰⁰, S. Bethke ¹¹⁵, A. Betti ²⁴, A.J. Bevan ⁹², J. Beyer ¹¹⁵, R. Bi ¹³⁹, R.M. Bianchi ¹³⁹, O. Biebel ¹¹⁴, D. Biedermann ¹⁹, R. Bielski ³⁶, K. Bierwagen ⁹⁹, N.V. Biesuz ^{71a,71b}, M. Biglietti ^{74a}, T.R.V. Billoud ¹⁰⁹, M. Bindi ⁵³, A. Bingul ^{12d}, C. Bini ^{72a,72b}, S. Biondi ^{23b,23a}, M. Birman ¹⁸⁰, T. Bisanz ⁵³, J.P. Biswal ¹⁶¹, A. Bitadze ¹⁰⁰, C. Bittrich ⁴⁸, K. Bjørke ¹³⁴, K.M. Black ²⁵, T. Blazek ^{28a}, I. Bloch ⁴⁶, C. Blocker ²⁶, A. Blue ⁵⁷, U. Blumenschein ⁹², G.J. Bobbink ¹²⁰, V.S. Bobrovnikov ^{122b,122a}, S.S. Bocchetta ⁹⁶, A. Bocci ⁴⁹, D. Boerner ⁴⁶, D. Bogavac ¹⁴, A.G. Bogdanchikov ^{122b,122a}, C. Böhm ^{45a}, V. Boisvert ⁹³, P. Bokan ^{53,172}, T. Bold ^{83a}, A.S. Boldyrev ¹¹³, A.E. Bolz ^{61b}, M. Bomben ¹³⁶, M. Bona ⁹², J.S. Bonilla ¹³¹, M. Boonekamp ¹⁴⁵, H.M. Borecka-Bielska ⁹⁰, A. Borisov ¹²³, G. Borissov ⁸⁹, J. Bortfeldt ³⁶, D. Bortoletto ¹³⁵, V. Bortolotto ^{73a,73b}, D. Boscherini ^{23b}, M. Bosman ¹⁴, J.D. Bossio Sola ¹⁰³, K. Bouaouda ^{35a}, J. Boudreau ¹³⁹, E.V. Bouhova-Thacker ⁸⁹, D. Boumediene ³⁸, S.K. Boutle ⁵⁷, A. Boveia ¹²⁶, J. Boyd ³⁶, D. Boye ^{33b,aq},

I.R. Boyko⁷⁹, A.J. Bozson⁹³, J. Bracinik²¹, N. Brahimi¹⁰¹, G. Brandt¹⁸², O. Brandt^{61a}, F. Braren⁴⁶, U. Bratzler¹⁶⁴, B. Brau¹⁰², J.E. Brau¹³¹, W.D. Breaden Madden⁵⁷, K. Brendlinger⁴⁶, L. Brenner⁴⁶, R. Brenner¹⁷², S. Bressler¹⁸⁰, B. Brickwedde⁹⁹, D.L. Briglin²¹, D. Britton⁵⁷, D. Britzger¹¹⁵, I. Brock²⁴, R. Brock¹⁰⁶, G. Brooijmans³⁹, W.K. Brooks^{147b}, E. Brost¹²¹, J.H. Broughton²¹, P.A. Bruckman de Renstrom⁸⁴, D. Bruncko^{28b}, A. Bruni^{23b}, G. Bruni^{23b}, L.S. Bruni¹²⁰, S. Bruno^{73a,73b}, B.H. Brunt³², M. Bruschi^{23b}, N. Bruscino¹³⁹, P. Bryant³⁷, L. Bryngemark⁹⁶, T. Buanes¹⁷, Q. Buat³⁶, P. Buchholz¹⁵¹, A.G. Buckley⁵⁷, I.A. Budagov⁷⁹, M.K. Bugge¹³⁴, F. Bühner⁵², O. Bulekov¹¹², T.J. Burch¹²¹, S. Burdin⁹⁰, C.D. Burgard¹²⁰, A.M. Burger¹²⁹, B. Burghgrave⁸, K. Burka⁸⁴, J.T.P. Burr⁴⁶, V. Büscher⁹⁹, E. Buschmann⁵³, P.J. Bussey⁵⁷, J.M. Butler²⁵, C.M. Buttar⁵⁷, J.M. Butterworth⁹⁴, P. Butti³⁶, W. Buttinger³⁶, A. Buzatu¹⁵⁸, A.R. Buzykaev^{122b,122a}, G. Cabras^{23b,23a}, S. Cabrera Urbán¹⁷⁴, D. Caforio⁵⁶, H. Cai¹⁷³, V.M.M. Cairo¹⁵³, O. Cakir^{4a}, N. Calace³⁶, P. Calafiura¹⁸, A. Calandri¹⁰¹, G. Calderini¹³⁶, P. Calfayan⁶⁵, G. Callea⁵⁷, L.P. Caloba^{80b}, S. Calvente Lopez⁹⁸, D. Calvet³⁸, S. Calvet³⁸, T.P. Calvet¹⁵⁵, M. Calvetti^{71a,71b}, R. Camacho Toro¹³⁶, S. Camarda³⁶, D. Camarero Munoz⁹⁸, P. Camarri^{73a,73b}, D. Cameron¹³⁴, R. Caminal Armadans¹⁰², C. Camincher³⁶, S. Campana³⁶, M. Campanelli⁹⁴, A. Camplani⁴⁰, A. Campoverde¹⁵¹, V. Canale^{69a,69b}, A. Canesse¹⁰³, M. Cano Bret^{60c}, J. Cantero¹²⁹, T. Cao¹⁶¹, Y. Cao¹⁷³, M.D.M. Capeans Garrido³⁶, M. Capua^{41b,41a}, R. Cardarelli^{73a}, F.C. Cardillo¹⁴⁹, I. Carli¹⁴³, T. Carli³⁶, G. Carlino^{69a}, B.T. Carlson¹³⁹, L. Carminati^{68a,68b}, R.M.D. Carney^{45a,45b}, S. Caron¹¹⁹, E. Carquin^{147b}, S. Carrá^{68a,68b}, J.W.S. Carter¹⁶⁷, M.P. Casado^{14,e}, A.F. Casha¹⁶⁷, D.W. Casper¹⁷¹, R. Castelijin¹²⁰, F.L. Castillo¹⁷⁴, V. Castillo Gimenez¹⁷⁴, N.F. Castro^{140a,140e}, A. Catinaccio³⁶, J.R. Catmore¹³⁴, A. Cattai³⁶, J. Caudron²⁴, V. Cavaliere²⁹, E. Cavallaro¹⁴, D. Cavalli^{68a}, M. Cavalli-Sforza¹⁴, V. Cavasinni^{71a,71b}, E. Celebi^{12b}, F. Ceradini^{74a,74b}, L. Cerda Alberich¹⁷⁴, A.S. Cerqueira^{80a}, A. Cerri¹⁵⁶, L. Cerrito^{73a,73b}, F. Cerutti¹⁸, A. Cervelli^{23b,23a}, S.A. Cetin^{12b}, D. Chakraborty¹²¹, S.K. Chan⁵⁹, W.S. Chan¹²⁰, W.Y. Chan⁹⁰, J.D. Chapman³², B. Chargeishvili^{159b}, D.G. Charlton²¹, T.P. Charman⁹², C.C. Chau³⁴, S. Che¹²⁶, A. Chegwidan¹⁰⁶, S. Chekanov⁶, S.V. Chekulaev^{168a}, G.A. Chelkov^{79,av}, M.A. Chelstowska³⁶, B. Chen⁷⁸, C. Chen^{60a}, C.H. Chen⁷⁸, H. Chen²⁹, J. Chen^{60a}, J. Chen³⁹, S. Chen¹³⁷, S.J. Chen^{15c}, X. Chen^{15b,au}, Y. Chen⁸², Y.-H. Chen⁴⁶, H.C. Cheng^{63a}, H.J. Cheng^{15a,15d}, A. Cheplakov⁷⁹, E. Cheremushkina¹²³, R. Cherkaoui El Moursli^{35e}, E. Cheu⁷, K. Cheung⁶⁴, T.J.A. Chevaléris¹⁴⁵, L. Chevalier¹⁴⁵, V. Chiarella⁵¹, G. Chiarelli^{71a}, G. Chiodini^{67a}, A.S. Chisholm^{36,21}, A. Chitan^{27b}, I. Chiu¹⁶³, Y.H. Chiu¹⁷⁶, M.V. Chizhov⁷⁹, K. Choi⁶⁵, A.R. Chomont^{72a,72b}, S. Chouridou¹⁶², Y.S. Chow¹²⁰, M.C. Chu^{63a}, J. Chudoba¹⁴¹, A.J. Chuinard¹⁰³, J.J. Chwastowski⁸⁴, L. Chytka¹³⁰, K.M. Ciesla⁸⁴, D. Cinca⁴⁷, V. Cindro⁹¹, I.A. Cioară^{27b}, A. Ciochio¹⁸, F. Ciotto^{69a,69b}, Z.H. Citron¹⁸⁰, M. Citterio^{68a}, D.A. Ciubotaru^{27b}, B.M. Ciungu¹⁶⁷, A. Clark⁵⁴, M.R. Clark³⁹, P.J. Clark⁵⁰, C. Clement^{45a,45b}, Y. Coadou¹⁰¹, M. Cokal^{66a,66c}, A. Coccaro^{55b}, J. Cochran⁷⁸, H. Cohen¹⁶¹, A.E.C. Coimbra³⁶, L. Colasurdo¹¹⁹, B. Cole³⁹, A.P. Colijn¹²⁰, J. Collot⁵⁸, P. Conde Muño^{140a,f}, E. Coniavitis⁵², S.H. Connell^{33b}, I.A. Connelly⁵⁷, S. Constantinescu^{27b}, F. Conventi^{69a,ax}, A.M. Cooper-Sarkar¹³⁵, F. Cormier¹⁷⁵, K.J.R. Cormier¹⁶⁷, L.D. Corpe⁹⁴, M. Corradi^{72a,72b}, E.E. Corrigan⁹⁶, F. Corriveau^{103,ac}, A. Cortes-Gonzalez³⁶, M.J. Costa¹⁷⁴, F. Costanza⁵, D. Costanzo¹⁴⁹, G. Cowan⁹³, J.W. Cowley³², J. Crane¹⁰⁰, K. Cranmer¹²⁴, S.J. Crawley⁵⁷, R.A. Creager¹³⁷, S. Crépe-Renaudin⁵⁸, F. Crescioli¹³⁶, M. Cristinziani²⁴, V. Croft¹²⁰, G. Crosetti^{41b,41a}, A. Cueto⁵, T. Cuhadar Donszelmann¹⁴⁹, A.R. Cukierman¹⁵³, S. Czekierda⁸⁴, P. Czodrowski³⁶, M.J. Da Cunha Sargedas De Sousa^{60b}, J.V. Da Fonseca Pinto^{80b}, C. Da Via¹⁰⁰, W. Dabrowski^{83a}, T. Dado^{28a}, S. Dahbi^{35e}, T. Dai¹⁰⁵, C. Dallapiccola¹⁰², M. Dam⁴⁰, G. D'amen^{23b,23a}, V. D'Amico^{74a,74b}, J. Damp⁹⁹, J.R. Dandoy¹³⁷, M.F. Daneri³⁰, N.P. Dang¹⁸¹, N.D. Dann¹⁰⁰, M. Danninger¹⁷⁵, V. Dao³⁶, G. Darbo^{55b}, O. Dartsis⁵, A. Dattagupta¹³¹, T. Daubney⁴⁶, S. D'Auria^{68a,68b}, W. Davey²⁴, C. David⁴⁶, T. Davidek¹⁴³, D.R. Davis⁴⁹, E. Dawe¹⁰⁴, I. Dawson¹⁴⁹, K. De⁸, R. De Asmundis^{69a}, M. De Beurs¹²⁰, S. De Castro^{23b,23a}, S. De Cecco^{72a,72b}, N. De Groot¹¹⁹, P. de Jong¹²⁰, H. De la Torre¹⁰⁶, A. De Maria^{15c}, D. De Pedis^{72a}, A. De Salvo^{72a}, U. De Sanctis^{73a,73b}, M. De Santis^{73a,73b}, A. De Santo¹⁵⁶, K. De Vasconcelos Corga¹⁰¹, J.B. De Vivie De Regie¹³², C. Debenedetti¹⁴⁶, D.V. Dedovich⁷⁹, A.M. Deiana⁴², M. Del Gaudio^{41b,41a}, J. Del Peso⁹⁸, Y. Delabat Diaz⁴⁶, D. Delgove¹³², F. Deliot¹⁴⁵, C.M. Delitzsch⁷, M. Della Pietra^{69a,69b}, D. Della Volpe⁵⁴, A. Dell'Acqua³⁶, L. Dell'Asta^{73a,73b}, M. Delmastro⁵, C. Delporte¹³², P.A. Delsart⁵⁸, D.A. DeMarco¹⁶⁷, S. Demers¹⁸³, M. Demichev⁷⁹, G. Demontigny¹⁰⁹, S.P. Denisov¹²³, D. Denysiuk¹²⁰, L. D'Eramo¹³⁶, D. Derendarz⁸⁴, J.E. Derkaoui^{35d},

F. Derue¹³⁶, P. Dervan⁹⁰, K. Desch²⁴, C. Deterre⁴⁶, K. Dette¹⁶⁷, C. Deutsch²⁴, M.R. Devesa³⁰, P.O. Deviveiros³⁶, A. Dewhurst¹⁴⁴, S. Dhaliwal²⁶, F.A. Di Bello⁵⁴, A. Di Ciaccio^{73a,73b}, L. Di Ciaccio⁵, W.K. Di Clemente¹³⁷, C. Di Donato^{69a,69b}, A. Di Girolamo³⁶, G. Di Gregorio^{71a,71b}, B. Di Micco^{74a,74b}, R. Di Nardo¹⁰², K.F. Di Petrillo⁵⁹, R. Di Sipio¹⁶⁷, D. Di Valentino³⁴, C. Diaconu¹⁰¹, F.A. Dias⁴⁰, T. Dias Do Vale^{140a}, M.A. Diaz^{147a}, J. Dickinson¹⁸, E.B. Diehl¹⁰⁵, J. Dietrich¹⁹, S. Díez Cornell⁴⁶, A. Dimitrievska¹⁸, W. Ding^{15b}, J. Dingfelder²⁴, F. Dittus³⁶, F. Djama¹⁰¹, T. Djobava^{159b}, J.I. Djuvsland¹⁷, M.A.B. Do Vale^{80c}, M. Dobre^{27b}, D. Dodsworth²⁶, C. Doglioni⁹⁶, J. Dolejsi¹⁴³, Z. Dolezal¹⁴³, M. Donadelli^{80d}, J. Donini³⁸, A. D'onofrio⁹², M. D'Onofrio⁹⁰, J. Dopke¹⁴⁴, A. Doria^{69a}, M.T. Dova⁸⁸, A.T. Doyle⁵⁷, E. Drechsler¹⁵², E. Dreyer¹⁵², T. Dreyer⁵³, A.S. Drobac¹⁷⁰, Y. Duan^{60b}, F. Dubinin¹¹⁰, M. Dubovsky^{28a}, A. Dubreuil⁵⁴, E. Duchovni¹⁸⁰, G. Duckeck¹¹⁴, A. Ducourthial¹³⁶, O.A. Ducu¹⁰⁹, D. Duda¹¹⁵, A. Dudarev³⁶, A.C. Dudder⁹⁹, E.M. Duffield¹⁸, L. Duflost¹³², M. Dührssen³⁶, C. Dülse¹⁸², M. Dumancic¹⁸⁰, A.E. Dumitriu^{27b}, A.K. Duncan⁵⁷, M. Dunford^{61a}, A. Duperrin¹⁰¹, H. Duran Yildiz^{4a}, M. Düren⁵⁶, A. Durglishvili^{159b}, D. Duschinger⁴⁸, B. Dutta⁴⁶, D. Duvnjak¹, G.I. Dyckes¹³⁷, M. Dyndal³⁶, S. Dysch¹⁰⁰, B.S. Dziedzic⁸⁴, K.M. Ecker¹¹⁵, R.C. Edgar¹⁰⁵, T. Eifert³⁶, G. Eigen¹⁷, K. Einsweiler¹⁸, T. Ekelof¹⁷², M. El Kacimi^{35c}, R. El Kosseifi¹⁰¹, V. Ellajosyula¹⁷², M. Ellert¹⁷², F. Ellinghaus¹⁸², A.A. Elliot⁹², N. Ellis³⁶, J. Elmsheuser²⁹, M. Elsing³⁶, D. Emelianov¹⁴⁴, A. Emerman³⁹, Y. Enari¹⁶³, J.S. Ennis¹⁷⁸, M.B. Epland⁴⁹, J. Erdmann⁴⁷, A. Ereditato²⁰, M. Errenst³⁶, M. Escalier¹³², C. Escobar¹⁷⁴, O. Estrada Pastor¹⁷⁴, E. Etzion¹⁶¹, H. Evans⁶⁵, A. Ezhilov¹³⁸, F. Fabbri⁵⁷, L. Fabbri^{23b,23a}, V. Fabiani¹¹⁹, G. Facini⁹⁴, R.M. Faisca Rodrigues Pereira^{140a}, R.M. Fakhruddinov¹²³, S. Falciano^{72a}, P.J. Falke⁵, S. Falke⁵, J. Faltova¹⁴³, Y. Fang^{15a}, Y. Fang^{15a}, G. Fanourakis⁴⁴, M. Fanti^{68a,68b}, A. Farbin⁸, A. Farilla^{74a}, E.M. Farina^{70a,70b}, T. Farooque¹⁰⁶, S. Farrell¹⁸, S.M. Farrington¹⁷⁸, P. Farthouat³⁶, F. Fassi^{35e}, P. Fassnacht³⁶, D. Fassouliotis⁹, M. Fauci Giannelli⁵⁰, W.J. Fawcett³², L. Fayard¹³², O.L. Fedin^{138,o}, W. Fedorko¹⁷⁵, M. Feickert⁴², S. Feigl¹³⁴, L. Feligioni¹⁰¹, A. Fell¹⁴⁹, C. Feng^{60b}, E.J. Feng³⁶, M. Feng⁴⁹, M.J. Fenton⁵⁷, A.B. Fenyuk¹²³, J. Ferrando⁴⁶, A. Ferrante¹⁷³, A. Ferrari¹⁷², P. Ferrari¹²⁰, R. Ferrari^{70a}, D.E. Ferreira de Lima^{61b}, A. Ferrer¹⁷⁴, D. Ferrere⁵⁴, C. Ferretti¹⁰⁵, F. Fiedler⁹⁹, A. Filipčič⁹¹, F. Filthaut¹¹⁹, K.D. Finelli²⁵, M.C.N. Fiolhais^{140a}, L. Fiorini¹⁷⁴, F. Fischer¹¹⁴, W.C. Fisher¹⁰⁶, I. Fleck¹⁵¹, P. Fleischmann¹⁰⁵, R.R.M. Fletcher¹³⁷, T. Flick¹⁸², B.M. Flierl¹¹⁴, L.F. Flores¹³⁷, L.R. Flores Castillo^{63a}, F.M. Follega^{75a,75b}, N. Fomin¹⁷, G.T. Forcolin^{75a,75b}, A. Formica¹⁴⁵, F.A. Förster¹⁴, A.C. Forti¹⁰⁰, A.G. Foster²¹, M.G. Foti¹³⁵, D. Fournier¹³², H. Fox⁸⁹, P. Francavilla^{71a,71b}, S. Francescato^{72a,72b}, M. Franchini^{23b,23a}, S. Franchino^{61a}, D. Francis³⁶, L. Franconi²⁰, M. Franklin⁵⁹, A.N. Fray⁹², B. Freund¹⁰⁹, W.S. Freund^{80b}, E.M. Freundlich⁴⁷, D.C. Frizzell¹²⁸, D. Froidevaux³⁶, J.A. Frost¹³⁵, C. Fukunaga¹⁶⁴, E. Fullana Torregrosa¹⁷⁴, E. Fumagalli^{55b,55a}, T. Fusayasu¹¹⁶, J. Fuster¹⁷⁴, A. Gabrielli^{23b,23a}, A. Gabrielli¹⁸, G.P. Gach^{83a}, S. Gadatsch⁵⁴, P. Gadow¹¹⁵, G. Gagliardi^{55b,55a}, L.G. Gagnon¹⁰⁹, C. Galea^{27b}, B. Galhardo^{140a}, G.E. Gallardo¹³⁵, E.J. Gallas¹³⁵, B.J. Gallop¹⁴⁴, P. Gallus¹⁴², G. Galster⁴⁰, R. Gamboa Goni⁹², K.K. Gan¹²⁶, S. Ganguly¹⁸⁰, J. Gao^{60a}, Y. Gao⁹⁰, Y.S. Gao^{31,l}, C. García¹⁷⁴, J.E. García Navarro¹⁷⁴, J.A. García Pascual^{15a}, C. Garcia-Argos⁵², M. Garcia-Sciveres¹⁸, R.W. Gardner³⁷, N. Garelli¹⁵³, S. Gargiulo⁵², V. Garonne¹³⁴, A. Gaudiello^{55b,55a}, G. Gaudio^{70a}, I.L. Gavrilenko¹¹⁰, A. Gavrilyuk¹¹¹, C. Gay¹⁷⁵, G. Gaycken²⁴, E.N. Gazis¹⁰, A.A. Geanta^{27b}, C.N.P. Gee¹⁴⁴, J. Geisen⁵³, M. Geisen⁹⁹, M.P. Geisler^{61a}, C. Gemme^{55b}, M.H. Genest⁵⁸, C. Geng¹⁰⁵, S. Gentile^{72a,72b}, S. George⁹³, T. Geralis⁴⁴, D. Gerbaudo¹⁴, L.O. Gerlach⁵³, P. Gessinger-Befurt⁹⁹, G. Gessner⁴⁷, S. Ghasemi¹⁵¹, M. Ghasemi Bostanabad¹⁷⁶, M. Ghneimat²⁴, A. Ghosh⁷⁷, B. Giacobbe^{23b}, S. Giagu^{72a,72b}, N. Giangiacomi^{23b,23a}, P. Giannetti^{71a}, A. Giannini^{69a,69b}, S.M. Gibson⁹³, M. Gignac¹⁴⁶, D. Gillberg³⁴, G. Gilles¹⁸², D.M. Gingrich^{3,aw}, M.P. Giordani^{66a,66c}, F.M. Giorgi^{23b}, P.F. Giraud¹⁴⁵, G. Giudliarelli^{66a,66c}, D. Giugni^{68a}, F. Giuli^{73a,73b}, S. Gkaitatzis¹⁶², I. Gkialas^{9,h}, E.L. Gkougkousis¹⁴, P. Gkoutoumis¹⁰, L.K. Gladilin¹¹³, C. Glasman⁹⁸, J. Glatzer¹⁴, P.C.F. Glaysher⁴⁶, A. Glazov⁴⁶, M. Goblirsch-Kolb²⁶, S. Goldfarb¹⁰⁴, T. Golling⁵⁴, D. Golubkov¹²³, A. Gomes^{140a,140b}, R. Goncalves Gama⁵³, R. Gonçalves^{140a,140b}, G. Gonella⁵², L. Gonella²¹, A. Gongadze⁷⁹, F. Gonnella²¹, J.L. Gonski⁵⁹, S. González de la Hoz¹⁷⁴, S. Gonzalez-Sevilla⁵⁴, G.R. Gonzalvo Rodriguez¹⁷⁴, L. Goossens³⁶, P.A. Gorbounov¹¹¹, H.A. Gordon²⁹, B. Gorini³⁶, E. Gorini^{67a,67b}, A. Gorišek⁹¹, A.T. Goshaw⁴⁹, C. Gössling⁴⁷, M.I. Gostkin⁷⁹, C.A. Gottardo²⁴, M. Gouighri^{35b}, D. Goujdami^{35c}, A.G. Goussiou¹⁴⁸, N. Govender^{33b,a}, C. Goy⁵, E. Gozani¹⁶⁰, I. Grabowska-Bold^{83a}, E.C. Graham⁹⁰, J. Gramling¹⁷¹, E. Gramstad¹³⁴, S. Grancagnolo¹⁹, M. Grandi¹⁵⁶, V. Gratchev¹³⁸, P.M. Gravila^{27f}, F.G. Gravili^{67a,67b},

C. Gray⁵⁷, H.M. Gray¹⁸, C. Grefe²⁴, K. Gregersen⁹⁶, I.M. Gregor⁴⁶, P. Grenier¹⁵³, K. Grevtsov⁴⁶, N.A. Grieser¹²⁸, J. Griffiths⁸, A.A. Grillo¹⁴⁶, K. Grimm^{31,k}, S. Grinstein^{14,w}, J.-F. Grivaz¹³², S. Groh⁹⁹, E. Gross¹⁸⁰, J. Grosse-Knetter⁵³, Z.J. Grout⁹⁴, C. Grud¹⁰⁵, A. Grummer¹¹⁸, L. Guan¹⁰⁵, W. Guan¹⁸¹, J. Guenther³⁶, A. Guerguichon¹³², F. Guescini^{168a}, D. Guest¹⁷¹, R. Gugel⁵², B. Gui¹²⁶, T. Guillemain⁵, S. Guindon³⁶, U. Gul⁵⁷, J. Guo^{60c}, W. Guo¹⁰⁵, Y. Guo^{60a,r}, Z. Guo¹⁰¹, R. Gupta⁴⁶, S. Gurbuz^{12c}, G. Gustavino¹²⁸, P. Gutierrez¹²⁸, C. Gutsche⁹⁴, C. Guyot¹⁴⁵, M.P. Guzik^{83a}, C. Gwenlan¹³⁵, C.B. Gwilliam⁹⁰, A. Haas¹²⁴, C. Haber¹⁸, H.K. Hadavand⁸, N. Haddad^{35e}, A. Hadeef^{60a}, S. Hageböck³⁶, M. Hagihara¹⁶⁹, M. Haleem¹⁷⁷, J. Haley¹²⁹, G. Halladjian¹⁰⁶, G.D. Hallewell¹⁰¹, K. Hamacher¹⁸², P. Hamal¹³⁰, K. Hamano¹⁷⁶, H. Hamdaoui^{35e}, G.N. Hamity¹⁴⁹, K. Han^{60a,qj}, L. Han^{60a}, S. Han^{15a,15d}, K. Hanagaki^{81,u}, M. Hance¹⁴⁶, D.M. Handl¹¹⁴, B. Haney¹³⁷, R. Hankache¹³⁶, P. Hanke^{61a}, E. Hansen⁹⁶, J.B. Hansen⁴⁰, J.D. Hansen⁴⁰, M.C. Hansen²⁴, P.H. Hansen⁴⁰, E.C. Hanson¹⁰⁰, K. Hara¹⁶⁹, A.S. Hard¹⁸¹, T. Harenberg¹⁸², S. Harkusha¹⁰⁷, P.F. Harrison¹⁷⁸, N.M. Hartmann¹¹⁴, Y. Hasegawa¹⁵⁰, A. Hasib⁵⁰, S. Hassani¹⁴⁵, S. Haug²⁰, R. Hauser¹⁰⁶, L.B. Havener³⁹, M. Havranek¹⁴², C.M. Hawkes²¹, R.J. Hawking³⁶, D. Hayden¹⁰⁶, C. Hayes¹⁵⁵, R.L. Hayes¹⁷⁵, C.P. Hays¹³⁵, J.M. Hays⁹², H.S. Hayward⁹⁰, S.J. Haywood¹⁴⁴, F. He^{60a}, M.P. Heath⁵⁰, V. Hedberg⁹⁶, L. Heelan⁸, S. Heer²⁴, K.K. Heidegger⁵², J. Heilman³⁴, S. Heim⁴⁶, T. Heim¹⁸, B. Heinemann^{46,ar}, J.J. Heinrich¹³¹, L. Heinrich³⁶, C. Heinz⁵⁶, J. Hejbal¹⁴¹, L. Helary^{61b}, A. Held¹⁷⁵, S. Hellesund¹³⁴, C.M. Helling¹⁴⁶, S. Hellman^{45a,45b}, C. Helsen³⁶, R.C.W. Henderson⁸⁹, Y. Heng¹⁸¹, S. Henkelmann¹⁷⁵, A.M. Henriques Correia³⁶, G.H. Herbert¹⁹, H. Herde²⁶, V. Herget¹⁷⁷, Y. Hernández Jiménez^{33c}, H. Herr⁹⁹, M.G. Herrmann¹¹⁴, T. Herrmann⁴⁸, G. Herten⁵², R. Hertenberger¹¹⁴, L. Hervas³⁶, T.C. Herwig¹³⁷, G.G. Hesketh⁹⁴, N.P. Hessey^{168a}, A. Higashida¹⁶³, S. Higashino⁸¹, E. Higón-Rodríguez¹⁷⁴, K. Hildebrand³⁷, E. Hill¹⁷⁶, J.C. Hill³², K.K. Hill²⁹, K.H. Hiller⁴⁶, S.J. Hillier²¹, M. Hils⁴⁸, I. Hinchliffe¹⁸, F. Hinterkeuser²⁴, M. Hirose¹³³, S. Hirose⁵², D. Hirschbuehl¹⁸², B. Hiti⁹¹, O. Hladik¹⁴¹, D.R. Hlaluku^{33c}, X. Hoad⁵⁰, J. Hobbs¹⁵⁵, N. Hod¹⁸⁰, M.C. Hodgkinson¹⁴⁹, A. Hoecker³⁶, F. Hoenig¹¹⁴, D. Hohn⁵², D. Hohov¹³², T.R. Holmes³⁷, M. Holzbock¹¹⁴, L.B.A.H. Hommels³², S. Honda¹⁶⁹, T. Honda⁸¹, T.M. Hong¹³⁹, A. Hönle¹¹⁵, B.H. Hooberman¹⁷³, W.H. Hopkins⁶, Y. Horii¹¹⁷, P. Horn⁴⁸, A.J. Horton¹⁵², L.A. Horyn³⁷, J.-Y. Hostachy⁵⁸, A. Hostiuc¹⁴⁸, S. Hou¹⁵⁸, A. Hoummada^{35a}, J. Howarth¹⁰⁰, J. Hoya⁸⁸, M. Hrabovsky¹³⁰, J. Hrdinka⁷⁶, I. Hristova¹⁹, J. Hrivnac¹³², A. Hrynevich¹⁰⁸, T. Hryn'ova⁵, P.J. Hsu⁶⁴, S.-C. Hsu¹⁴⁸, Q. Hu²⁹, S. Hu^{60c}, Y. Huang^{15a}, Z. Hubacek¹⁴², F. Hubaut¹⁰¹, M. Huebner²⁴, F. Hügging²⁴, T.B. Huffman¹³⁵, M. Huhtinen³⁶, R.F.H. Hunter³⁴, P. Huo¹⁵⁵, A.M. Hupe³⁴, N. Huseynov^{79,ae}, J. Huston¹⁰⁶, J. Huth⁵⁹, R. Hyneman¹⁰⁵, S. Hyrych^{28a}, G. Iacobucci⁵⁴, G. Iakovidis²⁹, I. Ibragimov¹⁵¹, L. Iconomidou-Fayard¹³², Z. Idrissi^{35e}, P.I. Iengo³⁶, R. Ignazzi⁴⁰, O. Igonkina^{120,y}, R. Iguchi¹⁶³, T. Iizawa⁵⁴, Y. Ikegami⁸¹, M. Ikeno⁸¹, D. Iliadis¹⁶², N. Ilic¹¹⁹, F. Iltzsche⁴⁸, G. Introzzi^{70a,70b}, M. Iodice^{74a}, K. Iordanidou³⁹, V. Ippolito^{72a,72b}, M.F. Isacson¹⁷², N. Ishijima¹³³, M. Ishino¹⁶³, M. Ishitsuka¹⁶⁵, W. Islam¹²⁹, C. Issever¹³⁵, S. Istin¹⁶⁰, F. Ito¹⁶⁹, J.M. Iturbe Ponce^{63a}, R. Iuppa^{75a,75b}, A. Ivina¹⁸⁰, H. Iwasaki⁸¹, J.M. Izen⁴³, V. Izzo^{69a}, P. Jacka¹⁴¹, P. Jackson¹, R.M. Jacobs²⁴, V. Jain², G. Jäkel¹⁸², K.B. Jakobi⁹⁹, K. Jakobs⁵², S. Jakobsen⁷⁶, T. Jakoubek¹⁴¹, J. Jamieson⁵⁷, K.W. Janas^{83a}, R. Jansky⁵⁴, J. Janssen²⁴, M. Janus⁵³, P.A. Janus^{83a}, G. Jarlskog⁹⁶, N. Javadov^{79,ae}, T. Javůrek³⁶, M. Javůrkova⁵², F. Jeanneau¹⁴⁵, L. Jeanty¹³¹, J. Jejelava^{159a,qf}, A. Jelinskas¹⁷⁸, P. Jenni^{52,b}, J. Jeong⁴⁶, N. Jeong⁴⁶, S. Jézéquel⁵, H. Ji¹⁸¹, J. Jia¹⁵⁵, H. Jiang⁷⁸, Y. Jiang^{60a}, Z. Jiang^{153,p}, S. Jiggins⁵², F.A. Jimenez Morales³⁸, J. Jimenez Pena¹⁷⁴, S. Jin^{15c}, A. Jinaru^{27b}, O. Jinnouchi¹⁶⁵, H. Jivan^{33c}, P. Johansson¹⁴⁹, K.A. Johns⁷, C.A. Johnson⁶⁵, K. Jon-And^{45a,45b}, R.W.L. Jones⁸⁹, S.D. Jones¹⁵⁶, S. Jones⁷, T.J. Jones⁹⁰, J. Jongmanns^{61a}, P.M. Jorge^{140a}, J. Jovicevic³⁶, X. Ju¹⁸, J.J. Junggeburth¹¹⁵, A. Juste Rozas^{14,w}, A. Kaczmarska⁸⁴, M. Kado^{72a,72b}, H. Kagan¹²⁶, M. Kagan¹⁵³, C. Kahra⁹⁹, T. Kaji¹⁷⁹, E. Kajomovitz¹⁶⁰, C.W. Kalderon⁹⁶, A. Kaluza⁹⁹, A. Kamenshchikov¹²³, L. Kanjir⁹¹, Y. Kano¹⁶³, V.A. Kantserov¹¹², J. Kanzaki⁸¹, L.S. Kaplan¹⁸¹, D. Kar^{33c}, M.J. Kareem^{168b}, E. Karentzos¹⁰, S.N. Karpov⁷⁹, Z.M. Karpova⁷⁹, V. Kartvelishvili⁸⁹, A.N. Karyukhin¹²³, L. Kashif¹⁸¹, R.D. Kass¹²⁶, A. Kastanas^{45a,45b}, Y. Kataoka¹⁶³, C. Kato^{60d,60c}, J. Katzy⁴⁶, K. Kawade⁸², K. Kawagoe⁸⁷, T. Kawaguchi¹¹⁷, T. Kawamoto¹⁶³, G. Kawamura⁵³, E.F. Kay¹⁷⁶, V.F. Kazanin^{122b,122a}, R. Keeler¹⁷⁶, R. Kehoe⁴², J.S. Keller³⁴, E. Kellermann⁹⁶, D. Kelsey¹⁵⁶, J.J. Kempster²¹, J. Kendrick²¹, O. Kepka¹⁴¹, S. Kersten¹⁸², B.P. Kerševan⁹¹, S. Ketabchi Haghighat¹⁶⁷, M. Khader¹⁷³, F. Khalil-Zada¹³, M. Khandoga¹⁴⁵, A. Khanov¹²⁹, A.G. Kharlamov^{122b,122a}, T. Kharlamova^{122b,122a}, E.E. Khoda¹⁷⁵, A. Khodinov¹⁶⁶, T.J. Khoo⁵⁴, E. Khramov⁷⁹, J. Khubua^{159b}, S. Kido⁸², M. Kiehn⁵⁴, C.R. Kilby⁹³,

Y.K. Kim³⁷, N. Kimura^{66a,66c}, O.M. Kind¹⁹, B.T. King^{90,*}, D. Kirchmeier⁴⁸, J. Kirk¹⁴⁴, A.E. Kiryunin¹¹⁵, T. Kishimoto¹⁶³, D.P. Kisliuk¹⁶⁷, V. Kitali⁴⁶, O. Kivernyk⁵, E. Kladiva^{28b,*}, T. Klapdor-Kleingrothaus⁵², M.H. Klein¹⁰⁵, M. Klein⁹⁰, U. Klein⁹⁰, K. Kleinknecht⁹⁹, P. Klimek¹²¹, A. Klimentov²⁹, T. Klingl²⁴, T. Klioutchnikova³⁶, F.F. Klitzner¹¹⁴, P. Kluit¹²⁰, S. Kluth¹¹⁵, E. Kneringer⁷⁶, E.B.F.G. Knoops¹⁰¹, A. Knue⁵², D. Kobayashi⁸⁷, T. Kobayashi¹⁶³, M. Kobel⁴⁸, M. Kocian¹⁵³, P. Kodys¹⁴³, P.T. Koenig²⁴, T. Koffas³⁴, N.M. Köhler¹¹⁵, T. Koi¹⁵³, M. Kolb^{61b}, I. Koletsou⁵, T. Komarek¹³⁰, T. Kondo⁸¹, N. Kondrashova^{60c}, K. Köneke⁵², A.C. König¹¹⁹, T. Kono¹²⁵, R. Konoplich^{124,am}, V. Konstantinides⁹⁴, N. Konstantinidis⁹⁴, B. Konya⁹⁶, R. Kopeliansky⁶⁵, S. Koperny^{83a}, K. Korcyl⁸⁴, K. Kordas¹⁶², G. Koren¹⁶¹, A. Korn⁹⁴, I. Korolkov¹⁴, E.V. Korolkova¹⁴⁹, N. Korotkova¹¹³, O. Kortner¹¹⁵, S. Kortner¹¹⁵, T. Kosek¹⁴³, V.V. Kostyukhin²⁴, A. Kotwal⁴⁹, A. Koulouris¹⁰, A. Kourkouveli-Charalampidi^{70a,70b}, C. Kourkouvelis⁹, E. Kourlitis¹⁴⁹, V. Kouskoura²⁹, A.B. Kowalewska⁸⁴, R. Kowalewski¹⁷⁶, C. Kozakai¹⁶³, W. Kozanecki¹⁴⁵, A.S. Kozhin¹²³, V.A. Kramarenko¹¹³, G. Kramberger⁹¹, D. Krasnopevtsev^{60a}, M.W. Krasny¹³⁶, A. Krasznahorkay³⁶, D. Krauss¹¹⁵, J.A. Kremer^{83a}, J. Kretzschmar⁹⁰, P. Krieger¹⁶⁷, F. Krieter¹¹⁴, A. Krishnan^{61b}, K. Krizka¹⁸, K. Kroeninger⁴⁷, H. Kroha¹¹⁵, J. Kroll¹⁴¹, J. Kroll¹³⁷, J. Krstic¹⁶, U. Kruchonak⁷⁹, H. Krüger²⁴, N. Krumnack⁷⁸, M.C. Kruse⁴⁹, T. Kubota¹⁰⁴, S. Kuday^{4b}, J.T. Kuechler⁴⁶, S. Kuehn³⁶, A. Kugel^{61a}, T. Kuhl⁴⁶, V. Kukhtin⁷⁹, R. Kukla¹⁰¹, Y. Kulchitsky^{107,ai}, S. Kuleshov^{147b}, Y.P. Kulinich¹⁷³, M. Kuna⁵⁸, T. Kunigo⁸⁵, A. Kupco¹⁴¹, T. Kupfer⁴⁷, O. Kuprash⁵², H. Kurashige⁸², L.L. Kurchaninov^{168a}, Y.A. Kurochkin¹⁰⁷, A. Kurova¹¹², M.G. Kurth^{15a,15d}, E.S. Kuwertz³⁶, M. Kuze¹⁶⁵, A.K. Kvam¹⁴⁸, J. Kvita¹³⁰, T. Kwan¹⁰³, A. La Rosa¹¹⁵, L. La Rotonda^{41b,41a}, F. La Ruffa^{41b,41a}, C. Lacasta¹⁷⁴, F. Lacava^{72a,72b}, D.P.J. Lack¹⁰⁰, H. Lacker¹⁹, D. Lacour¹³⁶, E. Ladygin⁷⁹, R. Lafaye⁵, B. Laforge¹³⁶, T. Lagouri^{33c}, S. Lai⁵³, S. Lammers⁶⁵, W. Lampl⁷, C. Lampoudis¹⁶², E. Lançon²⁹, U. Landgraf⁵², M.P.J. Landon⁹², M.C. Lanfermann⁵⁴, V.S. Lang⁴⁶, J.C. Lange⁵³, R.J. Langenberg³⁶, A.J. Lankford¹⁷¹, F. Lanni²⁹, K. Lantzsch²⁴, A. Lanza^{70a}, A. Lapertosa^{55b,55a}, S. Laplace¹³⁶, J.F. Laporte¹⁴⁵, T. Lari^{68a}, F. Lasagni Manghi^{23b,23a}, M. Lassnig³⁶, T.S. Lau^{63a}, A. Laudrain¹³², A. Laurier³⁴, M. Lavorgna^{69a,69b}, M. Lazzaroni^{68a,68b}, B. Le¹⁰⁴, O. Le Dortz¹³⁶, E. Le Guirriec¹⁰¹, M. LeBlanc⁷, T. LeCompte⁶, F. Ledroit-Guillon⁵⁸, C.A. Lee²⁹, G.R. Lee¹⁷, L. Lee⁵⁹, S.C. Lee¹⁵⁸, S.J. Lee³⁴, B. Lefebvre^{168a}, M. Lefebvre¹⁷⁶, F. Legger¹¹⁴, C. Leggett¹⁸, K. Lehmann¹⁵², N. Lehmann¹⁸², G. Lehmann Miotto³⁶, W.A. Leight⁴⁶, A. Leisos^{162,v}, M.A.L. Leite^{80d}, R. Leitner¹⁴³, D. Lellouch^{180,*}, K.J.C. Leney⁴², T. Lenz²⁴, B. Lenzi³⁶, R. Leone⁷, S. Leone^{71a}, C. Leonidopoulos⁵⁰, A. Leopold¹³⁶, G. Lerner¹⁵⁶, C. Leroy¹⁰⁹, R. Les¹⁶⁷, C.G. Lester³², M. Levchenko¹³⁸, J. Levêque⁵, D. Levin¹⁰⁵, L.J. Levinson¹⁸⁰, D.J. Lewis²¹, B. Li^{15b}, B. Li¹⁰⁵, C-Q. Li^{60a}, F. Li^{60c}, H. Li^{60a}, H. Li^{60b}, J. Li^{60c}, K. Li¹⁵³, L. Li^{60c}, M. Li^{15a}, Q. Li^{15a,15d}, Q.Y. Li^{60a}, S. Li^{60d,60c}, X. Li⁴⁶, Y. Li⁴⁶, Z. Li^{60b}, Z. Liang^{15a}, B. Liberti^{73a}, A. Liblong¹⁶⁷, K. Lie^{63c}, S. Liem¹²⁰, C.Y. Lin³², K. Lin¹⁰⁶, T.H. Lin⁹⁹, R.A. Linck⁶⁵, J.H. Lindon²¹, A.L. Lioni⁵⁴, E. Lipeles¹³⁷, A. Lipniacka¹⁷, M. Lisovyi^{61b}, T.M. Liss^{173,at}, A. Lister¹⁷⁵, A.M. Litke¹⁴⁶, J.D. Little⁸, B. Liu^{78,ab}, B.L. Liu⁶, H.B. Liu²⁹, H. Liu¹⁰⁵, J.B. Liu^{60a}, J.K.K. Liu¹³⁵, K. Liu¹³⁶, M. Liu^{60a}, P. Liu¹⁸, Y. Liu^{15a,15d}, Y.L. Liu¹⁰⁵, Y.W. Liu^{60a}, M. Livan^{70a,70b}, A. Lleres⁵⁸, J. Llorente Merino^{15a}, S.L. Lloyd⁹², C.Y. Lo^{63b}, F. Lo Sterzo⁴², E.M. Lobodzinska⁴⁶, P. Loch⁷, S. Loffredo^{73a,73b}, T. Lohse¹⁹, K. Lohwasser¹⁴⁹, M. Lokajicek¹⁴¹, J.D. Long¹⁷³, R.E. Long⁸⁹, L. Longo³⁶, K.A. Looper¹²⁶, J.A. Lopez^{147b}, I. Lopez Paz¹⁰⁰, A. Lopez Solis¹⁴⁹, J. Lorenz¹¹⁴, N. Lorenzo Martinez⁵, M. Losada²², P.J. Lösel¹¹⁴, A. Lösle⁵², X. Lou⁴⁶, X. Lou^{15a}, A. Lounis¹³², J. Love⁶, P.A. Love⁸⁹, J.J. Lozano Bahilo¹⁷⁴, M. Lu^{60a}, Y.J. Lu⁶⁴, H.J. Lubatti¹⁴⁸, C. Luci^{72a,72b}, A. Lucotte⁵⁸, C. Luedtke⁵², F. Luehring⁶⁵, I. Luise¹³⁶, L. Luminari^{72a}, B. Lund-Jensen¹⁵⁴, M.S. Lutz¹⁰², D. Lynn²⁹, R. Lysak¹⁴¹, E. Lytken⁹⁶, F. Lyu^{15a}, V. Lyubushkin⁷⁹, T. Lyubushkina⁷⁹, H. Ma²⁹, L.L. Ma^{60b}, Y. Ma^{60b}, G. Maccarrone⁵¹, A. Macchiolo¹¹⁵, C.M. Macdonald¹⁴⁹, J. Machado Miguens¹³⁷, D. Madaffari¹⁷⁴, R. Madar³⁸, W.F. Mader⁴⁸, N. Madysa⁴⁸, J. Maeda⁸², K. Maekawa¹⁶³, S. Maeland¹⁷, T. Maeno²⁹, M. Maerker⁴⁸, A.S. Maevskiy¹¹³, V. Magerl⁵², N. Magini⁷⁸, D.J. Mahon³⁹, C. Maidantchik^{80b}, T. Maier¹¹⁴, A. Maio^{140a,140b,140d}, O. Majersky^{28a}, S. Majewski¹³¹, Y. Makida⁸¹, N. Makovec¹³², B. Malaescu¹³⁶, Pa. Malecki⁸⁴, V.P. Maleev¹³⁸, F. Malek⁵⁸, U. Mallik⁷⁷, D. Malon⁶, C. Malone³², S. Maltezos¹⁰, S. Malyukov³⁶, J. Mamuzic¹⁷⁴, G. Mancini⁵¹, I. Mandić⁹¹, L. Manhaes de Andrade Filho^{80a}, I.M. Maniatis¹⁶², J. Manjarres Ramos⁴⁸, K.H. Mankinen⁹⁶, A. Mann¹¹⁴, A. Manousos⁷⁶, B. Mansoulie¹⁴⁵, I. Manthos¹⁶², S. Manzoni¹²⁰, A. Marantis¹⁶², G. Marceca³⁰, L. Marchese¹³⁵, G. Marchiori¹³⁶, M. Marcisovsky¹⁴¹, C. Marcon⁹⁶, C.A. Marin Tobon³⁶, M. Marjanovic³⁸, F. Marroquim^{80b}, Z. Marshall¹⁸, M.U.F. Martensson¹⁷², S. Marti-Garcia¹⁷⁴,

C.B. Martin¹²⁶, T.A. Martin¹⁷⁸, V.J. Martin⁵⁰, B. Martin dit Latour¹⁷, L. Martinelli^{74a,74b}, M. Martinez^{14,w}, V.I. Martinez Outschoorn¹⁰², S. Martin-Haugh¹⁴⁴, V.S. Martoiu^{27b}, A.C. Martyniuk⁹⁴, A. Marzin³⁶, S.R. Maschek¹¹⁵, L. Masetti⁹⁹, T. Mashimo¹⁶³, R. Mashinistov¹¹⁰, J. Masik¹⁰⁰, A.L. Maslennikov^{122b,122a}, L.H. Mason¹⁰⁴, L. Massa^{73a,73b}, P. Massarotti^{69a,69b}, P. Mastrandrea^{71a,71b}, A. Mastroberardino^{41b,41a}, T. Masubuchi¹⁶³, A. Matic¹¹⁴, P. Mättig²⁴, J. Maurer^{27b}, B. Maček⁹¹, S.J. Maxfield⁹⁰, D.A. Maximov^{122b,122a}, R. Mazini¹⁵⁸, I. Maznas¹⁶², S.M. Mazza¹⁴⁶, S.P. Mc Kee¹⁰⁵, T.G. McCarthy¹¹⁵, L.I. McClymont⁹⁴, W.P. McCormack¹⁸, E.F. McDonald¹⁰⁴, J.A. Mcfayden³⁶, M.A. McKay⁴², K.D. McLean¹⁷⁶, S.J. McMahon¹⁴⁴, P.C. McNamara¹⁰⁴, C.J. McNicol¹⁷⁸, R.A. McPherson^{176,ac}, J.E. Mdhluli^{33c}, Z.A. Meadows¹⁰², S. Meehan¹⁴⁸, T. Megy⁵², S. Mehlhase¹¹⁴, A. Mehta⁹⁰, T. Meideck⁵⁸, B. Meirose⁴³, D. Melini¹⁷⁴, B.R. Mellado Garcia^{33c}, J.D. Mellenthin⁵³, M. Melo^{28a}, F. Meloni⁴⁶, A. Melzer²⁴, S.B. Menary¹⁰⁰, E.D. Mendes Gouveia^{140a,140e}, L. Meng³⁶, X.T. Meng¹⁰⁵, S. Menke¹¹⁵, E. Meoni^{41b,41a}, S. Mergelmeyer¹⁹, S.A.M. Merkt¹³⁹, C. Merlassino²⁰, P. Mermod⁵⁴, L. Merola^{69a,69b}, C. Meroni^{68a}, O. Meshkov^{113,110}, J.K.R. Meshreki¹⁵¹, A. Messina^{72a,72b}, J. Metcalfe⁶, A.S. Mete¹⁷¹, C. Meyer⁶⁵, J. Meyer¹⁶⁰, J.-P. Meyer¹⁴⁵, H. Meyer Zu Theenhausen^{61a}, F. Miano¹⁵⁶, R.P. Middleton¹⁴⁴, L. Mijović⁵⁰, G. Mikenberg¹⁸⁰, M. Miestikova¹⁴¹, M. Mikuž⁹¹, H. Mildner¹⁴⁹, M. Milesi¹⁰⁴, A. Milic¹⁶⁷, D.A. Millar⁹², D.W. Miller³⁷, A. Milov¹⁸⁰, D.A. Milstead^{45a,45b}, R.A. Mina^{153,p}, A.A. Minaenko¹²³, M. Miñano Moya¹⁷⁴, I.A. Minashvili^{159b}, A.I. Mincer¹²⁴, B. Mindur^{83a}, M. Mineev⁷⁹, Y. Minegishi¹⁶³, Y. Ming¹⁸¹, L.M. Mir¹⁴, A. Mirto^{67a,67b}, K.P. Mistry¹³⁷, T. Mitani¹⁷⁹, J. Mitrevski¹¹⁴, V.A. Mitsou¹⁷⁴, M. Mittal^{60c}, A. Miucci²⁰, P.S. Miyagawa¹⁴⁹, A. Mizukami⁸¹, J.U. Mjörnmark⁹⁶, T. Mkrtchyan¹⁸⁴, M. Mlynarikova¹⁴³, T. Moa^{45a,45b}, K. Mochizuki¹⁰⁹, P. Mogg⁵², S. Mohapatra³⁹, R. Moles-Valls²⁴, M.C. Mondragon¹⁰⁶, K. Mönig⁴⁶, J. Monk⁴⁰, E. Monnier¹⁰¹, A. Montalbano¹⁵², J. Montejo Berlingen³⁶, M. Montella⁹⁴, F. Monticelli⁸⁸, S. Monzani^{68a}, N. Morange¹³², D. Moreno²², M. Moreno Llácer³⁶, C. Moreno Martinez¹⁴, P. Morettini^{55b}, M. Morgenstern¹²⁰, S. Morgenstern⁴⁸, D. Mori¹⁵², M. Morii⁵⁹, M. Morinaga¹⁷⁹, V. Morisbak¹³⁴, A.K. Morley³⁶, G. Mornacchi³⁶, A.P. Morris⁹⁴, L. Morvaj¹⁵⁵, P. Moschovakos³⁶, B. Moser¹²⁰, M. Mosidze^{159b}, T. Moskalets¹⁴⁵, H.J. Moss¹⁴⁹, J. Moss^{31,m}, K. Motohashi¹⁶⁵, E. Mountricha³⁶, E.J.W. Moyse¹⁰², S. Muanza¹⁰¹, J. Mueller¹³⁹, R.S.P. Mueller¹¹⁴, D. Muenstermann⁸⁹, G.A. Mullier⁹⁶, J.L. Munoz Martinez¹⁴, F.J. Munoz Sanchez¹⁰⁰, P. Murin^{28b}, W.J. Murray^{178,144}, A. Murrone^{68a,68b}, M. Muškinja¹⁸, C. Mwewa^{33a}, A.G. Myagkov^{123,an}, J. Myers¹³¹, M. Myska¹⁴², B.P. Nachman¹⁸, O. Nackenhorst⁴⁷, A. Nag Nag⁴⁸, K. Nagai¹³⁵, K. Nagano⁸¹, Y. Nagasaka⁶², M. Nagel⁵², E. Nagy¹⁰¹, A.M. Nairz³⁶, Y. Nakahama¹¹⁷, K. Nakamura⁸¹, T. Nakamura¹⁶³, I. Nakano¹²⁷, H. Nanjo¹³³, F. Napolitano^{61a}, R.F. Naranjo Garcia⁴⁶, R. Narayan¹¹, D.I. Narrias Villar^{61a}, I. Naryshkin¹³⁸, T. Naumann⁴⁶, G. Navarro²², H.A. Neal^{105,*}, P.Y. Nechaeva¹¹⁰, F. Nechansky⁴⁶, T.J. Neep²¹, A. Negri^{70a,70b}, M. Negrini^{23b}, C. Nellist⁵³, M.E. Nelson¹³⁵, S. Nemecek¹⁴¹, P. Nemethy¹²⁴, M. Nessi^{36,d}, M.S. Neubauer¹⁷³, M. Neumann¹⁸², P.R. Newman²¹, T.Y. Ng^{63c}, Y.S. Ng¹⁹, Y.W.Y. Ng¹⁷¹, H.D.N. Nguyen¹⁰¹, T. Nguyen Manh¹⁰⁹, E. Nibigira³⁸, R.B. Nickerson¹³⁵, R. Nicolaïdou¹⁴⁵, D.S. Nielsen⁴⁰, J. Nielsen¹⁴⁶, N. Nikiforou¹¹, V. Nikolaenko^{123,an}, I. Nikolic-Audit¹³⁶, K. Nikolopoulos²¹, P. Nilsson²⁹, H.R. Nindhito⁵⁴, Y. Ninomiya⁸¹, A. Nisati^{72a}, N. Nishu^{60c}, R. Nisius¹¹⁵, I. Nitsche⁴⁷, T. Nitta¹⁷⁹, T. Nobe¹⁶³, Y. Noguchi⁸⁵, M. Nomachi¹³³, I. Nomidis¹³⁶, M.A. Nomura²⁹, M. Nordberg³⁶, N. Norjoharuddeen¹³⁵, T. Novak⁹¹, O. Novgorodova⁴⁸, R. Novotny¹⁴², L. Nozka¹³⁰, K. Ntekas¹⁷¹, E. Nurse⁹⁴, F.G. Oakham^{34,aw}, H. Oberlack¹¹⁵, J. Ocariz¹³⁶, A. Ochi⁸², I. Ochoa³⁹, J.P. Ochoa-Ricoux^{147a}, K. O'Connor²⁶, S. Oda⁸⁷, S. Odaka⁸¹, S. Oerdek⁵³, A. Ogrodnik^{83a}, A. Oh¹⁰⁰, S.H. Oh⁴⁹, C.C. Ohm¹⁵⁴, H. Oide^{55b,55a}, M.L. Ojeda¹⁶⁷, H. Okawa¹⁶⁹, Y. Okazaki⁸⁵, Y. Okumura¹⁶³, T. Okuyama⁸¹, A. Olariu^{27b}, L.F. Oleiro Seabra^{140a}, S.A. Olivares Pino^{147a}, D. Oliveira Damazio²⁹, J.L. Oliver¹, M.J.R. Olsson¹⁷¹, A. Olszewski⁸⁴, J. Olszowska⁸⁴, D.C. O'Neil¹⁵², A. Onofre^{140a,140e}, K. Onogi¹¹⁷, P.U.E. Onyisi¹¹, H. Oppen¹³⁴, M.J. Oreglia³⁷, G.E. Orellana⁸⁸, Y. Oren¹⁶¹, D. Orestano^{74a,74b}, N. Orlando¹⁴, R.S. Orr¹⁶⁷, V. O'Shea⁵⁷, R. Ospanov^{60a}, G. Otero y Garzon³⁰, H. Otono⁸⁷, M. Ouchrif^{35d}, F. Ould-Saada¹³⁴, A. Ouraou¹⁴⁵, Q. Ouyang^{15a}, M. Owen⁵⁷, R.E. Owen²¹, V.E. Ozcan^{12c}, N. Ozturk⁸, J. Pacalt¹³⁰, H.A. Pacey³², K. Pachal⁴⁹, A. Pacheco Pages¹⁴, C. Padilla Aranda¹⁴, S. Pagan Griso¹⁸, M. Paganini¹⁸³, G. Palacino⁶⁵, S. Palazzo⁵⁰, S. Palestini³⁶, M. Palka^{83b}, D. Pallin³⁸, I. Panagoulas¹⁰, C.E. Pandini³⁶, J.G. Panduro Vazquez⁹³, P. Pani⁴⁶, G. Panizzo^{66a,66c}, L. Paolozzi⁵⁴, C. Papadatos¹⁰⁹, K. Papageorgiou^{9,h}, A. Paramonov⁶, D. Paredes Hernandez^{63b}, S.R. Paredes Saenz¹³⁵, B. Parida¹⁶⁶, T.H. Park¹⁶⁷,

A.J. Parker⁸⁹, M.A. Parker³², F. Parodi^{55b,55a}, E.W.P. Parrish¹²¹, J.A. Parsons³⁹, U. Parzefall⁵², L. Pascual Dominguez¹³⁶, V.R. Pascuzzi¹⁶⁷, J.M.P. Pasner¹⁴⁶, E. Pasqualucci^{72a}, S. Passaggio^{55b}, F. Pastore⁹³, P. Pasuwan^{45a,45b}, S. Patariaia⁹⁹, J.R. Pater¹⁰⁰, A. Pathak¹⁸¹, T. Pauly³⁶, B. Pearson¹¹⁵, M. Pedersen¹³⁴, L. Pedraza Diaz¹¹⁹, R. Pedro^{140a}, T. Peiffer⁵³, S.V. Peleganchuk^{122b,122a}, O. Penc¹⁴¹, H. Peng^{60a}, B.S. Peralva^{80a}, M.M. Perego¹³², A.P. Pereira Peixoto^{140a}, D.V. Perepelitsa²⁹, F. Peri¹⁹, L. Perini^{68a,68b}, H. Pernegger³⁶, S. Perrella^{69a,69b}, K. Peters⁴⁶, R.F.Y. Peters¹⁰⁰, B.A. Petersen³⁶, T.C. Petersen⁴⁰, E. Petit¹⁰¹, A. Petridis¹, C. Petridou¹⁶², P. Petroff¹³², M. Petrov¹³⁵, F. Petrucci^{74a,74b}, M. Pettee¹⁸³, N.E. Pettersson¹⁰², K. Petukhova¹⁴³, A. Peyaud¹⁴⁵, R. Pezoa^{147b}, L. Pezzotti^{70a,70b}, T. Pham¹⁰⁴, F.H. Phillips¹⁰⁶, P.W. Phillips¹⁴⁴, M.W. Phipps¹⁷³, G. Piacquadio¹⁵⁵, E. Pianori¹⁸, A. Picazio¹⁰², R.H. Pickles¹⁰⁰, R. Piegai³⁰, D. Pietreanu^{27b}, J.E. Pilcher³⁷, A.D. Pilkington¹⁰⁰, M. Pinamonti^{73a,73b}, J.L. Pinfold³, M. Pitt¹⁸⁰, L. Pizzimento^{73a,73b}, M.-A. Pleier²⁹, V. Pleskot¹⁴³, E. Plotnikova⁷⁹, D. Pluth⁷⁸, P. Podberczko^{122b,122a}, R. Poettgen⁹⁶, R. Poggi⁵⁴, L. Poggioli¹³², I. Pogrebnyak¹⁰⁶, D. Pohl²⁴, I. Pokharel⁵³, G. Polesello^{70a}, A. Poley¹⁸, A. Policicchio^{72a,72b}, R. Polifka¹⁴³, A. Polini^{23b}, C.S. Pollard⁴⁶, V. Polychronakos²⁹, D. Ponomarenko¹¹², L. Pontecorvo³⁶, S. Popa^{27a}, G.A. Popeneciu^{27d}, D.M. Portillo Quintero⁵⁸, S. Pospisil¹⁴², K. Potamianos⁴⁶, I.N. Potrap⁷⁹, C.J. Potter³², H. Potti¹¹, T. Poulsen⁹⁶, J. Poveda³⁶, T.D. Powell¹⁴⁹, G. Pownall⁴⁶, M.E. Pozo Astigarraga³⁶, P. Pralavorio¹⁰¹, S. Prell⁷⁸, D. Price¹⁰⁰, M. Primavera^{67a}, S. Prince¹⁰³, M.L. Proffitt¹⁴⁸, N. Proklova¹¹², K. Prokofiev^{63c}, F. Prokoshin^{147b}, S. Protopopescu²⁹, J. Proudfoot⁶, M. Przybycien^{83a}, D. Pudzha¹³⁸, A. Puri¹⁷³, P. Puzo¹³², J. Qian¹⁰⁵, Y. Qin¹⁰⁰, A. Quadt⁵³, M. Queitsch-Maitland⁴⁶, A. Qureshi¹, P. Rados¹⁰⁴, F. Ragusa^{68a,68b}, G. Rahal⁹⁷, J.A. Raine⁵⁴, S. Rajagopalan²⁹, A. Ramirez Morales⁹², K. Ran^{15a,15d}, T. Rashid¹³², S. Raspopov⁵, M.G. Ratti^{68a,68b}, D.M. Rauch⁴⁶, F. Rauscher¹¹⁴, S. Rave⁹⁹, B. Ravina¹⁴⁹, I. Ravinovich¹⁸⁰, J.H. Rawling¹⁰⁰, M. Raymond³⁶, A.L. Read¹³⁴, N.P. Readioff⁵⁸, M. Reale^{67a,67b}, D.M. Rebuzzi^{70a,70b}, A. Redelbach¹⁷⁷, G. Redlinger²⁹, K. Reeves⁴³, L. Rehnisch¹⁹, J. Reichert¹³⁷, D. Reikher¹⁶¹, A. Reiss⁹⁹, A. Rej¹⁵¹, C. Rembser³⁶, M. Renda^{27b}, M. Rescigno^{72a}, S. Resconi^{68a}, E.D. Resseguie¹³⁷, S. Rettie¹⁷⁵, E. Reynolds²¹, O.L. Rezanova^{122b,122a}, P. Reznicek¹⁴³, E. Ricci^{75a,75b}, R. Richter¹¹⁵, S. Richter⁴⁶, E. Richter-Was^{83b}, O. Ricken²⁴, M. Ridel¹³⁶, P. Rieck¹¹⁵, C.J. Riegel¹⁸², O. Rifki⁴⁶, M. Rijssenbeek¹⁵⁵, A. Rimoldi^{70a,70b}, M. Rimoldi²⁰, L. Rinaldi^{23b}, G. Ripellino¹⁵⁴, B. Ristić⁸⁹, E. Ritsch³⁶, I. Riu¹⁴, J.C. Rivera Vergara^{147a}, F. Rizatdinova¹²⁹, E. Rizvi⁹², C. Rizzi³⁶, R.T. Roberts¹⁰⁰, S.H. Robertson^{103,ac}, M. Robin⁴⁶, D. Robinson³², J.E.M. Robinson⁴⁶, A. Robson⁵⁷, E. Rocco⁹⁹, C. Roda^{71a,71b}, S. Rodriguez Bosca¹⁷⁴, A. Rodriguez Perez¹⁴, D. Rodriguez Rodriguez¹⁷⁴, A.M. Rodríguez Vera^{168b}, S. Roe³⁶, O. Röhne¹³⁴, R. Röhrig¹¹⁵, C.P.A. Roland⁶⁵, J. Roloff⁵⁹, A. Romaniouk¹¹², M. Romano^{23b,23a}, N. Rompotis⁹⁰, M. Ronzani¹²⁴, L. Roos¹³⁶, S. Rosati^{72a}, K. Rosbach⁵², N.-A. Rosien⁵³, G. Rosin¹⁰², B.J. Rosser¹³⁷, E. Rossi⁴⁶, E. Rossi^{74a,74b}, E. Rossi^{69a,69b}, L.P. Rossi^{55b}, L. Rossini^{68a,68b}, R. Rosten¹⁴, M. Rotaru^{27b}, J. Rothberg¹⁴⁸, D. Rousseau¹³², G. Rovelli^{70a,70b}, D. Roy^{33c}, A. Rozanov¹⁰¹, Y. Rozen¹⁶⁰, X. Ruan^{33c}, F. Rubbo¹⁵³, F. Rühr⁵², A. Ruiz-Martinez¹⁷⁴, A. Rummler³⁶, Z. Rurikova⁵², N.A. Rusakovich⁷⁹, H.L. Russell¹⁰³, L. Rustige^{38,47}, J.P. Rutherford⁷, E.M. Rüttinger^{46,j}, Y.F. Ryabov¹³⁸, M. Rybar³⁹, G. Rybkin¹³², A. Ryzhov¹²³, G.F. Rzehorz⁵³, P. Sabatini⁵³, G. Sabato¹²⁰, S. Sacerdoti¹³², H.F.-W. Sadrozinski¹⁴⁶, R. Sadykov⁷⁹, F. Safai Tehrani^{72a}, B. Safarzadeh Samani¹⁵⁶, P. Saha¹²¹, S. Saha¹⁰³, M. Sahinsoy^{61a}, A. Sahu¹⁸², M. Saimpert⁴⁶, M. Saito¹⁶³, T. Saito¹⁶³, H. Sakamoto¹⁶³, A. Sakharov^{124,am}, D. Salamani⁵⁴, G. Salamanna^{74a,74b}, J.E. Salazar Loyola^{147b}, P.H. Sales De Bruin¹⁷², D. Salihagic^{115,*}, A. Salnikov¹⁵³, J. Salt¹⁷⁴, D. Salvatore^{41b,41a}, F. Salvatore¹⁵⁶, A. Salvucci^{63a,63b,63c}, A. Salzburger³⁶, J. Samarati³⁶, D. Sammel⁵², D. Sampsonidis¹⁶², D. Sampsonidou¹⁶², J. Sánchez¹⁷⁴, A. Sanchez Pineda^{66a,66c}, H. Sandaker¹³⁴, C.O. Sander⁴⁶, I.G. Sanderswood⁸⁹, M. Sandhoff¹⁸², C. Sandoval²², D.P.C. Sankey¹⁴⁴, M. Sannino^{55b,55a}, Y. Sano¹¹⁷, A. Sansoni⁵¹, C. Santoni³⁸, H. Santos^{140a,140b}, S.N. Santpur¹⁸, A. Santra¹⁷⁴, A. Saproinov⁷⁹, J.G. Saraiva^{140a,140d}, O. Sasaki⁸¹, K. Sato¹⁶⁹, E. Sauvan⁵, P. Savard^{167,aw}, N. Savic¹¹⁵, R. Sawada¹⁶³, C. Sawyer¹⁴⁴, L. Sawyer^{95,ak}, C. Sbarra^{23b}, A. Sbrizzi^{23a}, T. Scanlon⁹⁴, J. Schaarschmidt¹⁴⁸, P. Schacht¹¹⁵, B.M. Schachtner¹¹⁴, D. Schaefer³⁷, L. Schaefer¹³⁷, J. Schaeffer⁹⁹, S. Schaepe³⁶, U. Schäfer⁹⁹, A.C. Schaffer¹³², D. Schaile¹¹⁴, R.D. Schamberger¹⁵⁵, N. Scharmberg¹⁰⁰, V.A. Schegelsky¹³⁸, D. Scheirich¹⁴³, F. Schenck¹⁹, M. Schernau¹⁷¹, C. Schiavi^{55b,55a}, S. Schier¹⁴⁶, L.K. Schildgen²⁴, Z.M. Schillaci²⁶, E.J. Schioppa³⁶, M. Schioppa^{41b,41a}, K.E. Schleicher⁵², S. Schlenker³⁶, K.R. Schmidt-Sommerfeld¹¹⁵, K. Schmieden³⁶, C. Schmitt⁹⁹, S. Schmitt⁴⁶, S. Schmitz⁹⁹,

J.C. Schmoeckel⁴⁶, U. Schnoor⁵², L. Schoeffel¹⁴⁵, A. Schoening^{61b}, E. Schopf¹³⁵, M. Schott⁹⁹, J.F.P. Schouwenberg¹¹⁹, J. Schovancova³⁶, S. Schramm⁵⁴, F. Schroeder¹⁸², A. Schulte⁹⁹, H.-C. Schultz-Coulon^{61a}, M. Schumacher⁵², B.A. Schumm¹⁴⁶, Ph. Schune¹⁴⁵, A. Schwartzman¹⁵³, T.A. Schwarz¹⁰⁵, Ph. Schwemling¹⁴⁵, R. Schwienhorst¹⁰⁶, A. Sciandra¹⁴⁶, G. Sciolla²⁶, M. Scodeggio⁴⁶, M. Scornajenghi^{41b,41a}, F. Scuri^{71a}, F. Scutti¹⁰⁴, L.M. Scyboz¹¹⁵, C.D. Sebastiani^{72a,72b}, P. Seema¹⁹, S.C. Seidel¹¹⁸, A. Seiden¹⁴⁶, T. Seiss³⁷, J.M. Seixas^{80b}, G. Sekhniaidze^{69a}, K. Sekhon¹⁰⁵, S.J. Sekula⁴², N. Semprini-Cesari^{23b,23a}, S. Sen⁴⁹, S. Senkin³⁸, C. Serfon⁷⁶, L. Serin¹³², L. Serkin^{66a,66b}, M. Sessa^{60a}, H. Severini¹²⁸, F. Sforza¹⁷⁰, A. Sfyrila⁵⁴, E. Shabalina⁵³, J.D. Shahinian¹⁴⁶, N.W. Shaikh^{45a,45b}, D. Shaked Renous¹⁸⁰, L.Y. Shan^{15a}, R. Shang¹⁷³, J.T. Shank²⁵, M. Shapiro¹⁸, A. Sharma¹³⁵, A.S. Sharma¹, P.B. Shatalov¹¹¹, K. Shaw¹⁵⁶, S.M. Shaw¹⁰⁰, A. Shcherbakova¹³⁸, Y. Shen¹²⁸, N. Sherafati³⁴, A.D. Sherman²⁵, P. Sherwood⁹⁴, L. Shi^{158,as}, S. Shimizu⁸¹, C.O. Shimmin¹⁸³, Y. Shimogama¹⁷⁹, M. Shimojima¹¹⁶, I.P.J. Shipsey¹³⁵, S. Shirabe⁸⁷, M. Shiyakova^{79,z}, J. Shlomi¹⁸⁰, A. Shmeleva¹¹⁰, M.J. Shochet³⁷, S. Shojaii¹⁰⁴, D.R. Shope¹²⁸, S. Shrestha¹²⁶, E. Shulga¹⁸⁰, P. Sicho¹⁴¹, A.M. Sickles¹⁷³, P.E. Sidebo¹⁵⁴, E. Sideras Haddad^{33c}, O. Sidiropoulou³⁶, A. Sidoti^{23b,23a}, F. Siegert⁴⁸, Dj. Sijacki¹⁶, M. Silva Jr.¹⁸¹, M.V. Silva Oliveira^{80a}, S.B. Silverstein^{45a}, S. Simion¹³², E. Simioni⁹⁹, R. Simoniello⁹⁹, P. Sinervo¹⁶⁷, N.B. Sinev¹³¹, M. Sioli^{23b,23a}, I. Siral¹⁰⁵, S.Yu. Sivoklov¹¹³, J. Sjölin^{45a,45b}, E. Skorda⁹⁶, P. Skubic¹²⁸, M. Slawinska⁸⁴, K. Sliwa¹⁷⁰, R. Slovak¹⁴³, V. Smakhtin¹⁸⁰, B.H. Smart¹⁴⁴, J. Smiesko^{28a}, N. Smirnov¹¹², S.Yu. Smirnov¹¹², Y. Smirnov¹¹², L.N. Smirnova^{113,s}, O. Smirnova⁹⁶, J.W. Smith⁵³, M. Smizanska⁸⁹, K. Smolek¹⁴², A. Smykiewicz⁸⁴, A.A. Snesarev¹¹⁰, H.L. Snoek¹²⁰, I.M. Snyder¹³¹, S. Snyder²⁹, R. Sobie^{176,ac}, A.M. Soffa¹⁷¹, A. Soffer¹⁶¹, A. Søgaard⁵⁰, F. Sohns⁵³, C.A. Solans Sanchez³⁶, E.Yu. Soldatov¹¹², U. Soldevila¹⁷⁴, A.A. Solodkov¹²³, A. Soloshenko⁷⁹, O.V. Solovyanov¹²³, V. Solovyev¹³⁸, P. Sommer¹⁴⁹, H. Son¹⁷⁰, W. Song¹⁴⁴, W.Y. Song^{168b}, A. Sopczak¹⁴², F. Sopkova^{28b}, C.L. Sotiropoulou^{71a,71b}, S. Sottocornola^{70a,70b}, R. Soualah^{66a,66c,g}, A.M. Soukharev^{122b,122a}, D. South⁴⁶, S. Spagnolo^{67a,67b}, M. Spalla¹¹⁵, M. Spangenberg¹⁷⁸, F. Spanò⁹³, D. Sperlich⁵², T.M. Spieker^{61a}, R. Spighi^{23b}, G. Spigo³⁶, M. Spina¹⁵⁶, D.P. Spiteri⁵⁷, M. Spousta¹⁴³, A. Stabile^{68a,68b}, B.L. Stamas¹²¹, R. Stamen^{61a}, M. Stamenkovic¹²⁰, E. Stanecka⁸⁴, R.W. Stanek⁶, B. Stanislaus¹³⁵, M.M. Stanitzki⁴⁶, M. Stankaityte¹³⁵, B. Stapf¹²⁰, E.A. Starchenko¹²³, G.H. Stark¹⁴⁶, J. Stark⁵⁸, S.H. Stark⁴⁰, P. Staroba¹⁴¹, P. Starovoitov^{61a}, S. Stärz¹⁰³, R. Staszewski⁸⁴, G. Stavropoulos⁴⁴, M. Stegler⁴⁶, P. Steinberg²⁹, A.L. Steinhebel¹³¹, B. Stelzer¹⁵², H.J. Stelzer¹³⁹, O. Stelzer-Chilton^{168a}, H. Stenzel⁵⁶, T.J. Stevenson¹⁵⁶, G.A. Stewart³⁶, M.C. Stockton³⁶, G. Stoica^{27b}, M. Stolarski^{140a}, P. Stolte⁵³, S. Stonjek¹¹⁵, A. Straessner⁴⁸, J. Strandberg¹⁵⁴, S. Strandberg^{45a,45b}, M. Strauss¹²⁸, P. Strizenec^{28b}, R. Ströhmer¹⁷⁷, D.M. Strom¹³¹, R. Stroynowski⁴², A. Strubig⁵⁰, S.A. Stucci²⁹, B. Stugu¹⁷, J. Stupak¹²⁸, N.A. Styles⁴⁶, D. Su¹⁵³, S. Suchek^{61a}, Y. Sugaya¹³³, V.V. Sulin¹¹⁰, M.J. Sullivan⁹⁰, D.M.S. Sultan⁵⁴, S. Sultansoy^{4c}, T. Sumida⁸⁵, S. Sun¹⁰⁵, X. Sun³, K. Suruliz¹⁵⁶, C.J.E. Suster¹⁵⁷, M.R. Sutton¹⁵⁶, S. Suzuki⁸¹, M. Svatos¹⁴¹, M. Swiatlowski³⁷, S.P. Swift², T. Swirski¹⁷⁷, A. Sydorenko⁹⁹, I. Sykora^{28a}, M. Sykora¹⁴³, T. Sykora¹⁴³, D. Ta⁹⁹, K. Tackmann^{46,x}, J. Taenzer¹⁶¹, A. Taffard¹⁷¹, R. Tafirout^{168a}, E. Tahirovic⁹², H. Takai²⁹, R. Takashima⁸⁶, K. Takeda⁸², T. Takeshita¹⁵⁰, E.P. Takeva⁵⁰, Y. Takubo⁸¹, M. Talby¹⁰¹, A.A. Talyshev^{122b,122a}, N.M. Tamir¹⁶¹, J. Tanaka¹⁶³, M. Tanaka¹⁶⁵, R. Tanaka¹³², B.B. Tannenwald¹²⁶, S. Tapia Araya¹⁷³, S. Tapprogge⁹⁹, A. Tarek Abouelfadl Mohamed¹³⁶, S. Tarem¹⁶⁰, G. Tarna^{27b,c}, G.F. Tartarelli^{68a}, P. Tas¹⁴³, M. Tasevsky¹⁴¹, T. Tashiro⁸⁵, E. Tassi^{41b,41a}, A. Tavares Delgado^{140a,140b}, Y. Tayalati^{35e}, A.J. Taylor⁵⁰, G.N. Taylor¹⁰⁴, W. Taylor^{168b}, A.S. Tee⁸⁹, R. Teixeira De Lima¹⁵³, P. Teixeira-Dias⁹³, H. Ten Kate³⁶, J.J. Teoh¹²⁰, S. Terada⁸¹, K. Terashi¹⁶³, J. Terron⁹⁸, S. Terzo¹⁴, M. Testa⁵¹, R.J. Teuscher^{167,ac}, S.J. Thais¹⁸³, T. Theveneaux-Pelzer⁴⁶, F. Thiele⁴⁰, D.W. Thomas⁹³, J.O. Thomas⁴², J.P. Thomas²¹, A.S. Thompson⁵⁷, P.D. Thompson²¹, L.A. Thomsen¹⁸³, E. Thomson¹³⁷, Y. Tian³⁹, R.E. Ticse Torres⁵³, V.O. Tikhomirov^{110,ao}, Yu.A. Tikhonov^{122b,122a}, S. Timoshenko¹¹², P. Tipton¹⁸³, S. Tisserant¹⁰¹, K. Todome^{23b,23a}, S. Todorova-Nova⁵, S. Todt⁴⁸, J. Tojo⁸⁷, S. Tokár^{28a}, K. Tokushuku⁸¹, E. Tolley¹²⁶, K.G. Tomiwa^{33c}, M. Tomoto¹¹⁷, L. Tompkins^{153,p}, K. Toms¹¹⁸, B. Tong⁵⁹, P. Tornambe¹⁰², E. Torrence¹³¹, H. Torres⁴⁸, E. Torró Pastor¹⁴⁸, C. Toscri¹³⁵, J. Toth^{101,aa}, D.R. Tovey¹⁴⁹, C.J. Treado¹²⁴, T. Trefzger¹⁷⁷, F. Tresoldi¹⁵⁶, A. Tricoli²⁹, I.M. Trigger^{168a}, S. Trincaz-Duvold¹³⁶, W. Trischuk¹⁶⁷, B. Trocmé⁵⁸, A. Trofymov¹³², C. Troncon^{68a}, M. Trovatelli¹⁷⁶, F. Trovato¹⁵⁶, L. Truong^{33b}, M. Trzebinski⁸⁴, A. Trzupek⁸⁴, F. Tsai⁴⁶, J.C.-L. Tseng¹³⁵, P.V. Tsiarehka^{107,ai}, A. Tsirigotis¹⁶², N. Tsirintanis⁹, V. Tsiskaridze¹⁵⁵, E.G. Tskhadadze^{159a}, M. Tsopoulou¹⁶²,

I.I. Tsukerman¹¹¹, V. Tsulaia¹⁸, S. Tsuno⁸¹, D. Tsybychev¹⁵⁵, Y. Tu^{63b}, A. Tudorache^{27b}, V. Tudorache^{27b}, T.T. Tulbure^{27a}, A.N. Tuna⁵⁹, S. Turchikhin⁷⁹, D. Turgeman¹⁸⁰, I. Turk Cakir^{4b,t}, R.J. Turner²¹, R.T. Turra^{68a}, P.M. Tuts³⁹, S. Tzamarias¹⁶², E. Tzovara⁹⁹, G. Ucchielli⁴⁷, K. Uchida¹⁶³, I. Ueda⁸¹, M. Ughetto^{45a,45b}, F. Ukegawa¹⁶⁹, G. Unal³⁶, A. Undrus²⁹, G. Unel¹⁷¹, F.C. Ungaro¹⁰⁴, Y. Unno⁸¹, K. Uno¹⁶³, J. Urban^{28b}, P. Urquijo¹⁰⁴, G. Usai⁸, J. Usui⁸¹, L. Vacavant¹⁰¹, V. Vacek¹⁴², B. Vachon¹⁰³, K.O.H. Vadla¹³⁴, A. Vaidya⁹⁴, C. Valderanis¹¹⁴, E. Valdes Santurio^{45a,45b}, M. Valente⁵⁴, S. Valentini^{23b,23a}, A. Valero¹⁷⁴, L. Valéry⁴⁶, R.A. Vallance²¹, A. Vallier³⁶, J.A. Valls Ferrer¹⁷⁴, T.R. Van Daalen¹⁴, P. Van Gemmeren⁶, I. Van Vulpen¹²⁰, M. Vanadia^{73a,73b}, W. Vandelli³⁶, A. Vaniachine¹⁶⁶, D. Vannicola^{72a,72b}, R. Vari^{72a}, E.W. Varnes⁷, C. Varni^{55b,55a}, T. Varol⁴², D. Varouchas¹³², K.E. Varvell¹⁵⁷, M.E. Vasile^{27b}, G.A. Vasquez¹⁷⁶, J.G. Vasquez¹⁸³, F. Vazeille³⁸, D. Vazquez Furelos¹⁴, T. Vazquez Schroeder³⁶, J. Veatch⁵³, V. Vecchio^{74a,74b}, M.J. Veen¹²⁰, L.M. Veloce¹⁶⁷, F. Veloso^{140a,140c}, S. Veneziano^{72a}, A. Ventura^{67a,67b}, N. Venturi³⁶, A. Verbytskyi¹¹⁵, V. Vercesi^{70a}, M. Verducci^{74a,74b}, C.M. Vergel Infante⁷⁸, C. Vergis²⁴, W. Verkerke¹²⁰, A.T. Vermeulen¹²⁰, J.C. Vermeulen¹²⁰, M.C. Vetterli^{152,aw}, N. Viaux Maira^{147b}, M. Vicente Barreto Pinto⁵⁴, T. Vickey¹⁴⁹, O.E. Vickey Boeriu¹⁴⁹, G.H.A. Viehhauser¹³⁵, L. Viganì¹³⁵, M. Villa^{23b,23a}, M. Villaplana Perez^{68a,68b}, E. Vilucchi⁵¹, M.G. Vinciter³⁴, V.B. Vinogradov⁷⁹, A. Vishwakarma⁴⁶, C. Vittori^{23b,23a}, I. Vivarelli¹⁵⁶, M. Vogel¹⁸², P. Vokac¹⁴², S.E. von Buddenbrock^{33c}, E. Von Toerne²⁴, V. Vorobel¹⁴³, K. Vorobev¹¹², M. Vos¹⁷⁴, J.H. Vosseveld⁹⁰, N. Vranjes¹⁶, M. Vranjes Milosavljevic¹⁶, V. Vrba¹⁴², M. Vreeswijk¹²⁰, T. Šfiligoj⁹¹, R. Vuillermet³⁶, I. Vukotic³⁷, T. Ženiš^{28a}, L. Živković¹⁶, P. Wagner²⁴, W. Wagner¹⁸², J. Wagner-Kuhr¹¹⁴, H. Wahlberg⁸⁸, K. Wakamiya⁸², V.M. Walbrecht¹¹⁵, J. Walder⁸⁹, R. Walker¹¹⁴, S.D. Walker⁹³, W. Walkowiak¹⁵¹, V. Wallangen^{45a,45b}, A.M. Wang⁵⁹, C. Wang^{60b}, F. Wang¹⁸¹, H. Wang¹⁸, H. Wang³, J. Wang¹⁵⁷, J. Wang^{61b}, P. Wang⁴², Q. Wang¹²⁸, R.-J. Wang⁹⁹, R. Wang^{60a}, R. Wang⁶, S.M. Wang¹⁵⁸, W.T. Wang^{60a}, W. Wang^{15c,ad}, W.X. Wang^{60a,ad}, Y. Wang^{60a,al}, Z. Wang^{60c}, C. Wanotayaroj⁴⁶, A. Warburton¹⁰³, C.P. Ward³², D.R. Wardrope⁹⁴, N. Warrack⁵⁷, A. Washbrook⁵⁰, A.T. Watson²¹, M.F. Watson²¹, G. Watts¹⁴⁸, B.M. Waugh⁹⁴, A.F. Webb¹¹, S. Webb⁹⁹, C. Weber¹⁸³, M.S. Weber²⁰, S.A. Weber³⁴, S.M. Weber^{61a}, A.R. Weidberg¹³⁵, J. Weingarten⁴⁷, M. Weirich⁹⁹, C. Weiser⁵², P.S. Wells³⁶, T. Wenaus²⁹, T. Wengler³⁶, S. Wenig³⁶, N. Wermes²⁴, M.D. Werner⁷⁸, P. Werner³⁶, M. Wessels^{61a}, T.D. Weston²⁰, K. Whalen¹³¹, N.L. Whallon¹⁴⁸, A.M. Wharton⁸⁹, A.S. White¹⁰⁵, A. White⁸, M.J. White¹, D. Whiteson¹⁷¹, B.W. Whitmore⁸⁹, F.J. Wickens¹⁴⁴, W. Wiedenmann¹⁸¹, M. Wielers¹⁴⁴, N. Wieseotte⁹⁹, C. Wiglesworth⁴⁰, L.A.M. Wiik-Fuchs⁵², F. Wilk¹⁰⁰, H.G. Wilkens³⁶, L.J. Wilkins⁹³, H.H. Williams¹³⁷, S. Williams³², C. Willis¹⁰⁶, S. Willocq¹⁰², J.A. Wilson²¹, I. Wingerter-Seez⁵, E. Winkels¹⁵⁶, F. Winklmeier¹³¹, O.J. Winston¹⁵⁶, B.T. Winter⁵², M. Wittgen¹⁵³, M. Wobisch⁹⁵, A. Wolf⁹⁹, T.M.H. Wolf¹²⁰, R. Wolff¹⁰¹, R.W. Wölker¹³⁵, J. Wollrath⁵², M.W. Wolter⁸⁴, H. Wolters^{140a,140c}, V.W.S. Wong¹⁷⁵, N.L. Woods¹⁴⁶, S.D. Worm²¹, B.K. Wosiek⁸⁴, K.W. Woźniak⁸⁴, K. Wraight⁵⁷, S.L. Wu¹⁸¹, X. Wu⁵⁴, Y. Wu^{60a}, T.R. Wyatt¹⁰⁰, B.M. Wynne⁵⁰, S. Xella⁴⁰, Z. Xi¹⁰⁵, L. Xia¹⁷⁸, D. Xu^{15a}, H. Xu^{60a,c}, L. Xu²⁹, T. Xu¹⁴⁵, W. Xu¹⁰⁵, Z. Xu^{60b}, Z. Xu¹⁵³, B. Yabsley¹⁵⁷, S. Yacoub^{33a}, K. Yajima¹³³, D.P. Yallup⁹⁴, D. Yamaguchi¹⁶⁵, Y. Yamaguchi¹⁶⁵, A. Yamamoto⁸¹, T. Yamanaka¹⁶³, F. Yamane⁸², M. Yamatani¹⁶³, T. Yamazaki¹⁶³, Y. Yamazaki⁸², Z. Yan²⁵, H.J. Yang^{60c,60d}, H.T. Yang¹⁸, S. Yang⁷⁷, X. Yang^{60b,58}, Y. Yang¹⁶³, Z. Yang¹⁷, W.-M. Yao¹⁸, Y.C. Yap⁴⁶, Y. Yasu⁸¹, E. Yatsenko^{60c,60d}, J. Ye⁴², S. Ye²⁹, I. Yeletskikh⁷⁹, M.R. Yexley⁸⁹, E. Yigitbasi²⁵, E. Yildirim⁹⁹, K. Yorita¹⁷⁹, K. Yoshihara¹³⁷, C.J.S. Young³⁶, C. Young¹⁵³, J. Yu⁷⁸, R. Yuan^{60b}, X. Yue^{61a}, S.P.Y. Yuen²⁴, B. Zabinski⁸⁴, G. Zacharis¹⁰, E. Zaffaroni⁵⁴, J. Zahreddine¹³⁶, R. Zaidan¹⁴, A.M. Zaitsev^{123,an}, T. Zakareishvili^{159b}, N. Zakharchuk³⁴, S. Zambito⁵⁹, D. Zanzi³⁶, D.R. Zaripovas⁵⁷, S.V. Zeiřner⁴⁷, C. Zeitnitz¹⁸², G. Zemaityte¹³⁵, J.C. Zeng¹⁷³, O. Zenin¹²³, D. Zerwas¹³², M. Zgubić¹³⁵, D.F. Zhang^{15b}, F. Zhang¹⁸¹, G. Zhang^{60a}, G. Zhang^{15b}, H. Zhang^{15c}, J. Zhang⁶, L. Zhang^{15c}, L. Zhang^{60a}, M. Zhang¹⁷³, R. Zhang^{60a}, R. Zhang²⁴, X. Zhang^{60b}, Y. Zhang^{15a,15d}, Z. Zhang^{63a}, Z. Zhang¹³², P. Zhao⁴⁹, Y. Zhao^{60b}, Z. Zhao^{60a}, A. Zhemchugov⁷⁹, Z. Zheng¹⁰⁵, D. Zhong¹⁷³, B. Zhou¹⁰⁵, C. Zhou¹⁸¹, M.S. Zhou^{15a,15d}, M. Zhou¹⁵⁵, N. Zhou^{60c}, Y. Zhou⁷, C.G. Zhu^{60b}, H.L. Zhu^{60a}, H. Zhu^{15a}, J. Zhu¹⁰⁵, Y. Zhu^{60a}, X. Zhuang^{15a}, K. Zhukov¹¹⁰, V. Zhulanov^{122b,122a}, D. Zieminska⁶⁵, N.I. Zimine⁷⁹, S. Zimmermann⁵², Z. Zinonos¹¹⁵, M. Ziolkowski¹⁵¹, G. Zobernig¹⁸¹, A. Zoccoli^{23b,23a}, K. Zoch⁵³, T.G. Zorbas¹⁴⁹, R. Zou³⁷, L. Zwalinski³⁶

¹ Department of Physics, University of Adelaide, Adelaide, Australia

- ² Physics Department, SUNY Albany, Albany NY, United States of America
- ³ Department of Physics, University of Alberta, Edmonton AB, Canada
- ⁴ ^(a) Department of Physics, Ankara University, Ankara; ^(b) Istanbul Aydin University, Istanbul; ^(c) Division of Physics, TOBB University of Economics and Technology, Ankara, Turkey
- ⁵ LAPP, Université Grenoble Alpes, Université Savoie Mont Blanc, CNRS/IN2P3, Annecy, France
- ⁶ High Energy Physics Division, Argonne National Laboratory, Argonne IL, United States of America
- ⁷ Department of Physics, University of Arizona, Tucson AZ, United States of America
- ⁸ Department of Physics, University of Texas at Arlington, Arlington TX, United States of America
- ⁹ Physics Department, National and Kapodistrian University of Athens, Athens, Greece
- ¹⁰ Physics Department, National Technical University of Athens, Zografou, Greece
- ¹¹ Department of Physics, University of Texas at Austin, Austin TX, United States of America
- ¹² ^(a) Bahcesehir University, Faculty of Engineering and Natural Sciences, Istanbul; ^(b) Istanbul Bilgi University, Faculty of Engineering and Natural Sciences, Istanbul; ^(c) Department of Physics, Bogazici University, Istanbul; ^(d) Department of Physics Engineering, Gaziantep University, Gaziantep, Turkey
- ¹³ Institute of Physics, Azerbaijan Academy of Sciences, Baku, Azerbaijan
- ¹⁴ Institut de Física d'Altes Energies (IFAE), Barcelona Institute of Science and Technology, Barcelona, Spain
- ¹⁵ ^(a) Institute of High Energy Physics, Chinese Academy of Sciences, Beijing; ^(b) Physics Department, Tsinghua University, Beijing; ^(c) Department of Physics, Nanjing University, Nanjing; ^(d) University of Chinese Academy of Science (UCAS), Beijing, China
- ¹⁶ Institute of Physics, University of Belgrade, Belgrade, Serbia
- ¹⁷ Department for Physics and Technology, University of Bergen, Bergen, Norway
- ¹⁸ Physics Division, Lawrence Berkeley National Laboratory and University of California, Berkeley CA, United States of America
- ¹⁹ Institut für Physik, Humboldt Universität zu Berlin, Berlin, Germany
- ²⁰ Albert Einstein Center for Fundamental Physics and Laboratory for High Energy Physics, University of Bern, Bern, Switzerland
- ²¹ School of Physics and Astronomy, University of Birmingham, Birmingham, United Kingdom
- ²² Facultad de Ciencias y Centro de Investigaciones, Universidad Antonio Nariño, Bogota, Colombia
- ²³ ^(a) INFN Bologna and Università di Bologna, Dipartimento di Fisica; ^(b) INFN Sezione di Bologna, Italy
- ²⁴ Physikalisches Institut, Universität Bonn, Bonn, Germany
- ²⁵ Department of Physics, Boston University, Boston MA, United States of America
- ²⁶ Department of Physics, Brandeis University, Waltham MA, United States of America
- ²⁷ ^(a) Transilvania University of Brasov, Brasov; ^(b) Horia Hulubei National Institute of Physics and Nuclear Engineering, Bucharest; ^(c) Department of Physics, Alexandru Ioan Cuza University of Iasi, Iasi; ^(d) National Institute for Research and Development of Isotopic and Molecular Technologies, Physics Department, Cluj-Napoca; ^(e) University Politehnica Bucharest, Bucharest; ^(f) West University in Timisoara, Timisoara, Romania
- ²⁸ ^(a) Faculty of Mathematics, Physics and Informatics, Comenius University, Bratislava; ^(b) Department of Subnuclear Physics, Institute of Experimental Physics of the Slovak Academy of Sciences, Kosice, Slovak Republic
- ²⁹ Physics Department, Brookhaven National Laboratory, Upton NY, United States of America
- ³⁰ Departamento de Física, Universidad de Buenos Aires, Buenos Aires, Argentina
- ³¹ California State University, CA, United States of America
- ³² Cavendish Laboratory, University of Cambridge, Cambridge, United Kingdom
- ³³ ^(a) Department of Physics, University of Cape Town, Cape Town; ^(b) Department of Mechanical Engineering Science, University of Johannesburg, Johannesburg; ^(c) School of Physics, University of the Witwatersrand, Johannesburg, South Africa
- ³⁴ Department of Physics, Carleton University, Ottawa ON, Canada
- ³⁵ ^(a) Faculté des Sciences Ain Chock, Réseau Universitaire de Physique des Hautes Energies - Université Hassan II, Casablanca; ^(b) Faculté des Sciences, Université Ibn-Tofail, Kénitra; ^(c) Faculté des Sciences Semlalia, Université Cadi Ayyad, LPHEA-Marrakech; ^(d) Faculté des Sciences, Université Mohamed Premier and LPTPM, Oujda; ^(e) Faculté des sciences, Université Mohammed V, Rabat, Morocco
- ³⁶ CERN, Geneva, Switzerland
- ³⁷ Enrico Fermi Institute, University of Chicago, Chicago IL, United States of America
- ³⁸ LPC, Université Clermont Auvergne, CNRS/IN2P3, Clermont-Ferrand, France
- ³⁹ Nevis Laboratory, Columbia University, Irvington NY, United States of America
- ⁴⁰ Niels Bohr Institute, University of Copenhagen, Copenhagen, Denmark
- ⁴¹ ^(a) Dipartimento di Fisica, Università della Calabria, Rende; ^(b) INFN Gruppo Collegato di Cosenza, Laboratori Nazionali di Frascati, Italy
- ⁴² Physics Department, Southern Methodist University, Dallas TX, United States of America
- ⁴³ Physics Department, University of Texas at Dallas, Richardson TX, United States of America
- ⁴⁴ National Centre for Scientific Research "Demokritos", Agia Paraskevi, Greece
- ⁴⁵ ^(a) Department of Physics, Stockholm University; ^(b) Oskar Klein Centre, Stockholm, Sweden
- ⁴⁶ Deutsches Elektronen-Synchrotron DESY, Hamburg and Zeuthen, Germany
- ⁴⁷ Lehrstuhl für Experimentelle Physik IV, Technische Universität Dortmund, Dortmund, Germany
- ⁴⁸ Institut für Kern- und Teilchenphysik, Technische Universität Dresden, Dresden, Germany
- ⁴⁹ Department of Physics, Duke University, Durham NC, United States of America
- ⁵⁰ SUPA - School of Physics and Astronomy, University of Edinburgh, Edinburgh, United Kingdom
- ⁵¹ INFN e Laboratori Nazionali di Frascati, Frascati, Italy
- ⁵² Physikalisches Institut, Albert-Ludwigs-Universität Freiburg, Freiburg, Germany
- ⁵³ II. Physikalisches Institut, Georg-August-Universität Göttingen, Göttingen, Germany
- ⁵⁴ Département de Physique Nucléaire et Corpusculaire, Université de Genève, Genève, Switzerland
- ⁵⁵ ^(a) Dipartimento di Fisica, Università di Genova, Genova; ^(b) INFN Sezione di Genova, Italy
- ⁵⁶ II. Physikalisches Institut, Justus-Liebig-Universität Giessen, Giessen, Germany
- ⁵⁷ SUPA - School of Physics and Astronomy, University of Glasgow, Glasgow, United Kingdom
- ⁵⁸ LPSC, Université Grenoble Alpes, CNRS/IN2P3, Grenoble INP, Grenoble, France
- ⁵⁹ Laboratory for Particle Physics and Cosmology, Harvard University, Cambridge MA, United States of America
- ⁶⁰ ^(a) Department of Modern Physics and State Key Laboratory of Particle Detection and Electronics, University of Science and Technology of China, Hefei; ^(b) Institute of Frontier and Interdisciplinary Science and Key Laboratory of Particle Physics and Particle Irradiation (MOE), Shandong University, Qingdao; ^(c) School of Physics and Astronomy, Shanghai Jiao Tong University, KLPPAC-MoE, SKLPPC, Shanghai; ^(d) Tsung-Dao Lee Institute, Shanghai, China
- ⁶¹ ^(a) Kirchhoff-Institut für Physik, Ruprecht-Karls-Universität Heidelberg, Heidelberg; ^(b) Physikalisches Institut, Ruprecht-Karls-Universität Heidelberg, Heidelberg, Germany
- ⁶² Faculty of Applied Information Science, Hiroshima Institute of Technology, Hiroshima, Japan
- ⁶³ ^(a) Department of Physics, Chinese University of Hong Kong, Shatin, N.T., Hong Kong; ^(b) Department of Physics, University of Hong Kong, Hong Kong; ^(c) Department of Physics and Institute for Advanced Study, Hong Kong University of Science and Technology, Clear Water Bay, Kowloon, Hong Kong, China
- ⁶⁴ Department of Physics, National Tsing Hua University, Hsinchu, Taiwan
- ⁶⁵ Department of Physics, Indiana University, Bloomington IN, United States of America
- ⁶⁶ ^(a) INFN Gruppo Collegato di Udine, Sezione di Trieste, Udine; ^(b) ICTP, Trieste; ^(c) Dipartimento Politecnico di Ingegneria e Architettura, Università di Udine, Udine, Italy
- ⁶⁷ ^(a) INFN Sezione di Lecce; ^(b) Dipartimento di Matematica e Fisica, Università del Salento, Lecce, Italy
- ⁶⁸ ^(a) INFN Sezione di Milano; ^(b) Dipartimento di Fisica, Università di Milano, Milano, Italy
- ⁶⁹ ^(a) INFN Sezione di Napoli; ^(b) Dipartimento di Fisica, Università di Napoli, Napoli, Italy

- ⁷⁰ (a) INFN Sezione di Pavia; (b) Dipartimento di Fisica, Università di Pavia, Pavia, Italy
- ⁷¹ (a) INFN Sezione di Pisa; (b) Dipartimento di Fisica E. Fermi, Università di Pisa, Pisa, Italy
- ⁷² (a) INFN Sezione di Roma; (b) Dipartimento di Fisica, Sapienza Università di Roma, Roma, Italy
- ⁷³ (a) INFN Sezione di Roma Tor Vergata; (b) Dipartimento di Fisica, Università di Roma Tor Vergata, Roma, Italy
- ⁷⁴ (a) INFN Sezione di Roma Tre; (b) Dipartimento di Matematica e Fisica, Università Roma Tre, Roma, Italy
- ⁷⁵ (a) INFN-TIFPA; (b) Università degli Studi di Trento, Trento, Italy
- ⁷⁶ Institut für Astro- und Teilchenphysik, Leopold-Franzens-Universität, Innsbruck, Austria
- ⁷⁷ University of Iowa, Iowa City IA, United States of America
- ⁷⁸ Department of Physics and Astronomy, Iowa State University, Ames IA, United States of America
- ⁷⁹ Joint Institute for Nuclear Research, Dubna, Russia
- ⁸⁰ (a) Departamento de Engenharia Elétrica, Universidade Federal de Juiz de Fora (UFJF), Juiz de Fora; (b) Universidade Federal do Rio De Janeiro COPPE/EE/IF, Rio de Janeiro;
- ^(c) Universidade Federal de São João del Rei (UFSJ), São João del Rei; ^(d) Instituto de Física, Universidade de São Paulo, São Paulo, Brazil
- ⁸¹ KEK, High Energy Accelerator Research Organization, Tsukuba, Japan
- ⁸² Graduate School of Science, Kobe University, Kobe, Japan
- ⁸³ (a) AGH University of Science and Technology, Faculty of Physics and Applied Computer Science, Krakow; (b) Marian Smoluchowski Institute of Physics, Jagiellonian University, Krakow, Poland
- ⁸⁴ Institute of Nuclear Physics Polish Academy of Sciences, Krakow, Poland
- ⁸⁵ Faculty of Science, Kyoto University, Kyoto, Japan
- ⁸⁶ Kyoto University of Education, Kyoto, Japan
- ⁸⁷ Research Center for Advanced Particle Physics and Department of Physics, Kyushu University, Fukuoka, Japan
- ⁸⁸ Instituto de Física La Plata, Universidad Nacional de La Plata and CONICET, La Plata, Argentina
- ⁸⁹ Physics Department, Lancaster University, Lancaster, United Kingdom
- ⁹⁰ Oliver Lodge Laboratory, University of Liverpool, Liverpool, United Kingdom
- ⁹¹ Department of Experimental Particle Physics, Jožef Stefan Institute and Department of Physics, University of Ljubljana, Ljubljana, Slovenia
- ⁹² School of Physics and Astronomy, Queen Mary University of London, London, United Kingdom
- ⁹³ Department of Physics, Royal Holloway University of London, Egham, United Kingdom
- ⁹⁴ Department of Physics and Astronomy, University College London, London, United Kingdom
- ⁹⁵ Louisiana Tech University, Ruston LA, United States of America
- ⁹⁶ Fysiska institutionen, Lunds universitet, Lund, Sweden
- ⁹⁷ Centre de Calcul de l'Institut National de Physique Nucléaire et de Physique des Particules (IN2P3), Villeurbanne, France
- ⁹⁸ Departamento de Física Teórica C-15 and CIAFF, Universidad Autónoma de Madrid, Madrid, Spain
- ⁹⁹ Institut für Physik, Universität Mainz, Mainz, Germany
- ¹⁰⁰ School of Physics and Astronomy, University of Manchester, Manchester, United Kingdom
- ¹⁰¹ CPPM, Aix-Marseille Université, CNRS/IN2P3, Marseille, France
- ¹⁰² Department of Physics, University of Massachusetts, Amherst MA, United States of America
- ¹⁰³ Department of Physics, McGill University, Montreal QC, Canada
- ¹⁰⁴ School of Physics, University of Melbourne, Victoria, Australia
- ¹⁰⁵ Department of Physics, University of Michigan, Ann Arbor MI, United States of America
- ¹⁰⁶ Department of Physics and Astronomy, Michigan State University, East Lansing MI, United States of America
- ¹⁰⁷ B.I. Stepanov Institute of Physics, National Academy of Sciences of Belarus, Minsk, Belarus
- ¹⁰⁸ Research Institute for Nuclear Problems of Byelorussian State University, Minsk, Belarus
- ¹⁰⁹ Group of Particle Physics, University of Montreal, Montreal QC, Canada
- ¹¹⁰ P.N. Lebedev Physical Institute of the Russian Academy of Sciences, Moscow, Russia
- ¹¹¹ Institute for Theoretical and Experimental Physics of the National Research Centre Kurchatov Institute, Moscow, Russia
- ¹¹² National Research Nuclear University MEPhI, Moscow, Russia
- ¹¹³ D.V. Skobeltsyn Institute of Nuclear Physics, M.V. Lomonosov Moscow State University, Moscow, Russia
- ¹¹⁴ Fakultät für Physik, Ludwig-Maximilians-Universität München, München, Germany
- ¹¹⁵ Max-Planck-Institut für Physik (Werner-Heisenberg-Institut), München, Germany
- ¹¹⁶ Nagasaki Institute of Applied Science, Nagasaki, Japan
- ¹¹⁷ Graduate School of Science and Kobayashi-Maskawa Institute, Nagoya University, Nagoya, Japan
- ¹¹⁸ Department of Physics and Astronomy, University of New Mexico, Albuquerque NM, United States of America
- ¹¹⁹ Institute for Mathematics, Astrophysics and Particle Physics, Radboud University Nijmegen/Nikhef, Nijmegen, Netherlands
- ¹²⁰ Nikhef National Institute for Subatomic Physics and University of Amsterdam, Amsterdam, Netherlands
- ¹²¹ Department of Physics, Northern Illinois University, DeKalb IL, United States of America
- ¹²² (a) Budker Institute of Nuclear Physics and NSU, SB RAS, Novosibirsk; (b) Novosibirsk State University Novosibirsk, Russia
- ¹²³ Institute for High Energy Physics of the National Research Centre Kurchatov Institute, Protvino, Russia
- ¹²⁴ Department of Physics, New York University, New York NY, United States of America
- ¹²⁵ Ochanomizu University, Otsuka, Bunkyo-ku, Tokyo, Japan
- ¹²⁶ Ohio State University, Columbus OH, United States of America
- ¹²⁷ Faculty of Science, Okayama University, Okayama, Japan
- ¹²⁸ Homer L. Dodge Department of Physics and Astronomy, University of Oklahoma, Norman OK, United States of America
- ¹²⁹ Department of Physics, Oklahoma State University, Stillwater OK, United States of America
- ¹³⁰ Palacký University, RPTM, Joint Laboratory of Optics, Olomouc, Czech Republic
- ¹³¹ Center for High Energy Physics, University of Oregon, Eugene OR, United States of America
- ¹³² LAL, Université Paris-Sud, CNRS/IN2P3, Université Paris-Saclay, Orsay, France
- ¹³³ Graduate School of Science, Osaka University, Osaka, Japan
- ¹³⁴ Department of Physics, University of Oslo, Oslo, Norway
- ¹³⁵ Department of Physics, Oxford University, Oxford, United Kingdom
- ¹³⁶ LPNHE, Sorbonne Université, Paris Diderot Sorbonne Paris Cité, CNRS/IN2P3, Paris, France
- ¹³⁷ Department of Physics, University of Pennsylvania, Philadelphia PA, United States of America
- ¹³⁸ Konstantinov Nuclear Physics Institute of National Research Centre "Kurchatov Institute", PNPI, St. Petersburg, Russia
- ¹³⁹ Department of Physics and Astronomy, University of Pittsburgh, Pittsburgh PA, United States of America
- ¹⁴⁰ (a) Laboratório de Instrumentação e Física Experimental de Partículas - LIP; (b) Departamento de Física, Faculdade de Ciências, Universidade de Lisboa, Lisboa; (c) Departamento de Física, Universidade de Coimbra, Coimbra; (d) Centro de Física Nuclear da Universidade de Lisboa, Lisboa; (e) Departamento de Física, Universidade do Minho, Braga; (f) Universidad de Granada, Granada (Spain); (g) Dep Física and CEFITEC of Faculdade de Ciências e Tecnologia, Universidade Nova de Lisboa, Caparica, Portugal
- ¹⁴¹ Institute of Physics of the Czech Academy of Sciences, Prague, Czech Republic
- ¹⁴² Czech Technical University in Prague, Prague, Czech Republic
- ¹⁴³ Charles University, Faculty of Mathematics and Physics, Prague, Czech Republic
- ¹⁴⁴ Particle Physics Department, Rutherford Appleton Laboratory, Didcot, United Kingdom

- ¹⁴⁵ IRFU, CEA, Université Paris-Saclay, Gif-sur-Yvette, France
- ¹⁴⁶ Santa Cruz Institute for Particle Physics, University of California Santa Cruz, Santa Cruz CA, United States of America
- ¹⁴⁷ ^(a) Departamento de Física, Pontificia Universidad Católica de Chile, Santiago; ^(b) Departamento de Física, Universidad Técnica Federico Santa María, Valparaíso, Chile
- ¹⁴⁸ Department of Physics, University of Washington, Seattle WA, United States of America
- ¹⁴⁹ Department of Physics and Astronomy, University of Sheffield, Sheffield, United Kingdom
- ¹⁵⁰ Department of Physics, Shinshu University, Nagano, Japan
- ¹⁵¹ Department Physik, Universität Siegen, Siegen, Germany
- ¹⁵² Department of Physics, Simon Fraser University, Burnaby BC, Canada
- ¹⁵³ SLAC National Accelerator Laboratory, Stanford CA, United States of America
- ¹⁵⁴ Physics Department, Royal Institute of Technology, Stockholm, Sweden
- ¹⁵⁵ Departments of Physics and Astronomy, Stony Brook University, Stony Brook NY, United States of America
- ¹⁵⁶ Department of Physics and Astronomy, University of Sussex, Brighton, United Kingdom
- ¹⁵⁷ School of Physics, University of Sydney, Sydney, Australia
- ¹⁵⁸ Institute of Physics, Academia Sinica, Taipei, Taiwan
- ¹⁵⁹ ^(a) E. Andronikashvili Institute of Physics, Iv. Javakishvili Tbilisi State University, Tbilisi; ^(b) High Energy Physics Institute, Tbilisi State University, Tbilisi, Georgia
- ¹⁶⁰ Department of Physics, Technion, Israel Institute of Technology, Haifa, Israel
- ¹⁶¹ Raymond and Beverly Sackler School of Physics and Astronomy, Tel Aviv University, Tel Aviv, Israel
- ¹⁶² Department of Physics, Aristotle University of Thessaloniki, Thessaloniki, Greece
- ¹⁶³ International Center for Elementary Particle Physics and Department of Physics, University of Tokyo, Tokyo, Japan
- ¹⁶⁴ Graduate School of Science and Technology, Tokyo Metropolitan University, Tokyo, Japan
- ¹⁶⁵ Department of Physics, Tokyo Institute of Technology, Tokyo, Japan
- ¹⁶⁶ Tomsk State University, Tomsk, Russia
- ¹⁶⁷ Department of Physics, University of Toronto, Toronto ON, Canada
- ¹⁶⁸ ^(a) TRIUMF, Vancouver BC; ^(b) Department of Physics and Astronomy, York University, Toronto ON, Canada
- ¹⁶⁹ Division of Physics and Tomonaga Center for the History of the Universe, Faculty of Pure and Applied Sciences, University of Tsukuba, Tsukuba, Japan
- ¹⁷⁰ Department of Physics and Astronomy, Tufts University, Medford MA, United States of America
- ¹⁷¹ Department of Physics and Astronomy, University of California Irvine, Irvine CA, United States of America
- ¹⁷² Department of Physics and Astronomy, University of Uppsala, Uppsala, Sweden
- ¹⁷³ Department of Physics, University of Illinois, Urbana IL, United States of America
- ¹⁷⁴ Instituto de Física Corpuscular (IFIC), Centro Mixto Universidad de Valencia - CSIC, Valencia, Spain
- ¹⁷⁵ Department of Physics, University of British Columbia, Vancouver BC, Canada
- ¹⁷⁶ Department of Physics and Astronomy, University of Victoria, Victoria BC, Canada
- ¹⁷⁷ Fakultät für Physik und Astronomie, Julius-Maximilians-Universität Würzburg, Würzburg, Germany
- ¹⁷⁸ Department of Physics, University of Warwick, Coventry, United Kingdom
- ¹⁷⁹ Waseda University, Tokyo, Japan
- ¹⁸⁰ Department of Particle Physics, Weizmann Institute of Science, Rehovot, Israel
- ¹⁸¹ Department of Physics, University of Wisconsin, Madison WI, United States of America
- ¹⁸² Fakultät für Mathematik und Naturwissenschaften, Fachgruppe Physik, Bergische Universität Wuppertal, Wuppertal, Germany
- ¹⁸³ Department of Physics, Yale University, New Haven CT, United States of America
- ¹⁸⁴ Yerevan Physics Institute, Yerevan, Armenia

^a Also at Centre for High Performance Computing, CSIR Campus, Rosebank, Cape Town; South Africa.

^b Also at CERN, Geneva; Switzerland.

^c Also at CPPM, Aix-Marseille Université, CNRS/IN2P3, Marseille; France.

^d Also at Département de Physique Nucléaire et Corpusculaire, Université de Genève, Genève; Switzerland.

^e Also at Departament de Física de la Universitat Autònoma de Barcelona, Barcelona; Spain.

^f Also at Departamento de Física, Instituto Superior Técnico, Universidade de Lisboa, Lisboa; Portugal.

^g Also at Department of Applied Physics and Astronomy, University of Sharjah, Sharjah; United Arab Emirates.

^h Also at Department of Financial and Management Engineering, University of the Aegean, Chios; Greece.

ⁱ Also at Department of Physics and Astronomy, University of Louisville, Louisville, KY; United States of America.

^j Also at Department of Physics and Astronomy, University of Sheffield, Sheffield; United Kingdom.

^k Also at Department of Physics, California State University, East Bay; United States of America.

^l Also at Department of Physics, California State University, Fresno; United States of America.

^m Also at Department of Physics, California State University, Sacramento; United States of America.

ⁿ Also at Department of Physics, King's College London, London; United Kingdom.

^o Also at Department of Physics, St. Petersburg State Polytechnical University, St. Petersburg; Russia.

^p Also at Department of Physics, Stanford University, Stanford CA; United States of America.

^q Also at Department of Physics, University of Fribourg, Fribourg; Switzerland.

^r Also at Department of Physics, University of Michigan, Ann Arbor MI; United States of America.

^s Also at Faculty of Physics, M.V. Lomonosov Moscow State University, Moscow; Russia.

^t Also at Giresun University, Faculty of Engineering, Giresun; Turkey.

^u Also at Graduate School of Science, Osaka University, Osaka; Japan.

^v Also at Hellenic Open University, Patras; Greece.

^w Also at Institut Català de Recerca i Estudis Avançats, ICREA, Barcelona; Spain.

^x Also at Institut für Experimentalphysik, Universität Hamburg, Hamburg; Germany.

^y Also at Institute for Mathematics, Astrophysics and Particle Physics, Radboud University Nijmegen/Nikhef, Nijmegen; Netherlands.

^z Also at Institute for Nuclear Research and Nuclear Energy (INRNE) of the Bulgarian Academy of Sciences, Sofia; Bulgaria.

^{aa} Also at Institute for Particle and Nuclear Physics, Wigner Research Centre for Physics, Budapest; Hungary.

^{ab} Also at Institute of High Energy Physics, Chinese Academy of Sciences, Beijing; China.

^{ac} Also at Institute of Particle Physics (IPP); Canada.

^{ad} Also at Institute of Physics, Academia Sinica, Taipei; Taiwan.

^{ae} Also at Institute of Physics, Azerbaijan Academy of Sciences, Baku; Azerbaijan.

^{af} Also at Institute of Theoretical Physics, Ilia State University, Tbilisi; Georgia.

^{ag} Also at Instituto de Física Teórica, IFT-UAM/CSIC, Madrid; Spain.

^{ah} Also at Istanbul University, Dept. of Physics, Istanbul; Turkey.

^{ai} Also at Joint Institute for Nuclear Research, Dubna; Russia.

^{aj} Also at LAL, Université Paris-Sud, CNRS/IN2P3, Université Paris-Saclay, Orsay; France.

^{ak} Also at Louisiana Tech University, Ruston LA; United States of America.

^{al} Also at LPNHE, Sorbonne Université, Paris Diderot Sorbonne Paris Cité, CNRS/IN2P3, Paris; France.

^{am} Also at Manhattan College, New York NY; United States of America.

^{an} Also at Moscow Institute of Physics and Technology State University, Dolgoprudny; Russia.

^{ao} Also at National Research Nuclear University MEPhI, Moscow; Russia.

^{ap} Also at Physics Department, An-Najah National University, Nablus; Palestine.

^{aq} Also at Physics Dept, University of South Africa, Pretoria; South Africa.

^{ar} Also at Physikalisches Institut, Albert-Ludwigs-Universität Freiburg, Freiburg; Germany.

^{as} Also at School of Physics, Sun Yat-sen University, Guangzhou; China.

^{at} Also at The City College of New York, New York NY; United States of America.

^{au} Also at The Collaborative Innovation Center of Quantum Matter (CICQM), Beijing; China.

^{av} Also at Tomsk State University, Tomsk, and Moscow Institute of Physics and Technology State University, Dolgoprudny; Russia.

^{aw} Also at TRIUMF, Vancouver BC; Canada.

^{ax} Also at Università di Napoli Parthenope, Napoli; Italy.

* Deceased.